1992

[Carbon-13] solid-state NMR study of ethylene oxidation over supported silver catalysts

Sadreddin Hosseini
Iowa State University

INFORMATION TO USERS

This manuscript has been reproduced from the microfilm master. UMI films the text directly from the original or copy submitted. Thus, some thesis and dissertation copies are in typewriter face, while others may be from any type of computer printer.

The quality of this reproduction is dependent upon the quality of the copy submitted. Broken or indistinct print, colored or poor quality illustrations and photographs, print bleedthrough, substandard margins, and improper alignment can adversely affect reproduction.

In the unlikely event that the author did not send UMI a complete manuscript and there are missing pages, these will be noted. Also, if unauthorized copyright material had to be removed, a note will indicate the deletion.

Oversize materials (e.g., maps, drawings, charts) are reproduced by sectioning the original, beginning at the upper left-hand corner and continuing from left to right in equal sections with small overlaps. Each original is also photographed in one exposure and is included in reduced form at the back of the book.

Photographs included in the original manuscript have been reproduced xerographically in this copy. Higher quality 6" x 9" black and white photographic prints are available for any photographs or illustrations appearing in this copy for an additional charge. Contact UMI directly to order.

UMI

University Microfilms International
A Bell & Howell Information Company
300 North Zeeb Road, Ann Arbor, MI 48106-1346 USA
313/761-4700 800/521-0600

Order Number 9234817

^{13}C solid-state NMR study of ethylene oxidation over supported silver catalysts

Hosseini, Sadreddin, Ph.D.

Iowa State University, 1992

U·M·I
300 N. Zeeb Rd.
Ann Arbor, MI 48106

^{13}C solid-state NMR study of ethylene oxidation over supported silver catalysts

by

Sadreddin Hosseini

A Dissertation Submitted to the

Graduate Faculty in Partial Fulfillment

of the Requirements for the Degree of

DOCTOR OF PHILOSOPHY

Department: Chemistry
Major: Physical Chemistry

Approved:

Signature was redacted for privacy.

In Charge of Major Work

Signature was redacted for privacy.

For the Major Department

Signature was redacted for privacy.

For the Graduate College

Iowa State University
Ames, Iowa

1992

Dedicated to my lovely wife Mitra and gracious parents whose enormous support, love and encouragement made this thesis possible.

TABLE OF CONTENTS

LIST OF FIGURES

CHAPTER I. SOME NMR BACKGROUND

Introduction

Nuclear magnetic resonance (NMR) spectroscopy is concerned with the interaction between an oscillating magnetic field (the rf field) and the net nuclear magnetization of a sample brought about by applying a static magnetic field. In 1924, Pauli suggested that exposure of certain atomic nuclei having properties of spin and magnetic moment to a magnetic field results in splitting of their energy levels. During the next decade, experimental verification of these postulates was obtained. However, it was not until 1946 that Bloch[1] at Stanford and Purcell[2] at Harvard, working independently, were able to demonstrate that nuclei absorb electromagnetic radiation in a strong magnetic field as a consequence of the energy level splitting induced by the magnetic force. The two physicists shared the 1952 Nobel prize for their work.

Nuclear magnetic resonance spectroscopy has, over the last 20 years or so, developed into a major spectroscopic technique for characterization of solids. Indeed, it is arguable that it is the single most important tool for obtaining detailed information on chemical systems at the molecular level. In explaining the nuclear magnetic resonance phenomenon, both classical and quantum mechanics are useful. In the case of an ensemble of weakly interacting spin 1/2 nuclei, the two treatments yield identical relationships.

Classical mechnics is more helpful in providing a physical picture of the absorption process and how it is measured, while quantum mechanics is more useful for relating absorption frequencies to energy states of nuclei. The fact that one can approach nuclear resonance from both classical viewpoints and quantum mechnical provides considerable advantages and is one of the beauties of the subject.

The general outline of the theory of nuclear magnetic resonance (NMR) is now quite common knowledge. There are many excellent books and monographs which deal at length with the subject[3,4,5]. Much of the description below relates to the net behaviour of the magnetization of the sample from the classical points of view. Fig. 1 is a conceptual block diagram of the pulsed NMR experiment. All nuclei with an odd mass number possess an intrinsic spin angular momentum denoted by I in units of $\hbar$ (Planck's constant divided by 2 π) and a magnetic moment $\mu = \gamma\hbar I$, where γ is the gyromagnetic ratio of the nucleus. A nucleus has (2I + 1) discrete states, equally spaced with a separation $\Delta E = \mu B_o / I$ where I is its spin quantum number. The component of angular momentum for these states in any chosen direction will have values of I, I - 1, I - 2,....., - I. In the absence of an external field, various states have identical energies (i.e, degenerate).

When a sample is placed in the magnet, the nuclei in the molecule generate a bulk macroscopic magnetization. The magnetization vector, M, for an ensemble of spins is the sum of the individual nuclear dipole vectors. At equilibrium, M is aligned parallel to external magnetic field, B_o, in the

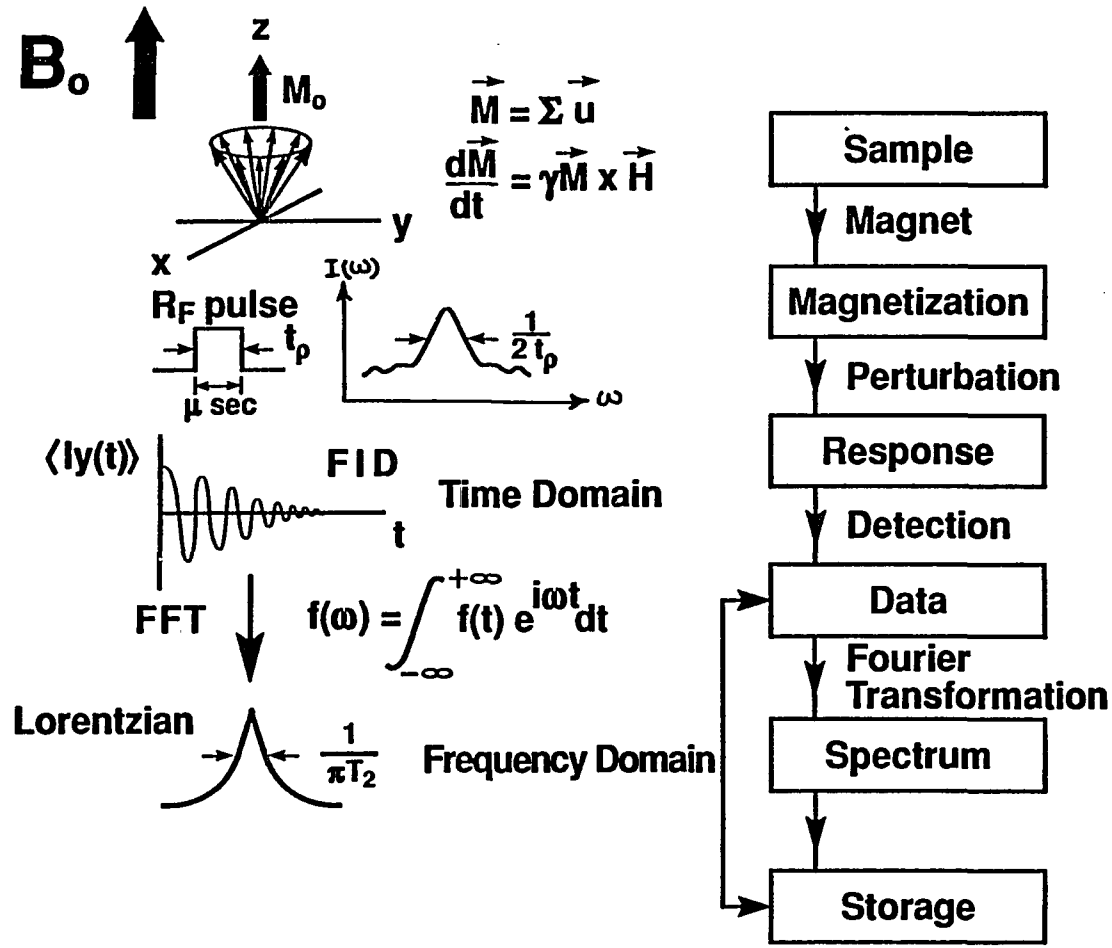

Fig. 1. A block diagram of the pulsed Fourier transform NMR experiment

Z - direction. This is because the Boltzmann distribution slightly favors the lower energy state, therefore, there are at equilibrium more nuclei aligned in the direction of B_o than opposed to it. Since the difference in population between the various states is very small (typically about 1 part in 10^5) and the separation between nuclear magnetic energy levels ($\Delta E \leqslant kT$) is typically 10^{-8} to 10^{-6} eV, NMR signals are weak in comparison with those observed with other forms of spectroscopy which have higher energy differences (i.e. $\Delta E \geqslant kT$). As with other types of quantum states, excitation to a higher nuclear magnetic quantum level can be brought about by absorption of a photon with energy $h\nu_o$ that just equals ΔE. The frequency (ν_o) of electromagnetic radiation (in Hz) adsorbed by nuclei which induces a transition between adjacent levels is given by the Larmor equation : $\nu_o = \gamma B_o / 2\pi$.

In continuous wave NMR, the disturbance of the magnetization is monitored as either the radio frequency is varied or the applied field is swept; in each case, only a single frequency is excited and detected at any one moment. In pulsed NMR on the other hand, the entire spectrum of interesting frequencies is stimulated by a pulse of radio frequency energy. Pulsed methods are often much more efficient, thus producing a very significant saving in time or improvement in signal/noise ratio.

Once the sample is brought into an external magnetic field, the system is disturbed from equilibrium with a strong, short (~ usec) pulse of RF power by applying an alternating voltage across the ends of the coil in the NMR probe. Ideally this alternating magnetic field would be uniform everywhere

in the sample and would fall abruptly to zero at the sample boundaries; naturally the true situation deviates from this ideal. The amplitude of the oscillating field is substantially smaller than that of the static field (thousands of times smaller) such that it does not alter the sample chemically, vibrationally or even rotationally. It is important to recognize that in order to observe NMR signals, we must pertube the system from equilibrium. The response of the system to this disturbance is then monitored. The phase-detected (demodulated) observed NMR signal is proportional to an induced voltage in a coil which is proportional to the expectation value of the transverse component of angular momentum as a function of time, e.g., $< I_y (t) >$. The signal obtained in the time domain is called the free induction decay (FID). We detect magnetization not in the fixed coordinate system of the lab but in the rotating frame or interaction frame of the Zeeman Hamiltonian. After perturbation, the system will behave like any other physical system and return to equilibrium. The population of the states will return to a Boltzmann distribution and magnetization will return to an equilibrium value M_o aligned along the field axis.

Up to this point, the signal that is observed is in time domain. We use the Fourier transform to convert data in the time domain to the frequency domain. The Fourier transform is a perfectly general mathematical transformation ($f(\omega) = \int_{-\infty}^{+\infty} f(t)\ e^{i\omega t}\ dt$). This transformatiom has two parts: real and imaginary. Each of these parts contains a representation of the spectrum, but with different forms of the Lorentzian line. The real part of

the transform contains absorption mode lines and the imaginary part of the transform contains dispersion mode lines. Conventionally, we display NMR spectra in absorption mode, so the real part of the spectrum is used for plotting. The fullwidth at half height of Lorentzian line is inversely proportional to T_2 which is the spin-spin or transverse relaxation time.

Application of NMR to Heterogeneous Catalysis

High- resolution NMR spectroscopy has been of such value in chemistry that one would hope to be able to apply it to surface studies. Indeed, this powerful spectroscopic technique has been used to study systems of catalytic interest for over two decades[6-12]. Heterogeneous catalysis is a surface phenomenon. Thus, in NMR studies, we need to be able to observe the NMR signal from the nuclei at the surface.

Two types of surfaces exist: (a) Oriented single crystals under conditions of ultrahigh vacuum (typically 1 cm^2 in area of metal surface under investigation contains about 10^{15} atom sites). Since a large number of nuclei are required to produce an observable NMR signal (typical NMR experiments requires 10^{18} - 10^{19} nuclei or 10 m^2 of surface), the NMR studies on macroscopic single crystals are presently impossible due to the weakness of NMR signals from surfaces.(b) very small particles, typically a few atom distances in radius, often supported on materials such as certain forms of Al_2O_3 (alumina) or SiO_2 (silica). These surfaces are representative of actual catalysts which typically have metal surface areas of 10's of square

meters for 1 cm^3 sample (1 g of a real catalyst may contain 1 to 10 m^2 of metal surface, presenting 10^{19} to 10^{20} atom sites).

Even though nuclear magnetic resonance is not sensitive enough for single crystal work, it has sufficient sensitivity for high surface area powder studies. Despite the obstacles to studying surface samples with NMR spectroscopy, the significance of the results often justify the effort. NMR allows us to undertake detailed microscopic investigations of the real catalysts. It provides information about the bonding of the molecules to the metal, lets us determine the structure that the molecules assume after adsorption, enables us to detect and measure rotational and translational motions of the molecules on the surface, and permits us to follow details of the breakup of the molecules induced by heating.

Applications of NMR spectroscopy of the solid state to the study of physically and chemically adsorbed species would help us understand more about the catalytic processes which occur on the surface of a catalyst. Most published studies involved molecules that are weakly bound to the surface, so-called physisorbed species. For catalysis, molecules that form chemical bonds with the surface, so called chemisorbed species, are of interest. Chemisorbed species have limited degrees of freedom on the surface which leads to broadband spectra. Physisorbed species on the other hand are more free to tumble on the surface such that the observed effects of many nuclear magnetic interactions are averaged to their isotropic, or scalar values, and therefore it is expected that one might detect their high- resolution NMR

spectra. Indeed, weakly adsorbed species can be identified based on their observed chemical shifts as compared with the data from liquid state NMR.

When formulating a NMR study of surfaces or adsorbates, several choices must be made. Unfortunately, many of the decisions, such as which nuclei to detect or which technique to apply, may be dictated by the capability of the available NMR spectrometer. The important consideration is which nuclear resonance to observe. For example, one might detect the ^{1}H resonance to investigate the adsorption of H_2 on metal oxides. To study oxidation of ethylene over supported silver catalyst one might consider ^{109} Ag, ^{17} O and ^{13} C NMR. There are however some limitations involved in this case. Experimentally, silver NMR presents severe challenges due to its low sensitivity (the inherent sensitivity of ^{109} Ag is only 1.01×10^{-4} compared with an equal number of protons, and 6.54×10^{-3} compared with an equal number of ^{13} C nuclei), long spin - lattice relaxation time T_1 and low natural abundance (49 %). Oxygen is a little - studied atom from the NMR point of view mainly because of its extremely low natural abundance (^{17} O, 0.037 %). Oxygen is also a quadrupolar nucleus (spin number I=5/2, quadrupole moment $eQ = -0.0263 \times 10^{-24}$ e cm^2) with relatively low Larmor frequency (ν_o = 13.5 MHz at B_o = 2.34 T). Because of experimental difficulties, quadrupolar nuclei have been used only rarely to study catalytic systems.

The work presented in this thesis focuses on the application of solid state ^{13} C NMR to study oxidation of ethylene over supported silver catalysts. Even though the NMR signals from ^{13} C are weak due to its low

natural isotopic abundance (1.1 %) and the small gyromagnetic ratios, there are some advantages associated with using ^{13} C NMR to study catalytic systems. ^{13} C NMR provides information about the backbone of hydrocarbon molecules rather than the periphery. The chemical shift range for ^{13} C in a majority of organic compounds is ~ 200 ppm (compared with ~10 -15 ppm ^{1} H), which results in less overlap of peaks. Because of the low abundance of ^{13} C, there is no homonuclear spin - spin coupling between carbon atoms. Heteronuclear spin coupling between ^{13} C - ^{12} C does not occur because ^{12} C is an inactive nucleus (I = 0). Finally, there are effective methods to suppress the heteronuclear dipolar coupling to ^{1} H. Decoupling the interaction between ^{13} C atoms and ^{1} H has become possible through advances in double - resonance techniques and improvements in instrumentation. A combination of high power proton decoupling, sensitivity enhancement techniques like cross polarization and spinning of the sample at the "magic angle" of $54^{\circ}44'$ to the magnetic field provide a powerful tool for obtaining high - resolution ^{13} C NMR of molecules adsorbed on surfaces. In what follows, we describe in some detail the theory of the cross - polarization experiment which is used for studying oxidation of ethylene over supported silver catalyst.

Theory of Cross Polarization (CP) Experiments

The solid state NMR signals of many nuclei (e.g.,^{13} C, ^{15} N) which can give valuable information regarding the chemical functionalities of molecules are weak relative to signals obtained from higher energy spectroscopies mainly because of 1) the low sensitivity due to low natural abundance and small gyromagnetic ratio, 2) relatively long spin-lattice relaxation times which make data acquisition a difficult task and 3) spectral broadening due to dipolar interactions with protons. These factors contribute to the difficulty of obtaining satisfactory solid-state spectra for dilute spins such as ^{13} C. Fortunately, a wealth of double resonance techniques have been developed to overcome this problem and have made high resolution solid state NMR of dilute spin systems possible. The basic idea of the double resonance technique was proposed by Hartmann and Hahn[13]. In 1962, they introduced a double nuclear resonance spectroscopy method which depends upon magnetic dipole-dipole coupling between two different nuclear species. Since the NMR signals of dilute and/or insensitive nuclei are so weak, sensitivity can be enhanced by taking advantage of the dipolar reservoir of abundant spins. This can be accomplished in two ways: 1) by the indirect method[14], where the dilute spins are detected via the abundant spins and 2) by the direct method[15], where the dilute spins are polarized by the abundant spins. The latter technique has furnished most of the high resolution double resonance NMR spectra in solids of dilute spins to date.

The dynamics of the different double resonance methods are detailed in chapter 4 of Mehring[16]and chapter 6 of Gerstein and Dybowski[3]. Using ideas suggested in 1962 by Hartmann-Hahn[13], Pines, Gibby and Waugh[17] in 1973 developed the cross-polarization technique with high powered decoupling of the abundant spins and dilute-spin observation and recorded the first enhanced NMR spectra of dilute spins in solids. The basic principle of a double resonance experiment as suggested by Hartmann and Hahn[13] is shown schematically in Fig. 2. The coupling between the abundant and rare spin reservoirs is represented by the cross relaxation time T_{C-H}. Under spin-lock conditions in the rotating frame, the nuclear spin-lattice relaxation times of abundant ^{1}H spin and rare ^{13}C spin are $T_{1\rho}$ ^{1}H and $T_{1\rho}$ ^{13}C, respectively. There are three steps in a polarization transfer experiment: (I) cooling of the abundant ^{1}H spin reservoir, (II) transfer of polarization between the two reservoirs by bringing the abundant and the rare spins into contact, and (III) observation of the rare spin. Cooling of the abundant ^{1}H spin system can be achieved by locking the spins in the rotating frame with a field $B_1 << B_0$. In the high-temperature limit, the equilibrium spin density matrix is given by

$$\rho = 1 - \hbar H / kT \qquad (1)$$

where H is the Hamiltonian operator for the system in question.
The magnetization and energy are given by appropriate traces :

$$M_i = \hbar\gamma \, Tr \{\rho I_i\} \quad (i= x, y , z) \qquad (2)$$

$$E = Tr \{\rho H\} \qquad (3)$$

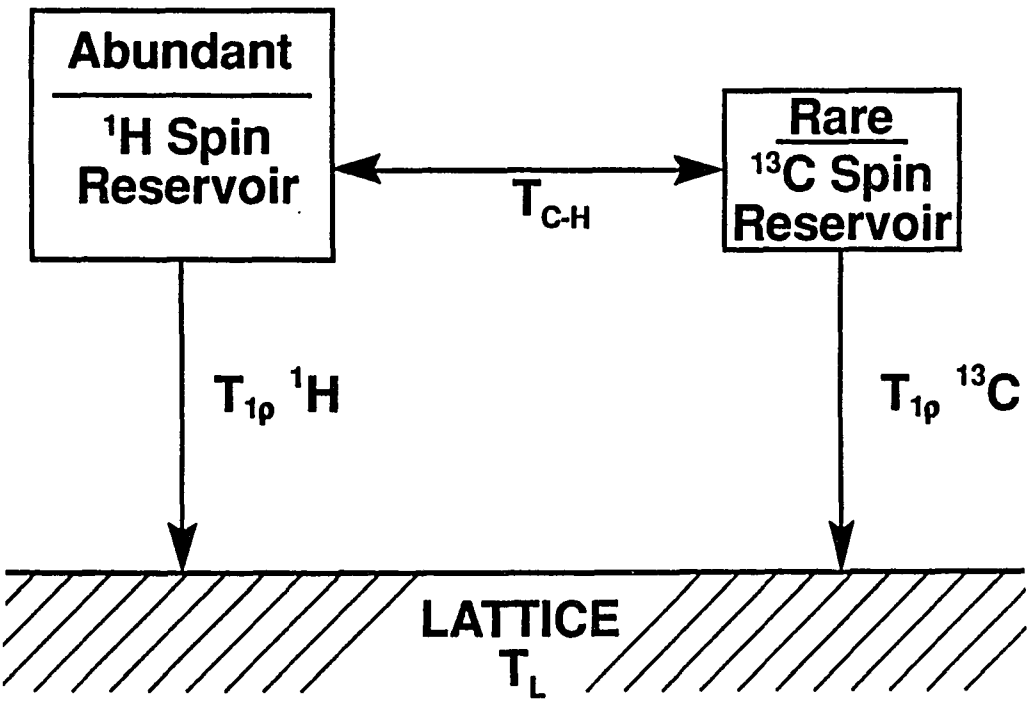

Fig. 2. Schematic representation of an abundant spin reservoir (^{1}H) and a rare spin reservoir (^{13}C). $T_{1\rho}$ ^{1}H and $T_{1\rho}$ ^{13}C are nuclear spin-lattice relaxation times in the rotating frames of abundant ^{1}H spin and rare ^{13}C spin, respectively. The ^{1}H and ^{13}C spins may be coupled by some interaction represented by the cross relaxation time T_{C-H}

In the high-temperature limit when placing a sample into the static magnetic field B_0 along z,

$$M_0 = CB_0 / T \tag{4}$$

$$E = CB_0^2 / T \tag{5}$$

Equation (4) is known as Curie's law. According to (4), a low spin temperature implies large polarization of the magnetic moments in a small field.

The proton magnetization produced in the laboratory frame by equilibration with the lattice is given by Curie's law as

$$M_0 (H) = C_H B_0 / T_L \tag{6}$$

where $C_H = (1/4) \gamma_H^2 \hbar^2 N_H / k$ and T_L is the lattice temperature. This equilibrium magnetization is transferred to the rotating frame by spin-locking, but it is of course, no longer at equilibrium, since $B_1 << B_0$. In fact the situation can be expressed in terms of a spin temperature in the rotating frame, T_P. Thus

$$C_H B_0 / T_L = C_H B_{1H} / T_P \tag{7}$$

i.e. $T_P = (B_{1H} / B_0) T_L$

Since $B_1 << B_0$, the proton spin temperature T_P in B_{1H} is very low compared to that of the proton spins T_L at equilibrium in the field B_0. Given $B_0 = 10^4$ G, $B_1 = 60$ G and $T_L = 300$ K, T_P is calculated to be 1.80 K. Since the ^{1}H spins are "cold" and the ^{13}C spins are "hot", an energy exchange can take place with time constant T_{C-H}. This energy exchange is impossible in the laboratory frame since such a process need occur under total energy conservation. However, a matching of the energy levels is

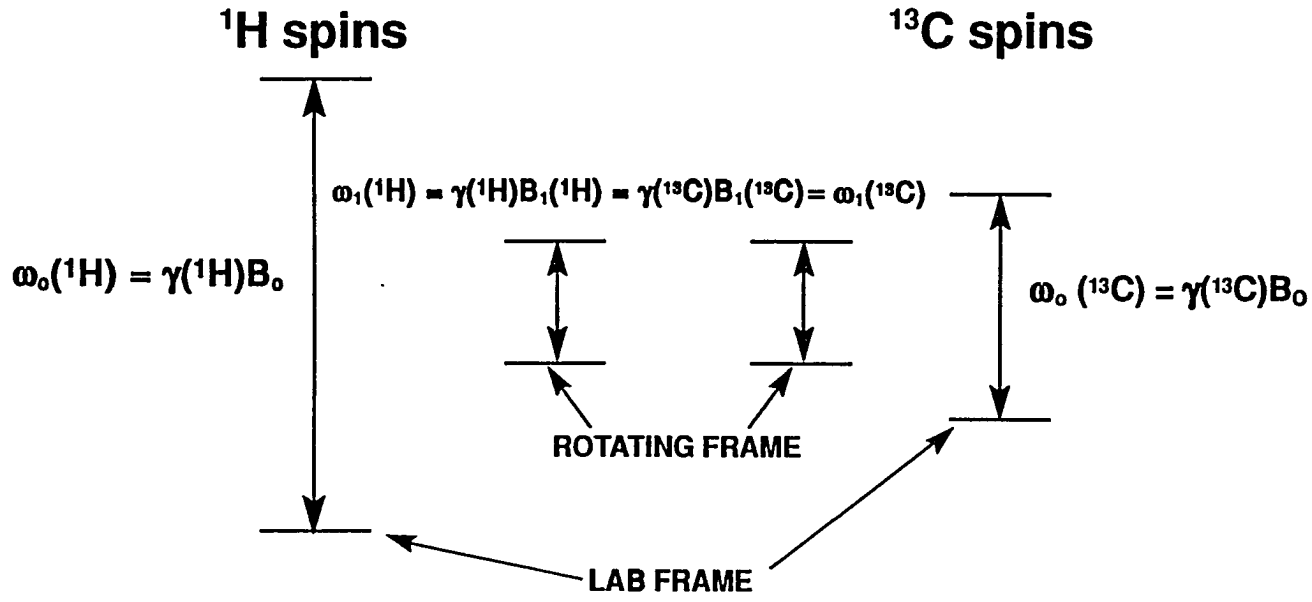

Fig. 3. The energy level diagram of the ^{1}H and ^{13}C spin systems. Under Hartmann - Hahn condition, the energy levels of the two systems are equal in the rotating frame

possible in the rotating frame as shown in Fig. 3, allowing rapid transfer under energy conservation if the Hartmann - Hahn condition, Equation (8), is fulfilled

$$\gamma(^{13}C)\, B_1(^{13}C) = \gamma(^{1}H)\, B_1(^{1}H) \qquad (8)$$

or $$\omega_1(^{13}C) = \omega_1(^{1}H)$$

where $B_1(^{13}C)$ and $B_1(^{1}H)$ are the r.f. field in the rotating frame of the proton and carbon spins respectively.

The Hartmann - Hahn matching condition implies that in their respective rotating frames of reference the protons and carbons precess at equal rates and that the effective energies (also in the rotating frames) are comparable, thus allowing a rapid transfer of magnetization. Under this condition, the large , cold ^{1}H reservoir can cool the small, hotter ^{13}C reservoir with time constant $T_{C\text{-}H}$. In other words, the ^{1}H magnetization is larger than the ^{13}C magnetization so cross polarization from protons to carbon will cause the ^{13}C magnetization to increase, whereas the ^{1}H magnetization decreases. The enhanced magnetization in the carbon spins is detected by monitoring the FID following the cross polarization. It can be shown that the polarization transfer rate is a maximum when the precession frequencies of ^{1}H and ^{13}C in their respective rotating frames are equal: $\gamma(^{13}C)\, B_1(^{13}C) = \gamma(^{1}H)\, B_1(^{1}H)$. Fig. 4 schematically shows that cross-polarization builds-up the magnetization which then decays due to $T_1\rho$ processes. So the advantage of cross-polarization is the enhancement of the NMR signals from dilute, low-gyromagnetic ratio spins. For the ^{1}H -

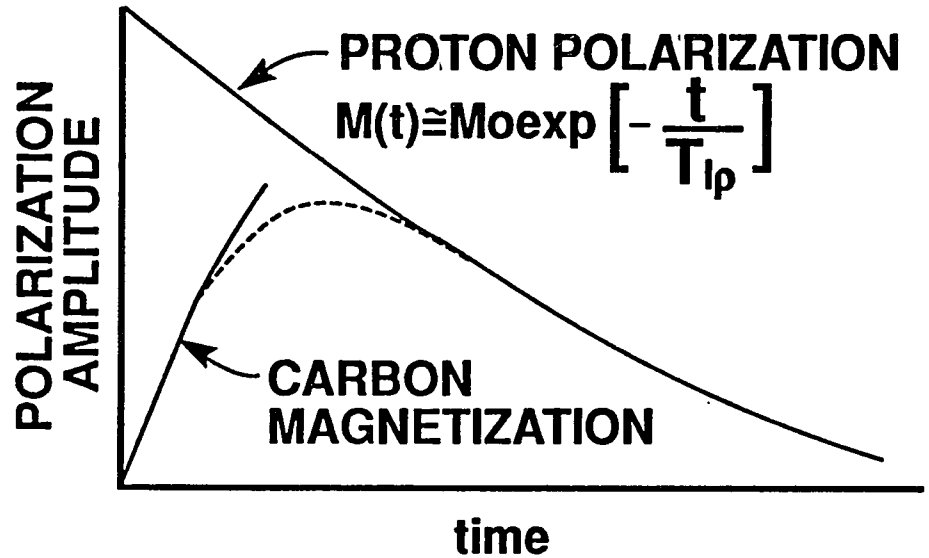

Fig. 4. The time evolution of the ^{13}C spin magnetization M (t) during contact time with the ^{1}H spins

^{13} C system, the ^{13} C signal is enhanced by a factor of four and the spectral averaging time is reduced by a factor of sixteen. The magnitude of the ^{13} C signal which is determined by the ratio of $\gamma(^{1}H) / \gamma(^{13}C) \sim 4$ is not usually reached in practice but one does obtain a useful increase in sensitivity. Furthermore, under conditions of cross-polarization, the rate at which the experiment may be repeated is determined by the spin-lattice relaxation rate of ^{1} H (proton T_1's are typically seconds) rather than the slower ^{13} C relaxation rate (^{13} C T_1's can be as long as 200 seconds). Therfore, the cross-polarization is repeated every five proton T_1, rather than every five ^{13} C T_1 . This effect is the major factor in sensitivity enhancement of ^{13} C by ^{1} H in solids.

Fig. 5 illustrates the cross-polarization pulse sequence and the corresponding behaviour of the ^{1} H and ^{13} C spin magnetization during this sequence. The actual cross polarization experiment consists of a three step process:

(1) a 90°_{x} pulse is applied to the ^{1}H-spin system to flip the proton magnetization from the d.c. field direction (z-axis) to a transverse direction (y-axis) in the rotating frame; (2) immediately following a 90°_{x} pulse to the protons, the r.f. field is not switched off, but is phase shifted by 90° with respect to the 90°_{x} pulse to be along the y-axis to spin-lock the magnetization[18]. During application of the transverse locking field, the proton magnetization along this field decays with time constant $T_{1\rho}$, or spin-lattice relaxation in the rotating frame. Once the proton magnetization is spin locked along y-axis, a suitable ^{13} C radio-frequency field in the ^{13} C

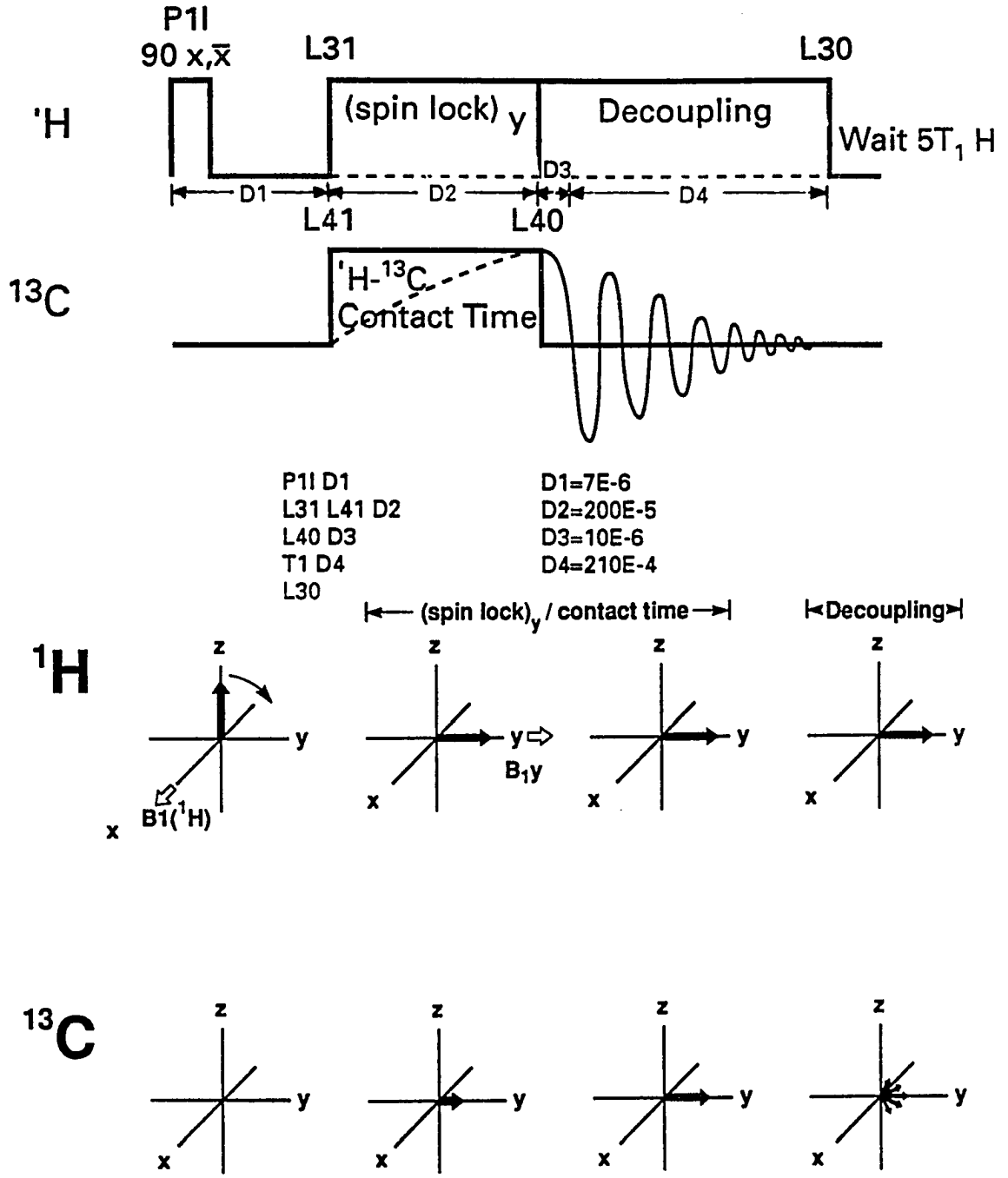

Fig. 5. The cross-polarization pulse sequence and the corresponding behaviour of the ^{1}H and ^{13}C spin magnetization during this sequence

channel is switched on, and the amplitude of the magnetic field B_1 (^{13}C) adjusted so that the Hartmann - Hahn matching condition, Eqn. (8), is fulfilled. This condition which is maintained for about 1-10 msec is known as the cross-polarization or contact time. More carbon atoms in relatively mobile systems generally take longer to cross polarize because molecular motion attenuates the ^{13}C - ^{1}H and the ^{1}H - ^{1}H dipolar interactions. Thus a longer cross-polarization time is required. Based on the theoretical model of Demco[19], carbon atoms should polarize according to the following relative rates: CH_3(static) > CH_2 > CH > CH_3(rotating) > C(nonprotonated). (3) after the cross polarization time, the ^{13}C radiofrequency field is removed, and the ^{1}H transmitter is left on to provide heteronuclear dipolar decoupling between the carbon and the neighboring protons while monitoring the response of the ^{13}C spin system. It suffices to say that maintenance of a $1x10^{-3}$ T (45 kHz) proton r.f. field is sufficient to decouple the ^{13}C - ^{1}H dipolar interaction, which is of order of 30 kHz. The ^{13}C-^{13}C homonuclear dipolar interactions are already small because the carbon-13 nuclei are dilute (natural abundance 1.1 %).

The full Hamiltonian of a system of two spin 1/2 species, e.g., ^{1}H and ^{13}C has the form,

$$H = H_{Z_I} + H_{CS_I} + H_{Z_S} + H_{CS_S} + H_{D_{II}} + H_{D_{IS}} + H_{D_{SS}} + H_{rf} \qquad (9)$$

where I stands for an abundant spin system (i.e. ^{1}H), S is a rare spin system (i.e. ^{13}C), H_{Z_I} and H_{Z_S} are the Zeeman interactions of I and S spins

with the external field, cs is chemical shift, H_D is the full dipolar interaction and H_{rf} is the Hamiltonian for the rf excitation. Because of the low natural abundance of carbon ^{13} C (1.1 %), the homonuclear ^{13} C- ^{13} C coupling (H_D) is negligible. The heteronuclear interaction for a ^{13} C- ^{1} H pair, on the other hand, has a magnitude of 30 kHz which dominates the ^{13} C spectrum. The ^{13} C - ^{1} H dipole - dipole couplings must be removed by incorporating irradiational techniques.

The orientational dependence of the chemical shift is given by

$$\omega = \omega_o [1-\tilde{\sigma} - 1/2\ \delta ((\ 3\ \cos^2\theta - 1) + \eta\ \sin^2\theta\ \cos 2\phi)] \qquad (10)$$

where $\tilde{\sigma}$, δ and η are termed the isotropic chemical shift, shielding anisotropy and asymmetry parameters, respectively.

The secular Hamiltonians for the homonuclear and the heteronuclear interactions are given by

$$H_{II} = 1/4\ (\gamma_I^2\ \hbar^2 / r^3)\ [1 - 3\ \cos^2\theta]\ [\ 3\ I_{z_1}\ I_{z_2} - I_1.I_2] \qquad (11)$$

$$H_{IS} = (\gamma_I\gamma_S\ \hbar^2/ r^3)\ (1 - 3\ \cos^2\theta)\ I_z\ S_z \qquad (12)$$

where γ_I and γ_S are the nuclear gyromagnetic ratios of ^{1} H and ^{13} C, respectively. $\hbar$ is Planck's constant divided by 2 π, r, the distance between the two nuclei, θ, the angle between the internuclear axis and the external magnetic field, and I_Z and S_Z are the Z component of the angular

momentum operators for the spin ensemble I (i.e. ^{1} H) and S (i.e. ^{13} C), respectively.

In solution, rapid isotropic motion averages dipolar splitting and chemical shift anisotropy (CSA) to zero, allowing us to observe sharp lines at the isotropic chemical shift. In solids, strong continuous wave radio frequency irradiation of the ^{1} H at the proton frequency will decouple the ^{1} H - ^{13} C dipolar interaction. In this case, the Z component of the I magnetization (i.e. ^{1} H) is periodically inverted such that the S spins (i.e. ^{13} C) spend half their time in the normal field from I and half in the inverted field. Thus the average Hamiltonian for such a sequence is zero and the effects of the I spins are removed. Then sample spinning at the " magic angle", $\theta = 54°44'$, to the external magnetic field[20] will average the shielding anisotropy to zero and thus makes possible important improvements in resolution. Magic-angle spinning was originally proposed independently by Andrew and by Lowe[21]. The combined cross-polarization / dipolar decoupling sequence may be applied to a sample that is spinning at the magic angle to give what is commonly called a CPMAS experiment yielding high resolution NMR spectra of rare spins (^{13} C) in the presence of abundant spins (^{1} H). The typical lineshapes of NMR absorptions are shown in Fig. 6. In experiments where the chemical shift anisotropy (CSA) linewidth is larger than the spinning frequency, one observes a set of sharp lines (also known as sidebands) spaced at the rotation frequency and centered on the isotropic (averaged) chemical shift. In this case, the spinning sidebands make it difficult to interpret the spectra, forcing one to rely on the

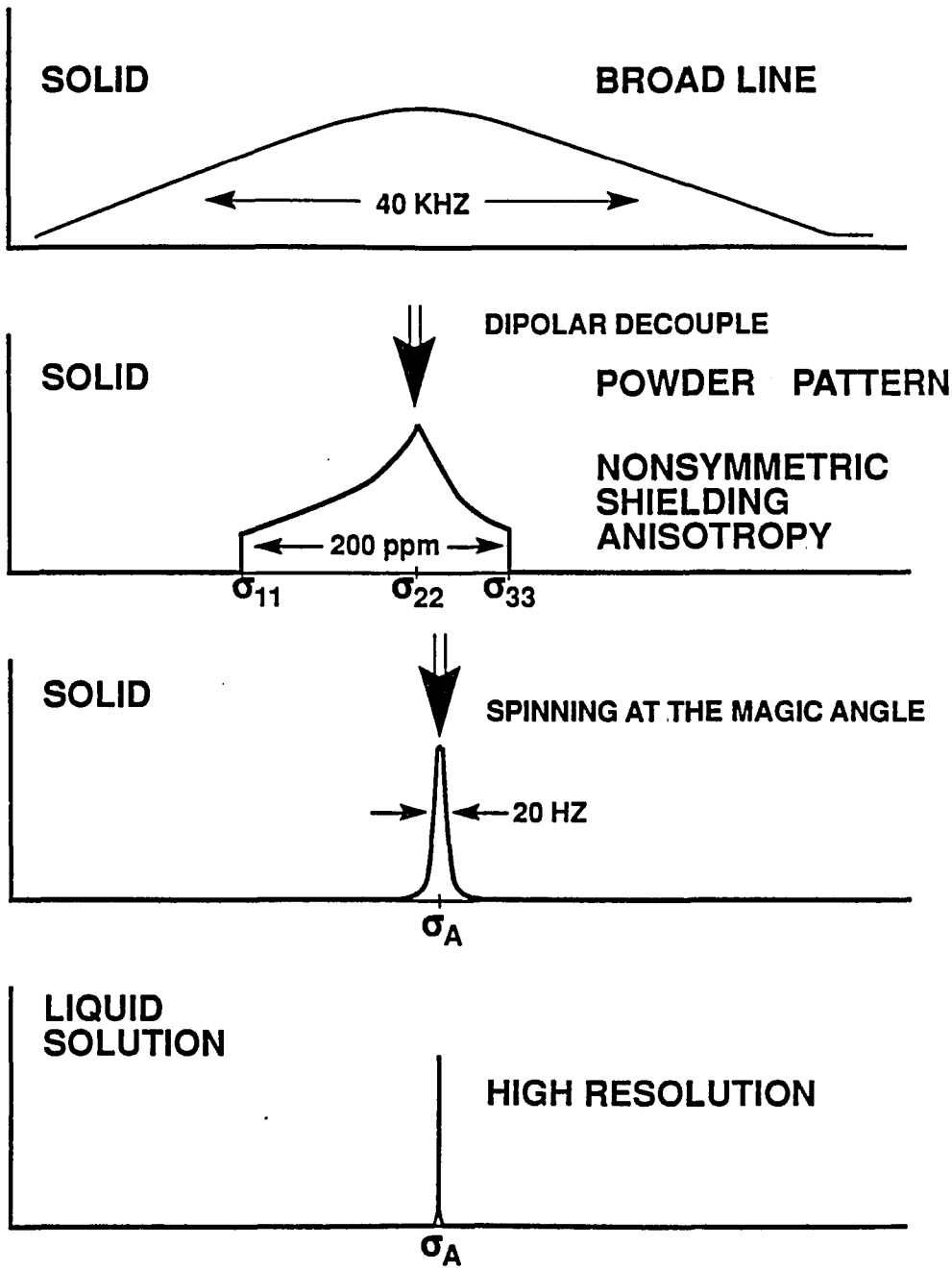

Fig. 6. Typical lineshapes of NMR absorptions

chemical shifts for assignments. A method has been reported for minimizing sideband intensities[22]. In the limit of very rapid rotation, the peaks are effectively removed from the observed frequency range and only the isotropic peak remains.

Thus, CPMAS uses high-power decoupling to remove the dipolar broadening of carbon spectra, magic angle spinning to remove chemical shift anisotropy, and proton-carbon cross-polarization to enhance the ^{13}C signals.

Cross-polarization experiments may be difficult to set up because we must optimize several variables in order for the experiments to work well. The probe must be tuned to ensure efficient transfer of power, the angle of spinning must be well adjusted and the proton 90° pulse must be checked. An adamantane sample will give very narrow lines and a good signal-to-noise ratio, and is a good test sample for optimizing the Hartmann-Hahn match. Mismatches in the field strengths in regard to the Hartmann - Hahn condition causes the actual cross - polarization process from the ideal case[19]. The cross - polarization process cannot tolerate mismatches much greater than about 10 %. Once the tuning is complete, the Hartmann-Hahn match can be made by adjusting the output power of the ^{13}C transmitter while monitoring the ^{13}C FID. The center of symmetry of the observed pattern is assumed to best present the exact Hartmann-Hahn match.

A schematic representation of the homebuilt spectrometer used in our research group, which is capable of performing cross polarization-double resonance experiments for obtaining high resolution NMR spectra of dilute

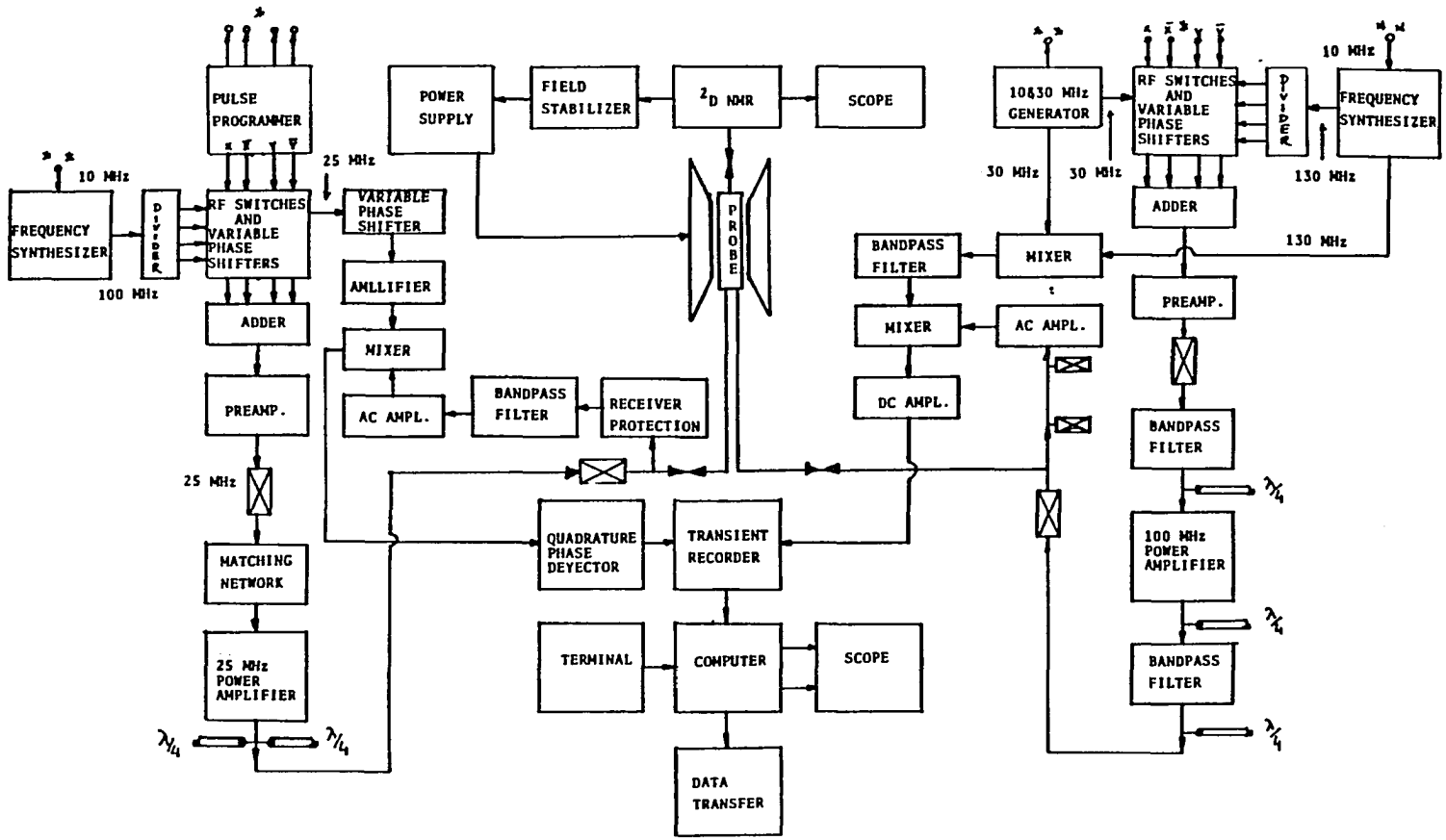

Fig. 7. A schematic diagram of a double - resonance NMR spectrometer

spins is shown in Figure. 7. This particular home-built spectrometer operates at 100.06 MHz and 25.16 MHz for ^{1}H and ^{13}C, respectively. The reference frequency source is a stable rf oscillator or frequency synthesizer which supplies the rf gating unit with a source of continous wave sinusoidal signal at angular frequency ω in the megahertz range. This signal is divided into a signal that is fed in pulse mode by means of a gating switch controlled by a pulse programmer, and a reference signal. A 10-MHz reference clock establishes a phase coherency between the pulses from the pulse programmer and the rf pulses from the rf gating unit. The rf gating unit has four channels, X,Y,$\overline{X}$,$\overline{Y}$, successively differing in phase by 90°. For example, if X is the reference phase then Y is 90°, - X is 180°, and - Y is 270° out of phase. The gating of all rf pulses, levels, triggers, looping and microprogram sequencing is controlled by a microprocessor based pulse programmer which is the heart of a pulse spectrometer. The 'pulse programmer' is in fact a small high-speed computer that is loaded with the instructions by the main computer but takes over control of the spectrometer when instructed to do so. The output of the rf unit goes through a band pass filter before the signal reaches the transmitter. Since we need to irradiate two different kinds of nuclei, we need two frequency synthesizers as well as two transmitters or power amplifiers. The transmitters must be very stable not only in frequency but in amplitude in order to maintain the Hartmann-Hahn condition. In order to satisfy the Hartmann-Hahn condition, the ^{13}C B_1 field must be higher by a factor of four (γ_H / γ_C). This requires a high-power transmitter. The ^{13}C transmitter is a high power Varian pulse amplifier

Model V4420, and the ^{1}H transmitter is Amplifier Research Model 150 LA which gives linear amplification of signals in the frequency range of 1 to 150 MHz with pulses of 150 Watts. In our experiments, a proton B_1 field of 50 KHz coresponding to a 90° pulse of 5.0 μsec length is used for cross-polarization and decoupling. This field is sufficient to decouple the ^{13}C-^{1}H dipolar interaction (order of 30 KHz). The series crossed diodes at the output of the transmitter reduce transmitter noise during signal reception. The signal, following suitable filtering and amplification, enters a double-resonance probe. The probe is mounted inside a high-resolution Varian XL-100 15-inch electromagnet which has some original or modified Varian accessories (magnet power supply, field stabilizer and lock, and shimming system) and provides the permanent magnetic field B_o of 2.348 T, necessary for the separation of the nuclear spin energy. The probe is single coil and double-tuned at 100.06 MHz and 25.16 MHz for ^{1}H and ^{13}C, respectively. The spinning assembly is a modified version of the Shoemaker - Apple design[23]. with macor and torlon used as stator and rotor materials, respectively. With this design, magic angle spinning of sealed samples at rates exceeding 5 KHz (with an air drive) is achieved. A Magic angle spinning rate of 5 KHz is sufficient to avoid sideband problems of ^{13}C at the resonance frequency of 25 MHz. The response of the sample to the pulse is fed to a high-gain amplifier (a receiver). Using quarter-wavelength cables and sets of cross diodes to ground reduces the high voltage transmitter pulse to a few volts at the input of the amplifier thus preventing amplifier failure from overload during the rf pulse. The receiving system consists of an AC or

video preamplifier with a linear amplification over the range of 0.1 μV to several mV, a device known as a 'mixer' or a demodulator and a DC or audio amplifier which behaves both as an amplifier and as a low pass filter with the characteristic of not passing signals of frequency higher than 1 MHz. A Nicolet 2090-III-A transient recorder with a minimum sampling time of 500 nsec is used to accumulate all data. The Nicolet is interfaced with a computer for signal averaging and data manipulation.

CHAPTER II. ^{13}C SOLID-STATE NMR OF ETHYLENE OXIDATION OVER SUPPORTED SILVER CATALYSTS

Introduction

The selective oxidation of ethylene to ethylene oxide (EO) is an important industrial catalytic reaction. The subject has been extensively reviewed[24-28]. The industrial reaction is usually carried out at 473 - 573 K, with a catalyst consisting of silver dispersed on α-alumina.

High-resolution nuclear magnetic resonance (NMR) spectroscopy is emerging as a powerful technique for the study of real catalyst systems. Duncan and Dybowski[29], Slichter[30] and Wang et al.[31] have reviewed much of the previous work and advances that have made NMR a valuable method for studying species adsorbed on metal surfaces. An understanding of the chemistry taking place on the catalyst surface, through the detection and identification of the reaction intermediates, could lead to the development of modified catalysts with higher selectivity toward the production of ethylene oxide.

Only a limited amount of work has been reported concerning the direct observation of surface structures which might relate to the progress of the oxidation reaction. For example, in a recent solid-state NMR study, Plischke et al.[32] have identified a variety of surface species formed after ethylene was adsorbed on an oxygen-covered $Ag/\eta\text{-}Al_2O_3$ catalyst. Ethylene oxide was not clearly detected by these authors. Force and Bell have studied the

infrared spectra of the species adsorbed over a Ag/SiO_2 catalyst during the oxidation of ethylene[33] and, based on the surface structures identified by infrared spectroscopy, postulated a mechanism for the epoxidation and combustion reactions[34].

Chin and Ellis[35] used ^{13}C to investigate dynamics, structures and reaction of acetylene and ethylene over $Ag/\gamma\text{-}Al_2O_3$. These authors identified a π-complexed ethylene species which was stable to air at room temperature. Furthermore, in the presence of pure oxygen or air, they assigned an isotropic peak resonating at 61 ppm to ethylene oxide. Pruski and co-workers[36] have reported solid-state ^{13}C NMR in ethylene adsorbed on Ru/SiO_2. The application of transient techniques including cross-polarization with magic angle spinning (CP/MAS)[37], CP/MAS with dipolar dephasing[38] and single-pulse experiments allowed these authors to observe the decomposition of ethylene at room temperature to form strongly adsorbed acetylide and alkyl groups followed by subsequent recombination of adsorbed alkyl species and hydrogenation of ethylene to form weakly adsorbed ethane, butane and butene.

In the present study, we have used solid-state NMR to study the reaction of ethylene with oxygen over silica-supported silver catalysts. None of the catalysts in this work have been deliberately moderated by adding chlorinated hydrocarbons, as is done commercially in industrial processes to improve catalyst selectivity for ethylene oxide. A variety of experimental nuclear spin dynamics including standard cross-polarization with magic angle spinning (CP/MAS), CP/MAS with dipolar dephasing and direct ^{13}C

excitation (Bloch decay) have been applied to identify the surface species formed on the surface of a Ag/SiO_2 catalyst at various temperatures. No ethylene oxide could be unambiguously detected. However, under the experimental conditions employed in this study, we were able to identify ethylene, acetic acid, ethane and an alkoxy species at the temperature range 298 - 613 K.

Furthermore, we have studied the interaction of C_2H_4, CO_2, C_2H_4O, i.e., the reactant, and products of the reaction, with Ag/SiO_2 as well as the pure SiO_2 support. This study provided insight into the adsorption characteristics of these species. In particular, it is found that under conditions of epoxidation, ethylene oxide reacts with both metal and silica support and thus could not be observed as the reaction product. Under the experimental conditions employed in this study, we have been able to observe ethylene oxide after the saturation of silica surface with unlabeled ethylene oxide prior to ethylene oxidation. In addition, it was determined that under identical conditions the silica support does not possess any activity toward formation of ethylene oxide.

Literature Review

Ethylene oxide which is used for the manufacture of ethylene glycol (used in antifreeze (40 %) in the cooling system of motor vehicles), detergents, synthetic fibers and polymers (such as polyethylene teraphtalate)[39] has been first prepared by Wurtz[40] by reacting potassium

hydroxide, chlorohydrin and ethylene. In 1863, he reported the lack of success in preparing ethylene oxide via direct oxidation. In 1931, Lefort[41] succeeded in preparing ethylene oxide from oxygen and ethylene over a silver catalyst. Today, the standard industrial process to produce ethylene oxide (also known as ethylene epoxide) involves the vapor-phase partial oxidation of ethylene with oxygen or air in a tubular reactor.

The unique aspects of this partial oxidation are the following[42-44].

1) Only ethylene can be epoxidized with high yields compared to higher olefins. It is not fully understood why epoxidation is only efficient for ethylene while higher olefins combust mostly to CO_2 and H_2O. A possible explanation is that hydrocarbons such as butylene or propylene are probably adsorbed in the form of a π-bonded allyl that is readily oxidized to carbon dioxide and water.

2) Silver has a unique role in the epoxidation of ethylene to synthesize ethylene oxide (EO) with high selectivity and the minimum formation of carbon dioxide and water. It is not well understood why silver is so exceptional. Metals other than silver generally produce CO_2 and H_2O, the thermodynamically preferred products. Consequently, no other metal is at all comparable to silver in selectivity. The fact that silver is unique among metals in its ability to promote the epoxidation reaction with significantly high selectivities is a very interesting aspect of this catalytic system, and has thus been the subject of numerous studies.

3) Chlorine, calcium, potassium and cesium are among the known promoters of the reaction. In the industrial epoxidation process, trace

quantities (ppm) of chlorine (usually in the form of 1,2-dichloroethane), cesium (in the form of aqueous solution of CsOH, $CsNO_3$, or Cs_2CO_3), and other promoters are added in order to increase the activity and selectivity of the catalyst. It is known that alkali metals and chlorine inhibit total combustion of the olefin to CO_2 and H_2O which is a competitive process.

The hypothesis is that the predominant effect of chlorine is on the "primary chemistry" (i.e., C_2H_4 -> C_2H_4O and C_2H_4 -> $CO_2 + H_2O$) whereas alkali metals act principally on the "secondary chemistry" (i.e., C_2H_4O -> $CO_2 + H_2O$) by inhibiting isomerization of ethylene oxide. It is known that adsorbed chlorine enhances ethylene adsorption on Ag. This effect is attributed to a strongly increased heat of adsorption. Chlorine acts to create Ag^+ sites on the surface by electron withdrawal, and that these electron - deficient Ag atoms more favorably accept π - electron donation by the ethylene molecule. Chlorine seems to inhibit the dissociative adsorption of oxygen leading to carbon dioxide. Enhancement in selectivity results since chlorine inhibits CO_2 production more strongly than ethylene oxide production. Atomically adsorbed chlorine on Ag (110) gives the same qualitative effects as known for chlorinated feed additives on high surface area supported Ag catalysts, i.e., the selectivity is improved at the cost of loss in activity. This result is in accord with the idea that chlorine promoters actually function as chlorine adatoms bonded directly to the Ag surface, and that a support material (Al_2O_3, SiO_2) is unnecessary in achieving the promoter effect.

As was pointed out earlier, alkali metals inhibit isomerization of ethylene oxide. Low or zero apparent selectivities observed with many catalysts could be caused by further reaction of ethylene oxide on sites supplied by the support material. Isomerization of ethylene oxide is known to take place on acidic sites of metal oxides. To investigate ethylene oxide isomerization/oxidation, surface acidity of the support materials (e.g., SiO_2, Al_2O_3) can be modified by impregnation with alkali metals. For example, it is known that Cs enhances selectivity toward ethylene oxide. It is thus argued that Cs acts to block acidic sites on the surface of the support, by ion exchange of Cs^+ with H^+ thereby reducing the concentrations of silanol protons, and inhibiting isomerization, and further oxidation of ethylene oxide.

The process for the production of ethylene oxide was first developed and utilized by Union Carbide in 1937. UCC has rarely licensed their process to others. Ethylene oxide is a highly reactive, toxic, inflammable and in certain circumstances even autoexplosive carcinogen. It therefore requires a rather sophisticated approach in manufacturing and handling. The modern catalyzed direct oxidation technology which uses air and pure oxygen accounts for essentially all ethylene oxide produced industrially. In the oxygen case, ethylene and oxygen gas enter a multitublar reactor where the reaction to ethylene oxide and by-products takes place at an optimum reaction temperature 503 K. In the air case the optimum reaction temperature is about 533 - 553 K. Above 573 K, complete combustion occurs. The most common catalyst is silver (8 to 12 wt %) supported on α-Al_2O_3, of

1 m^2 /g -specific surface area, promoted up to 0.35 % concentration of lithium, sodium, as well as 0.025 % cesium. Ethylene concentrations are usually between 20-30 % vol (in the air case around 5 %) and oxygen concentrations are 5-10 %.

Because of its industrial as well as fundamental scientific importance, the catalytic oxidation of ethylene to ethylene oxide has received great attention and been the subject of intense research activity. Related studies of this important and complex catalytic system involve: (1) the application of modern surface science techniques to well defined surfaces (e.g., Ag (110) and Ag (111)) under ultrahigh vacuum (UHV) conditions[45-47], (2) reactor studies performed under relatively high pressures[48-50], (3) experiments concerned with characterization of silver crystallites supported on oxides such as Al_2O_3, TiO_2 and SiO_2[51-53], and (4) more recently nuclear magnetic resonance (NMR) spectroscopy[32,35]. During the past 20 years, much experimental research has been devoted to getting a better understanding of the epoxidation reaction, with the ultimate goal to be able to increase the selectivity (moles of ethylene oxide / moles of ethylene converted) for epoxide formation. The epoxidation of ethylene to ethylene oxide has consequently created a challenging problem to fundamental research in catalysis.

The kinetics of ethylene oxidation over silver catalysts have been studied by many investigators. Fig. 8 presents the most widely accepted kinetic pattern which is consistent with a triangular scheme of first-order reactions. The selective oxidation of ethylene to ethylene oxide over a silver catalyst is midly exothermic (-146 kJ/mol), utilizing only 1/2 mole of oxygen

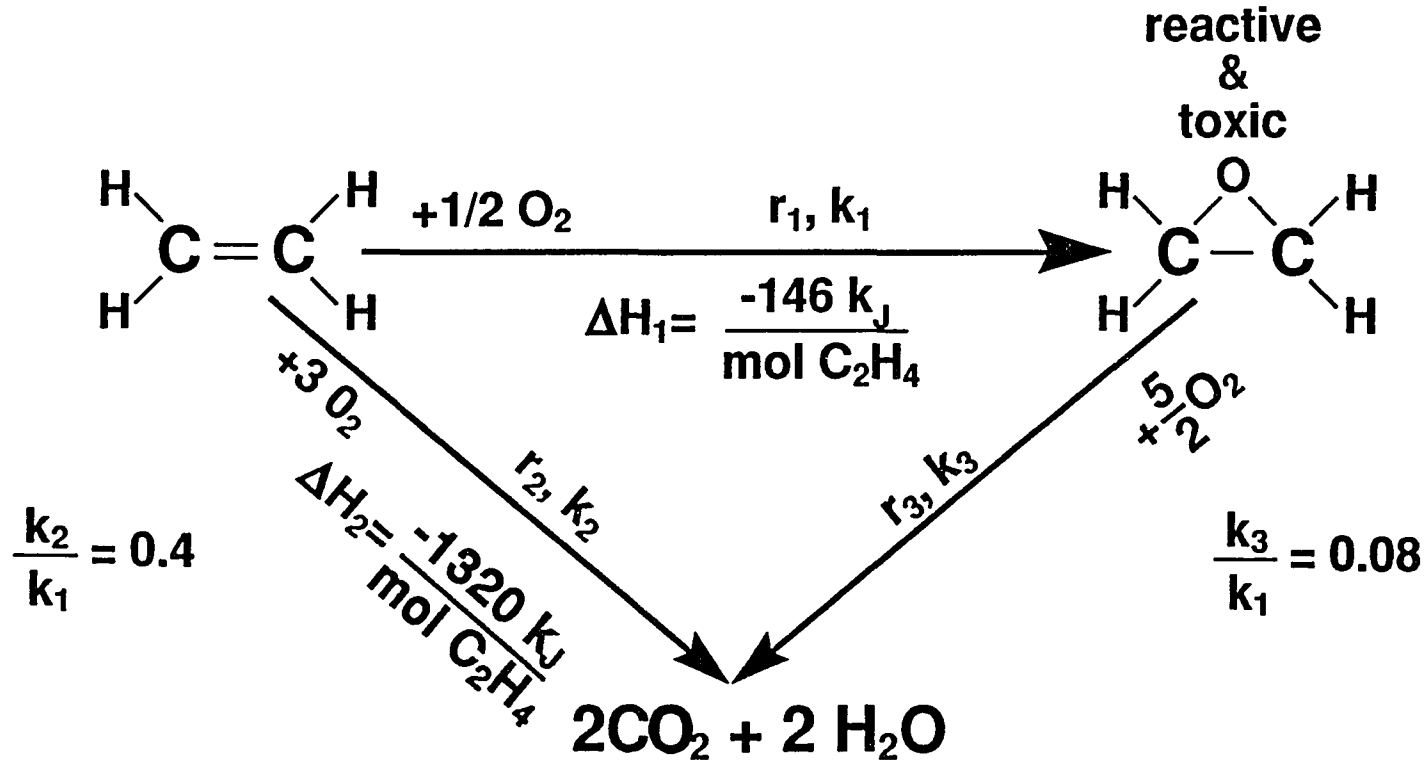

Fig. 8. A triangular kinetic scheme of ethylene oxidation

per mole of ethylene reacted to ethylene oxide. The production of CO_2 releases 9 times as much heat as the production of ethylene oxide. Therefore the reaction conditions are critical. If they are too mild, little oxide is produced; if they are too severe, CO_2 and water are formed either by complete oxidation of ethylene or by further oxidation of the ethylene oxide. The corresponding rate expressions are

$$r_1 = k_1 P_{C2H4} P_{O2} \exp(-E_1 / RT)$$
$$r_2 = k_2 P_{C2H4} P_{O2} \exp(-E_2 / RT)$$

The ratios $k_3/k_1 = 0.08$ and $k_2/k_1 = 0.40$ have been found, indicating that under industrial conditions, most of the carbon dioxide is formed by parallel oxidation of ethylene (i.e., reaction 2) rather than consecutive oxidation of ethylene oxide (i.e., reaction 3). It is believed that the further oxidation of the product (i.e., reaction 3) plays an important role in determining the selectivity in industrial processes. Much emphasis has been placed on achieving maximum selectivity to ethylene oxide (i.e, minimum combustion). Today, ethylene is converted with a selectivity of around 80 % under commercial conditions, whereas in the early 1960s the selectivity was 68 % at a comparable conversion level. Greater selectivity toward ethylene oxide is achieved by adding trace amounts of organic chlorine. The selectivity to ethylene oxide is highly sensitive to the mode of adsorption of oxygen on silver.

Despite the fact that the epoxidation reaction is a simple example of a kinetically controlled, selective heterogenous catalytic reaction, there remains great controversy over the precise nature of the active form of oxygen (atomic versus molecular). Even though the process has been in commercial use for more than a half century, yet the fundamental question concerning the nature of the surface oxygen species responsible for the epoxidation and combustion reactions has not been conclusively resolved.

The interaction between oxygen and silver has received much attention for over 50 years. There have been two general approaches to the study of interaction of oxygen with silver surfaces. The first approach which deals with measuring coverages and heats of adsorption and desorption over a range of oxygen pressure (10^{-3} to 300 Torr) have been performed on silver powders[54-56] and crystallites supported on oxides such as Al_2O_3, TiO_2 and SiO_2[52,53,57,58]. The second approach involves the application of modern surface science techniques which mainly include the interaction of oxygen with clean and well defined single crystal surfaces under ultrahigh vacuum (UHV) conditions[59-62]. The main advantage of working on a single crystal cut along well defined crystal planes is the possibility of studying surface reactions on systems which are much more simple and homogenous than those represented by polycrystalline materials.

Experimental techniques which have been used by many authors to investigate the interaction between silver metal and oxygen include electron spin resonance[63], field emission microscopy[64], X-ray and electron diffraction investigation of surface structures[65], Auger electron

spectroscopy[59,66], infrared spectroscopy[67], ultraviolet spectroscopy[68], secondary ionic emission[69], and classical methods such as those based on adsorption and desorption kinetics and isotherms[70,71]. The results have been contradictory mainly due to the different catalyst preparation and pretreatment procedures, the adsorption conditions and surface contamination by impurities. It is generally agreed that oxygen adsorbs on silver in more than one energy state and that such states are associated with several different adsorbed species. Whether these species include O_2^-, O_2^{2-}, O^-, or O^{2-} remains a matter of debate and interpretation of experimental data.

Many surface science techniques have been used to study oxygen adsorption and desorption on silver single crystals. Among them are LEED[72-74], UPS[75,76], TPD[72,77,78], AES[72,74], XPS[74,75], HREELS[79,80]. Much of the work has been carried out on a Ag(110) surface due to its higher reactivity towards O_2 than Ag(111), though adsorption of oxygen on a Ag(111) surface has also been examined by several researchers. There is consistent evidence from single crystal studies[81,82] of Ag(110) and Ag (111) that a molecularly adsorbed oxygen species, O_2(a) exists at very low temperatures (120-150 K) which desorbs at around (190-217 K), and atomically adsorbed oxygen, O(a), at ~500 K which desorbs at around 600 K. A third state of oxygen, probably a subsurface atomic state, also appears to exist below 600 K with a strong binding energy. It appears that subsurface oxygen is required for ethylene oxide formation. Van santen and Backs[83] have performed electronic structure calculations on the chemisorption of

atomic oxygen on Ag(110) and on the subsequent reaction of this chemisorbed oxygen with ethylene. These authors have shown that the presence of subsurface oxygen reduces the bond energy between silver and adsorbed oxygen and converts the repulsion interaction between adsorbed oxygen and gas-phase ethylene into an attractive one, thus making possible the epoxidation reaction. The fact that subsurface oxygen may play an important mechanistic role in the epoxidation of ethylene is one of the most important features of the epoxidation reaction which is still poorly understood.

Considerable attention has been given to understanding the mechanism by which ethylene is oxidized to ethylene oxide over a silver catalyst. The mechanism of the epoxidation reaction is not certain and still very much a matter for debate. Currently, there is no generally accepted mechanism for the epoxidation reaction and considerable differences of interpretation still exist. In heterogenous catalytic oxidations the mechanism essentially involves interaction between a hydrocarbon and surface oxygen species. It is believed the type of adsorbed oxygen species involved in the interaction determines the course of the reaction and hence the selectivity. Consequently, the main differences in the reported mechanism and the derived kinetic equations of ethylene oxidation over silver are due to the type of chemisorbed oxygen present at the catalyst surface and the role played by ethylene chemisorption.

The first mechanism of ethylene oxidation over silver catalyst was proposed by Worbs in 1942. According to Worbs[84] it was diatomic oxygen

that reacted with ethylene to form ethylene oxide (EO), whereas oxygen atoms were responsible for the combustion reaction. This theory was later extended by Voge and Adams in 1967[85] and Kilty and Sachtler in 1974[86]. Sachtler and Kilty[86,87] observed three kinetically distinguishable oxygen adsorption on Ag/α-Al_2O_3 catalyst. The first reaction is related to dissociative adsorption of an oxygen molecule on an ensemble of four adjacent silver atoms with a low activation energy (~ 3 Kcal/mol)

$O_2 + 4\ Ag\ (adj) \rightarrow 2\ O^{2-}\ (adj) + 4\ Ag^{+}\ (adj)$

The second process was dissociative adsorption with the highest activation energy (14 Kcal/mol). This process was thought to be due to the migration of adsorbed species, of ensembles of adjacent silver atoms

$O_2 + 4\ Ag\ (nonadj) \rightarrow 2\ O^{2-}\ (ads) + 4\ Ag^{+}\ (adj)$

The third process was nondissociative with an activation energy of 7.9 Kcal/mol. This process required only one electron and occured when gas phase oxygen is adsorbed on to a single silver atom resulting a superoxide ion (O_2^-)

$O_2 + Ag \rightarrow O_2^-\ (ads) + Ag^{+}$

The first reaction was shown to be completely inhibited when 25 % of the surface was covered by chlorine. Since it is known that chlorine increases selectivity of the ethylene oxidation over silver catalysts, Kilty and Sachtler concluded that diatomic chemisorbed oxygen (O_2^-) is responsible for the selective oxidation while dissociatively adsorbed oxygen ions lead to carbon dioxide.

Ethylene selectively reacts with the diatomic oxygen species

$C_2H_4 + O_2$ (ads) -> C_2H_4O + O (ads)

The oxygen atoms produced react with ethylene, resulting in combustion products

O (ads) + C_2H_4 -> OC_2H_4 (ads)

OC_2H_4 (ads) + 5 O (ads) -> 2 CO_2 + 2 H_2O

The overall reaction is

7 C_2H_4 + 6 O_2 -> 6 C_2H_4O + 2 CO_2 + 2 H_2O

The maximum selectivity achievable according to this mechanism is 6/7 or 85.7 % assuming that there is no oxidation of ethylene oxide in a consecutive reaction. In practice, ethylene oxide is oxidized in a consecutive reaction to undesired products causing a decrease in selectivity below 80 %.

According to their data, Kilty and Sachtler[86,87] proposed that the oxidation of ethylene over silver catalyst proceeds via a Rideal rather than a Langmuir - Hinshelwood mechanism

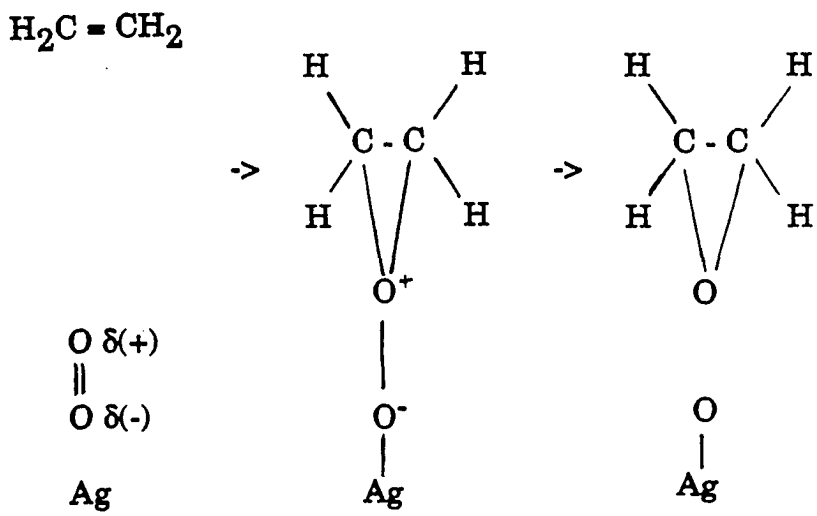

The adsorbed oxygen molecule is polarized to satisfy the nucleophilic properties of the incoming ethylene molecule. Ethylene is strongly adsorbed on to a diatomic oxygen ion (O_2^-) to form a complex. This complex splits at the O-O bond to form ethylene oxide and leave an adsorbed oxygen atom.

Some authors[33,34] on the other hand proposed that chemisorbed atomic oxygen leads to both epoxidation and complete oxidation. Recent studies however, suggest that chemisorbed atomic oxygen reacts with adsorbed ethylene to yield both ethylene oxide and byproducts, provided that subsurface oxygen is present[47,88,89].

Experimental

A detailed description of how the catalysts have been prepared, characterized and preatreated prior to the NMR experiments, and the experimental techniques and equipment employed to investigate ethylene oxidation over supported silver catalysts by NMR is provided in the following sections.

Catalyst Preparation

The 10 and 20 % (by weight) Ag/SiO_2 catalysts were prepared by an ion-exchange technique. This technique makes the most efficient use of a catalytic metal (particularly for a costly noble metal such as silver) by providing a more highly dispersed Ag/SiO_2 catalyst compared with the incipient wetness

technique. The key step consists of fixing metal cations through exchange reactions with ions in the surface of the silica support; subsequent reduction in hydrogen produces the supported free metal. The "ion-exchanged" silver - silica catalyst was prepared by adding ammonium hydroxide (NH_4OH) solution to an appropriate weight of Ag_2O (Fisher Scientific, 99.99 %) slowly under the hood with constant stirring until Ag_2O was completely dissolved (2.2 ml NH_4OH / g SiO_2). A silver - amine complex ($Ag(NH_3)_2^+$) was prepared from silver oxide and ammonium hydroxide. The pH of the mixture was adjusted to 9 with ammonium hydroxide. It is important to note that a mixture of ammonium hydroxide and Ag_2O can be explosive, therefore some precautions are necessary while preparing the catalysts. A dried Cab-O-Sil HS5 (300 m^2/g BET surface area) amorphous fumed silica support was slowly added to the solution and vigorously stirred throughout to obtain uniform dispersion until a slurry was formed. A pure silica sample was also prepared by adding ammonium hydroxide (2.2 ml NH_4OH / g SiO_2) to an appropriate weight of silica support. The slurry and pure silica obtained were then dried for 24 hr at room temperature and 4 hr in air at 383 K. The samples were then ground into fine powder in an agate mortar and stored in a desicator.

Catalyst Characterization

Selective gas phase chemisorption is a standard technique for determining surface area, and dispersion (fraction exposed) and thus the crystallite size for many metal catalysts dispersed on a support. The technique requires that the

adsorbate form a chemisorbed monolayer and that a simple relationship exists between the number of molecules sorbed and the number of surface atoms. Oxygen chemisorption is the most commonly used method for measuring the metal surface area of a supported silver catalyst because oxygen is one of the few gases that chemisorbs on reduced silver to the extent that monolayer coverages can be attained[54,55,90]. Other simple diatomic gases such as H_2 and CO which are routinely used for measuring the surface area of group VIII metals do not adsorb significantly on reduced Ag surfaces to provide complete, well-defined monolayer coverages. However, one of the problems with the adsorption of oxygen on silver is a slow, continous uptake of oxygen following a rapid initial uptake, which is the result of 'subsurface' or 'bulk' oxygen formation which has complicated measurement of the actual silver surface area[91-93]. This is particularly severe with larger Ag crystalites. The mechanisms of formation and the exact nature of this form of oxygen is not known although it has been proposed that subsurface oxygen plays a significant role in the selectivity toward ethylene oxide[94].

The pretreatment procedure for determining the surface area of supported silver catalyst was as follows. The catalyst sample (~ 1.10 g) was first heated to 403 K in He (~ 1 atm) for 30 min followed by evacuation for 10 min to remove excess moisture. The temperature setpoint of the heater was gradually raised until it reached the final reduction temperature. The catalyst was then reduced at 613 K for 4 hr under static hydrogen pressure of 760 Torr. At temperatures in the region of (570 - 770 K) the reduction of the metal oxide to the metal is thermodynamically favored for all group VIII elements plus Ag.

To insure complete reduction of the catalyst sample, The static reduction was repeated every 30 min with fresh dosage of hydrogen. The catalyst sample was then cooled to 473 K and the system was evacuated overnight to 3.5 X 10^{-6} Torr. The catalyst sample was then further cooled to 443 K. Oxygen adsorption experiments were performed over a typical range of 30 to 200 Torr. The isotherms were measured at 443 K, which is an optimum temperature for oxygen adsorption over silver based on previous studies[95-97]. For the total O_2 isotherm, the sample was allowed to equilibrate up to 2 hr before the first pressure measurement . Subsequent pressure measurements were taken after 30 min intervals. The system was then evacuted for 2 hr to 1 X 10^{-5} Torr. For the O_2 reversible isotherm, the pressure measurements were taken after 30 min. Adsorption isotherms for 10 % Ag / SiO_2 are shown in Fig. 9. The adsorption isotherms were a linear function of the equilibration pressures. Correction for physical (reversible) adsorption on the catalyst surface and support were made by extrapolating the linear portion of the isotherms to zero pressure by a least squares linear regression. From the adsorption stoichiometry, the metal dispersion (fraction of atoms exposed at the surface) can be determined. The dispersion was calculated by dividing the number of irreversibly chemisorbed O atoms ($O_{2,irrev} = O_{2,tot} - O_{2,rev}$) by the number of Ag atoms. An adsorption stoichiometry of O_a / Ag_s = 1, where Ag_s is a surface atom was used to calculate the dispersion[96,97,98]. Corresponding silver dispersions ($O_{2,irrev}$ / Ag_{atoms}) of 10 % and 20 % Ag/SiO_2 catalysts in this study were calculated to be 11.0 % and 6.0 %, respectively.

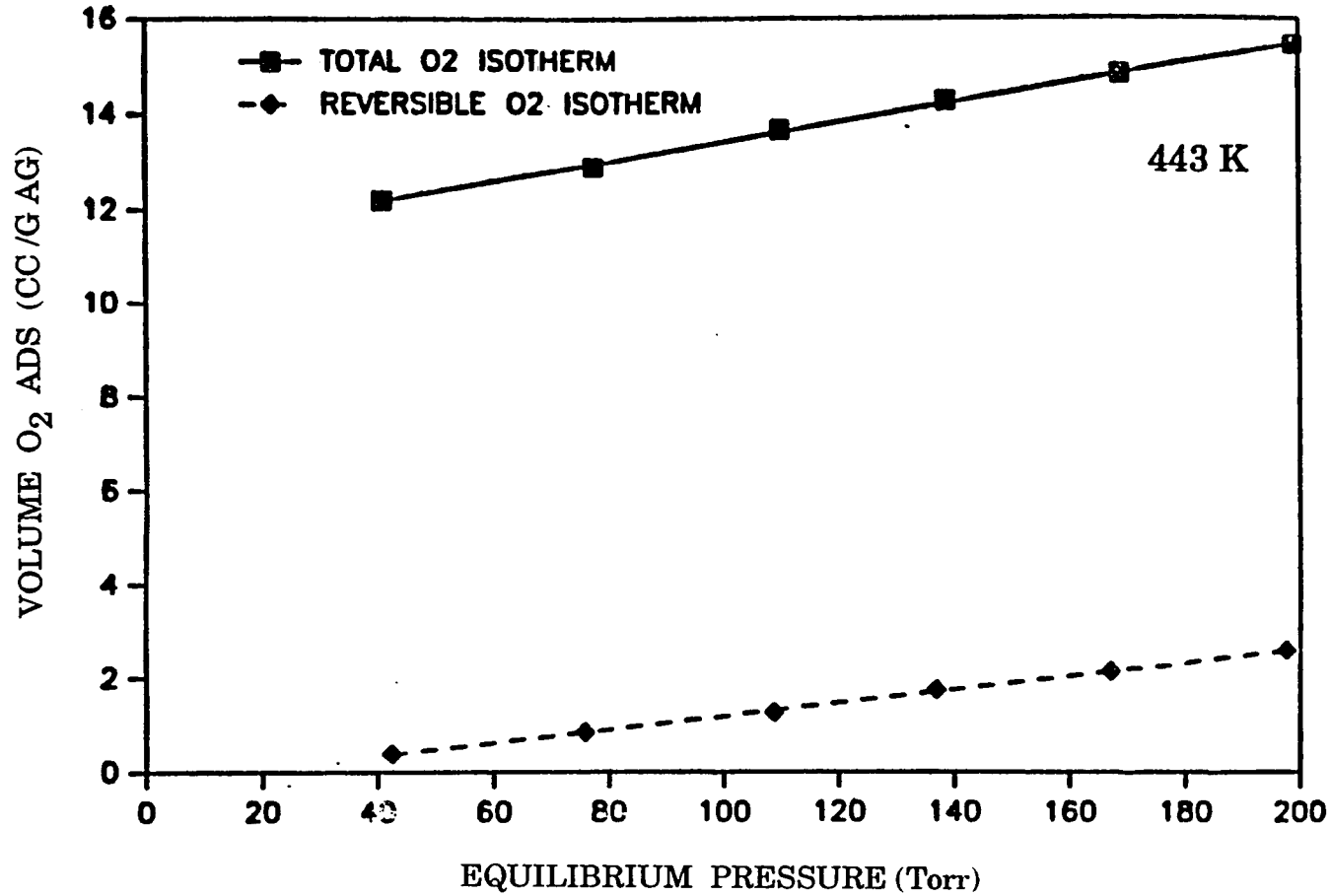

Fig. 9. Oxygen adsorption isotherms at 443 K for 10 % Ag/SiO_2 ■,$(O_2)_{tot}$, ◆ ,$(O_2)_{rev}$

Adsorption Apparatus

A multiport high-vacuum Pyrex glass apparatus was used for sample preparation prior to the NMR experiments as well as chemisorption measurements. A detailed description of this apparatus is given in chapter III of this dissertation.

NMR Sample Preparation

Approximately 130 mg of sample was loaded into the 5 mm-OD Norell XR-55 NMR sample tube with a sample depth of about 2 cm, which was then attached to one of the sample ports of the high vacuum glass manifold. A mini - heater was then carefully fitted to the NMR sample tube. The details of the NMR sample pretreatment procedures are given below.

Preatreatment (A): The 10 % Ag/SiO_2 catalyst was dried, reduced and evacuated in a manner similar to the oxygen chemisorption measurements described previously. Nitrous oxide was allowed to adsorbed for 2 hr at 443 K under atmospheric pressure followed by evacuation for 10 min. The sample tube was then immersed in liquid nitrogen and the sample dosed with ethylene (double ^{13}C labeled). Approximately 3 Torr of ethylene was condensed into the sample tube at the liquid nitrogen temperature which resulted in an exposure of $\Theta = 4$ (i.e., $\Theta = C_2H_4$ molecules / Ag surface atoms). After adsorption has ceased the sample was sealed off with a micro - torch

keeping the sample at 78 K to prevent any possible thermal damage during sealing.

Preatreatment (B): The pure silica support was dried at 403 K for 4 hr under vacuum. The 20 % Ag/SiO_2 catalyst was dried, reduced and evacuated overnight as before. Only labeled C_2H_4, CO_2 or C_2H_4O were used. The adsorptions were carried out individually at room temperature under 10 Torr pressure for 30 min. The samples were then sealed at liquid nitrogen temperature without evacuation.

Preatreatment (C): The pure silica support was dried at 403 K for 4 hr under vacuum. The 20 % Ag/SiO_2 catalyst was dried, reduced and evacuated overnight as stated before. The saturation experiments were carried out on Ag/SiO_2 as well as pure SiO_2 by dosing them individually with 10 Torr of unlabeled C_2H_4O for 2 hr followed by dosing with 10 Torr of labeled C_2H_4O for 30 min at 298 or 523 K. The samples were evacuated for 10 min after each unlabeled C_2H_4O saturation run. Samples were finally sealed off at liquid nitrogen temperature.

Preatreatment (D): Under identical conditions, the reduced Ag/SiO_2 as well as dried pure SiO_2 samples were saturated with only unlabeled C_2H_4O according to the procedure given in preatreatment (C). They were then dosed individually with oxygen at 443 K for 2 hr under atmospheric pressure followed by 10 min evacuation. Subsequently, double-labeled C_2H_4 adsorptions were carried out individually on each sample with an exposure of $\Theta = 1$ at liquid nitrogen temperature without further evacuation followed by sealing the samples.

NMR Experimental Techniques and Equipment

Transient techniques in NMR employed to identify adsorbed surface species on the Ag catalyst as well as pure SiO_2 include CP/MAS[37], CP/MAS with dipolar dephasing[38] and ^{13}C excitation (Bloch decay). All high-resolution ^{13}C NMR spectra were obtained on an in-house constructed spectrometer operating at 100.06 MHz for ^{1}H and 25.16 MHz for ^{13}C. Magic angle spinning of sealed samples in 5 mm NMR tubes was performed at rates exceeding 5 KHz (with air drive) in a double-tuned, single coil probe with macor and torlon used as stator and rotor material, respectively[99]. The spinning rate of 5 KHz is sufficient to avoid side band problems of ^{13}C at the resonance frequency of 25 MHz. In this work, a proton B_1 field of 50 KHz corresponding to a 90° pulse of 5.0 μsec length was used for cross-polarization and decoupling. This field was sufficient to decouple the ^{13}C - ^{1}H dipolar interaction (order of 30 KHz). The data were obtained with proton spin temperature inversion[100] which attenuates base line distortion associated with receiver recovery and pulse breakthrough. ^{13}C chemical shifts are conventionally measured relative to the ^{13}C resonance of tetramethylsilane [$(CH_3)_4Si$], abbreviated TMS. Typical ^{13}C shifts of diamagnetic molecules cover a total range of some 250 ppm. All

resonance line positions in this study were determined in the range of 400 to -300 ppm with respect to TMS in the scale with positive numbers being downfield (deshielded). In all the CP/MAS measurements, a recycle time of 1 sec between scans, dwell time of 10 μsec, optimum cross-polarization contact time of 2 msec, an acquisition time of 200 msec and dipolar dephasing time of 50 μsec were used. The data were acquired by using 2 K quadrature detection and Fourier transformed after zero filling to 8 K. In order to achieve a satisfactory signal-to-noise ratio for ^{13}C in some spectra, up to 150,000 free-induction decays were accumulated.

Results and Discussion

^{13}C solid-state NMR techniques used in the present work to identify the species adsorbed on the Ag catalyst as well as pure SiO_2 were (a) standard cross-polarization with magic angle spinning (CP/MAS), (b) CP/MAS with 50 μsec of dipolar dephasing and (c) direct ^{13}C excitation (Bloch decay).

The theory of the CP/MAS experiment was explained in some detail in chapter I of this thesis. In short, the cross-polarization technique enhances sensitivity from dilute, low-gyromagnetic ratio ^{13}C spins via polarization transfer mechanisms from abundant, higher gyromagnetic ratio ^{1}H spins. In solids, the static dipolar coupling is the interaction used for polarization

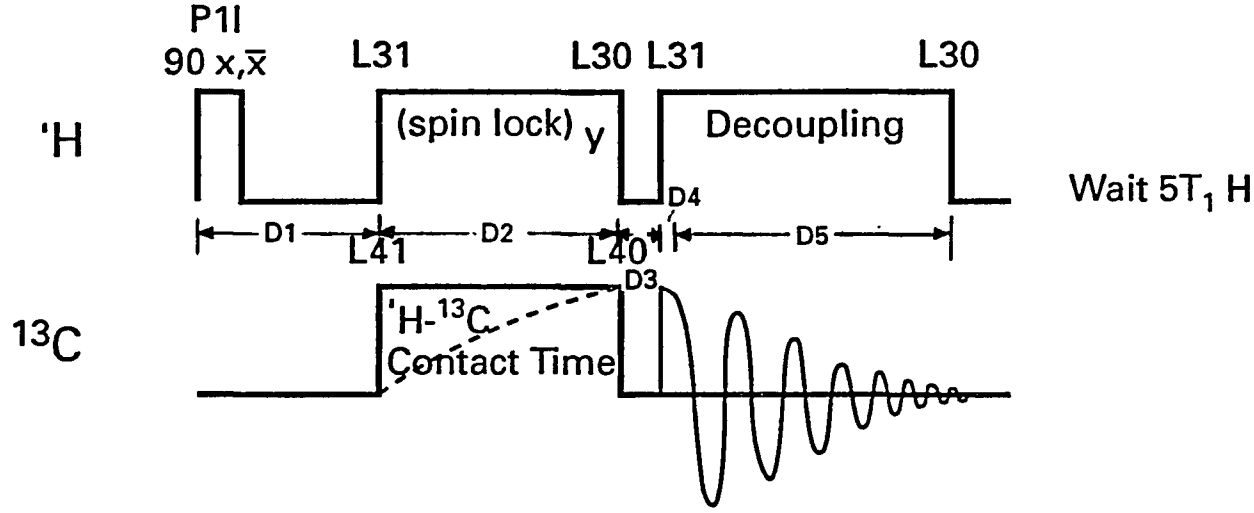

Fig. 10. Dipolar dephasing pulse sequence

transfer between ^{1}H and ^{13}C spins. In liquids, the static dipolar coupling is motionally averaged to zero. However, the indirect or scalar coupling which results from the hyperfine interactions of electrons and nuclei provides the means of polarization transfer. The CP/MAS experiment allowes us to simultaneously observe molecules that are weakly bound to the surface, so-called physisorbed species and molecules that form chemical bonds with the surface, so-called chemisorbed species. Identification of weakly (physisorbed) adsorbed species is based on isotropic chemical shifts as compared with the liquid state ^{13}C NMR chemical shifts even though they might be slightly different from each other due to Van der waals interactions and bulk susceptibility[101].

The dipolar dephasing experiment is similar to a conventional cross-polarization experiment except for the introduction of a delay or dipolar dephasing time, T_{DD}, between the cross-polarization and the acquisition of the carbon FID where the proton field is turned off. The pulse sequence[38] for the dipolar dephasing experiment is illustrated in Fig. 10. During the dipolar dephasing period, the transverse magnetization of the rare spins (^{13}C) strongly coupled to abundant spins (^{1}H) dephases very quickly compared to carbon spins with no attached proton due to heteronuclear dipolar interactions, and so are removed from observation. The delay or dipolar dephasing time, T_{DD}, used in this work was 50 μsec, which has been shown[102] to cause virtually complete destruction of signals from carbons with a directly bonded hydrogen and only small effects on C more distant from H. After this delay, the proton spin decoupling pulse is reapplied to

decouple the dipolar interactions during the acquisition of the carbons free induction decay, which is now due to only the quarternary and methyl carbons which are the only ones not completely dephased during the delay. The dipolar dephasing technique thus achieves preferential suppression of the signal due to non-quaternary carbons (e.g., CH and CH_2) but is less effective for suppressing methyl groups (e.g., CH_3) where rapid internal rotation reduces the dipolar interaction. With a dipolar dephasing time of 50 μsec, signals from rotating methyl groups are reduced but not eliminated[103]. Conventional cross-polarization and dipolar dephasing results are complementary and together can provide valuable information regarding the nature of adsorbed species on the surface of a catalyst.

Fig. 11 presents ^{13}C CP/MAS spectra of C_2H_4 - N_2O on a 10 % Ag/SiO_2 in the temperature range of 298 - 473 K. The catalyst preparation and the NMR sample pretreatment (A) were described earlier. Each spectrum results from 150,000 scans with a spectral range of 50 KHz. Only the region between 400 to - 300 ppm is exhibited in all spectra since no features were observed outside of this region. The procedure involved first taking the spectra at room temperature and then heating the sample to various temperatures outside of the probe for 1 hr, allowing the surface reaction to proceed between ethylene and chemisorbed oxygen. The spectra at different temperatures were recorded at room temperature.

Recent experimental investigations have tended to support O_a as the crucial epoxidising species responsible for the epoxidation reaction[47,89]. Indeed, to probe the reaction mechanism, some workers [104,105] have used

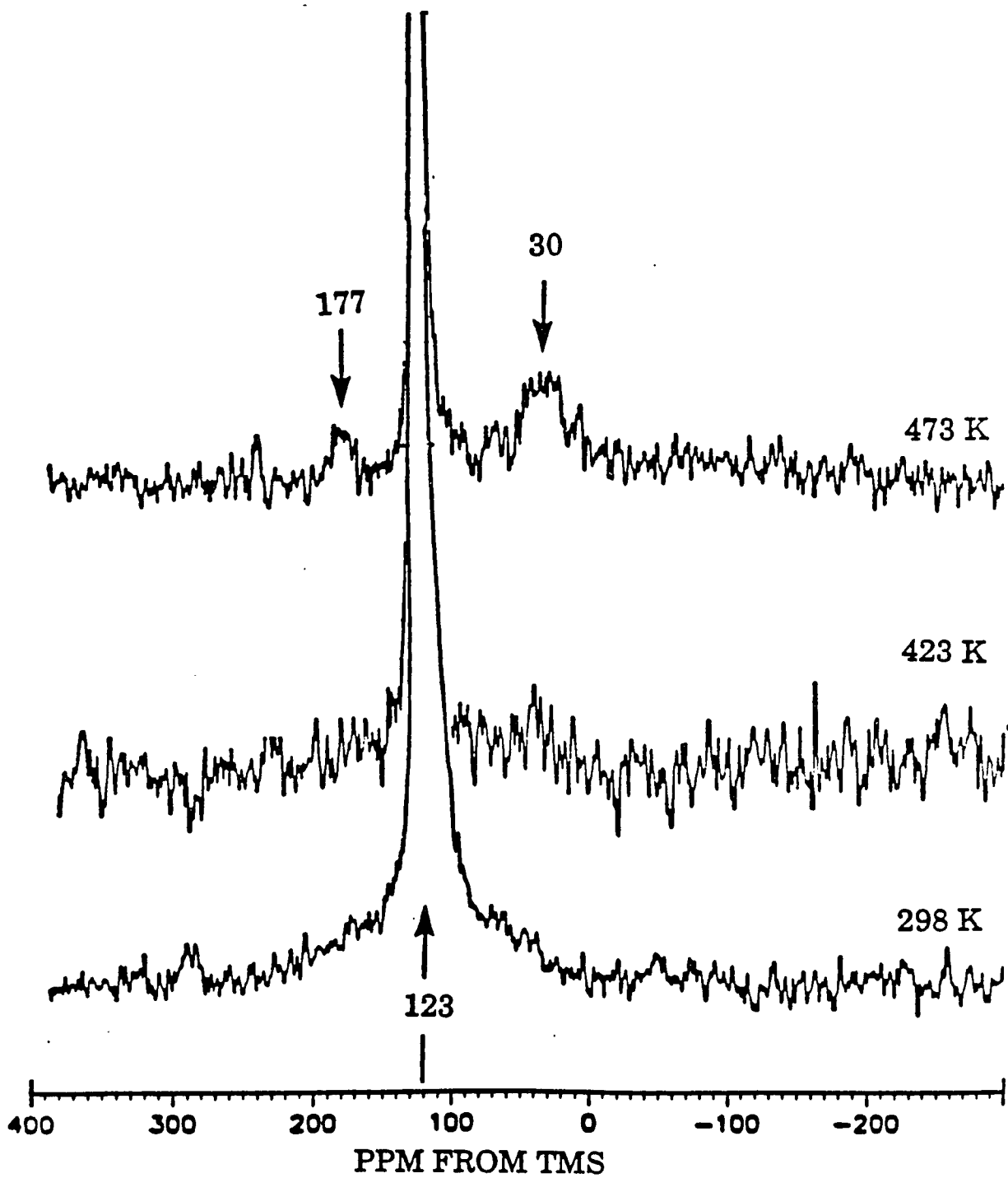

Fig. 11. ^{13}C CP/MAS spectra of C_2H_4 - N_2O on 10 % Ag/SiO_2 in the temperature range of 298 - 473 K

N_2O rather than O_2 as the oxidant in the oxidation of ethylene over silver catalysts to examine the "atomic oxygen hypothesis" vs "diatomic oxygen hypothesis". Oxygen adsorption via decomposition of N_2O on supported silver catalysts, N_2O (g) + Ag_s -> Ag_s - O_a + N_2 (g), was also shown to provide oxygen coverages similar to those obtained using O_2 as the adsorbate[51,53]. On transition metal single - crystal surfaces, dissociative chemisorption of N_2O occurs from 298 to 900 K producing adsorbed atomic oxygen and gaseous N_2[106-108]. On Ag (111), Tan et al.[109] have shown that N_2O does not decompose at 300 K, whereas negligible decomposition occurs at 400 K. Further heating the surface to 520 K produced O_a.

The CP/MAS spectra of C_2H_4 adsorbed on an oxygenated silver surface as illustrated in Fig. 11, show the presence of a narrow peak located at 123 ppm which represents species of high mobility that are not rigidly attached to the surface. This peak consistently appears in other CP/MAS spectra at higher temperatures. Based on the isotropic chemical shift, this peak is identified as gas-phase weakly adsorbed ethylene[110]. Indeed, throughout this work we have observed resonances at 123 ppm for ethylene adsorbed on silica - supported reduced, oxygen-covered silver surfaces as well as pure SiO_2. This assignment is consistent with the previous studies which showed gas-phase ethylene resonating between 119 - 123 ppm[111]. Further confirmation for the presence of the reversibly adsorbed state of ethylene was provided by the CP/MAS dipolar dephasing experiment indicating that rapid isotropic motion of ethylene sufficiently reduces the dipolar interaction that its resonance survives a delay of 50 μsec. Resonances for irreversibly

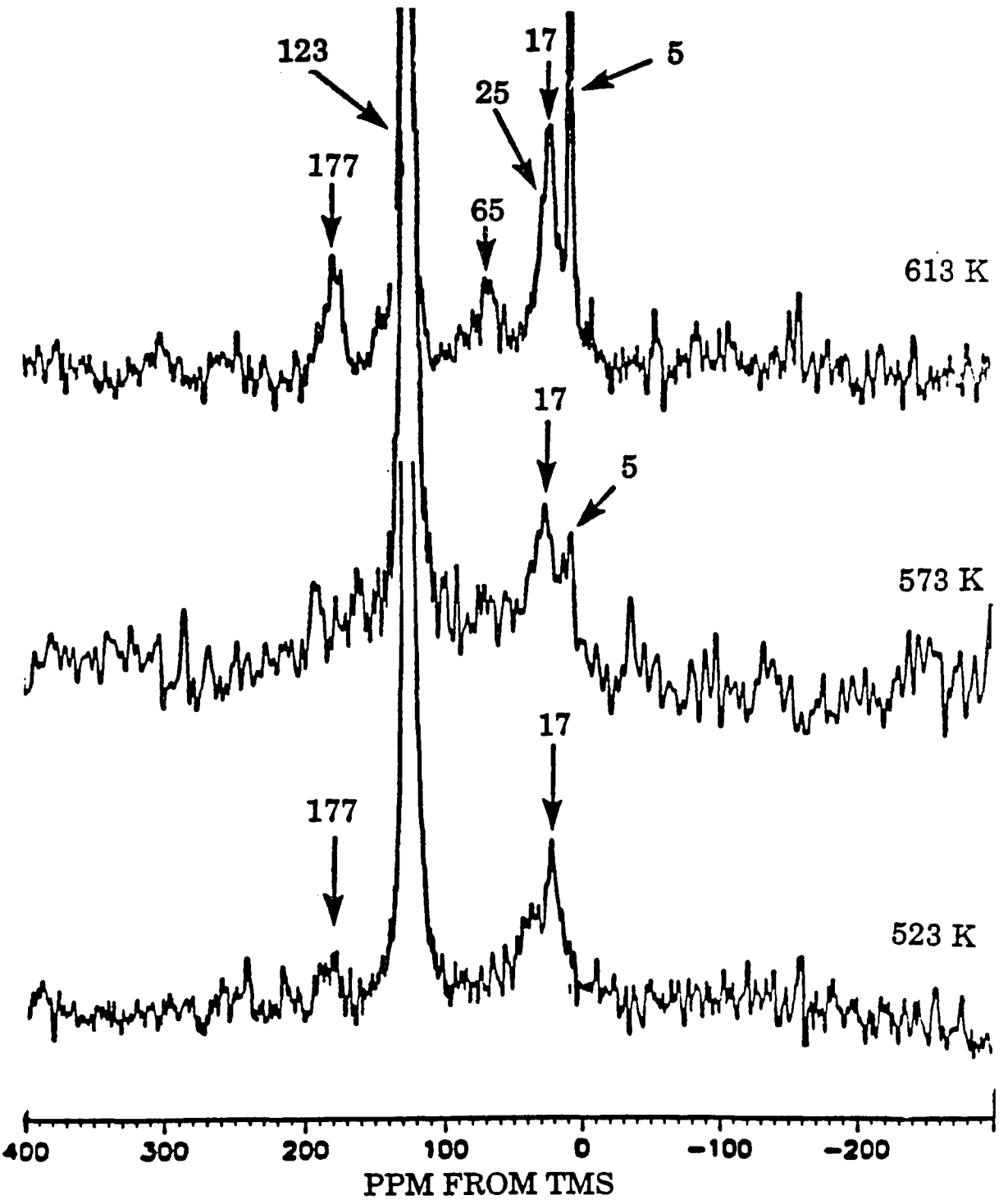

Fig. 12. ^{13}C CP/MAS spectra of C_2H_4 - N_2O on 10 % Ag/SiO_2 in the temperature range of 523 - 613 K

and reversibly adsorbed states of ethylene have been reported at 103 and 111 ppm on oxygen-covered Al_2O_3 - supported silver catalysts[32]. In the presence of oxygen on a Ag/Al_2O_3 catalyst, Chin and Ellis[35] have assigned an isotropic peak resonating at 108 ppm to a π-bonded ethylene where C = C axis is possibly parrallel to silver surface.

Fig. 12 illustrates the CP/MAS spectra of C_2H_4 adsorbed on an oxygenated silver surface in the temperature range of 523 - 613 K. When the sample is heated to higher temperatures, several new features are observed due to the formation of a variety of intermediate products. This is attributed to the fact that at high temperature decomposition of N_2O is significant and the reaction between ethylene and chemisorbed oxygen becomes evident. Notable in every spectrum is the low signal-to-noise ratio due to the small concentrations of the reaction products. Thus, a large number of scans were required to achieve a satisfactory signal/noise ratio. The CP/MAS spectrum at 473 K clearly shows the presence of two resonances : a downfield peak centered at 177 ppm and an upfield peak centered at 30 ppm. The former peak consistently appears in other CP/MAS spectra at higher temperatures while the latter peak is transformed into other species on the surface as the temperature is increased from 473 to 613 K. As was stated earlier, identification of the various peaks are based upon the chemical shifts and the verification of the identity as quaternary or methyl carbons is made from the dipolar dephasing experiments. ^{13}C chemical shifts of some compounds are given in table 1. The CP/MAS spectra with 50 μsec dipolar dephasing of C_2H_4 adsorbed on oxygenated silver surface in the

Table 1. ^{13}C chemical shifts in ppm (from TMS) from liquid state NMR[110]

COMPOUND	FORMULA	C^a	C^b
Ethane	$C^aH_3 - C^aH_3$	5.7	-
Ethylene	$C^aH_2 = C^aH_2$	123	-
Ethylene oxide	$C^aH_2 - C^aH_2$ (O)	40	-
Carbon dioxide	$O = C = O$	124	-
Acetaldehyde	$C^aH_3 - C^b(H) = O$	30	199
Acetic acid	$C^aH_3 - C^b(OH) = O$	20	177
Formaldehyde	$H - C^a(H) = O$	166	-
Acetone	$C^aH_3 - C^b(C^aH_3) = O$	30	206
Ethylene glycol	$C^aH_2(OH) - C^aH_2(OH)$	63	-
Propoxide	$CH_3 - C^aH_2 - C^bH_2 - O -$	25	65

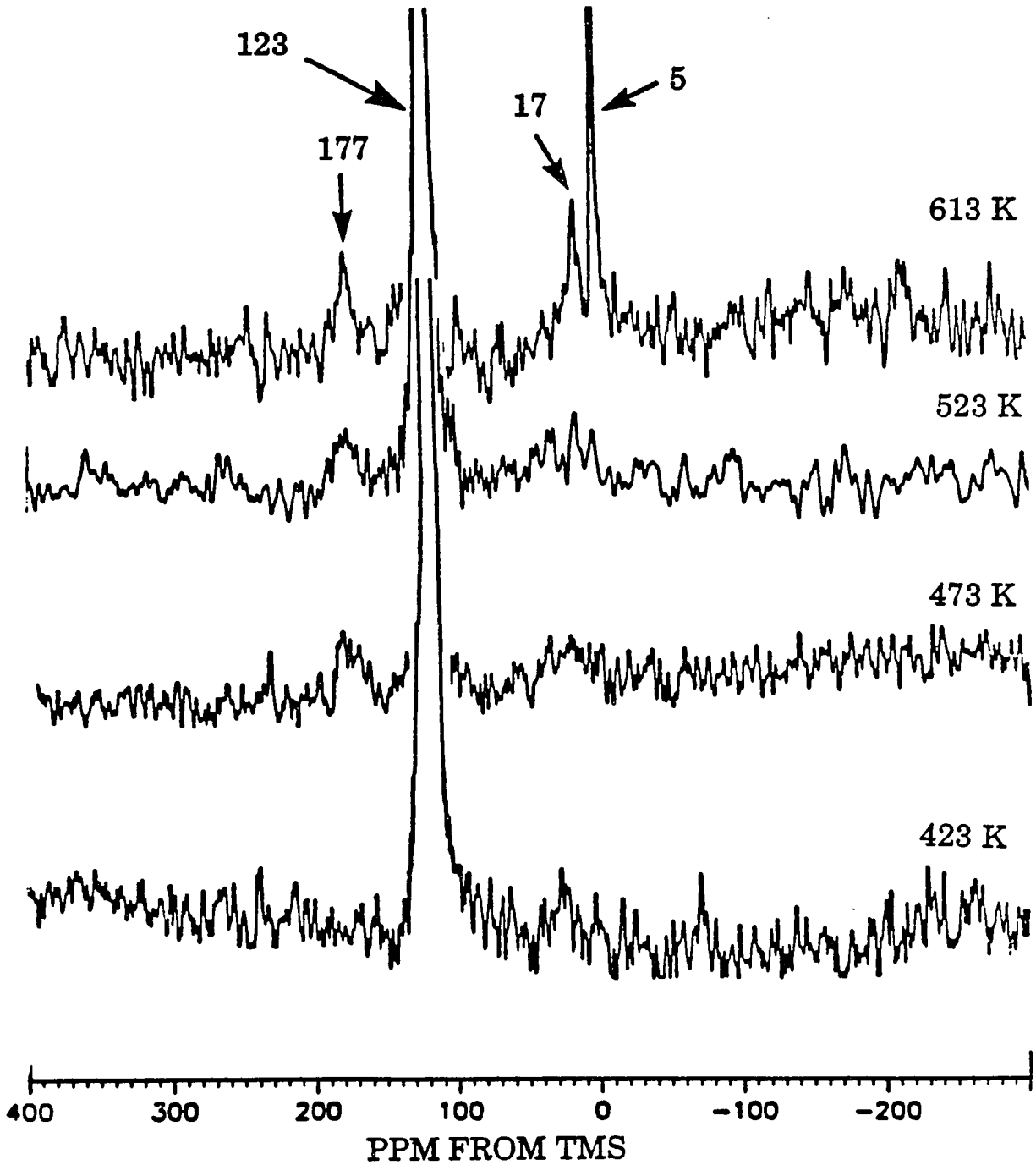

Fig. 13. ^{13}C CP/MAS spectra with dipolar dephasing of C_2H_4 - N_2O on 10 % Ag/SiO_2 in the temperature range of 423 - 613 K

temperature range of 423 - 613 K are shown in Fig. 13. It is evident from these spectra that the downfield peak centered at 177 ppm survived a delay of 50 μsec associated with CP/MAS dipolar dephasing experiment. The upfield peak centered at 30 ppm, however, did not survive this delay at 473 - 573 K indicating relatively rigid protonated ^{13}C nuclei. Based on these observations, it can be reasonably assumed that the downfield peak centered at 177 ppm corresponds to an unprotonated carbon species on the surface of the silver catalyst in the temperature range of 473 - 613 K. Hence, we ascribe this resonance to a carboxyl functional group (- $\overset{O}{\overset{\|}{C}}$ - O -). The results also reveal that the peak centered at 30 ppm contains a contribution from a methyl group (- CH_3). We therefore identify this species as acetic acid.

The presence of acetic acid as an intermediate in the oxidation process has been reported by Kobayashi[112] who used a transient response method with N_2O pulses to study mechanism of the epoxidation reaction. On Ag (111), Grant and Lambert[47] have identified acetic acid as a reaction intermediate in the further oxidation of ethylene oxide. Recent NMR studies of ethylene adsorbed on oxygen - covered alumina - supported silver catalysts have shown resonances at 19 and 179 ppm associated with acetic acid[32,35].

The CP/MAS spectra as shown in Fig. 12 indicate that several features are developed at successively higher temperatures. A narrow peak resonating at 123 ppm, an upfield peak at 17 ppm and a downfield peak centered at 177 ppm have been previously identified as physisorbed ethylene

and chemisorbed acetic acid, respectively. Furthermore, the CP/MAS spectra reveal the presence of a narrow upfield peak located at 5 ppm associated with a species of high mobility which is not rigidly bound to the surface as well as resonances at 65 and 25 ppm. Based on the isotropic chemical shifts and the results obtained from the dipolar dephasing experiments, the peak resonating at 5 ppm and the resonances at 65 and 25 ppm have been identified as ethane and alkoxy species Ag- O - CH_2 - CH_2 - CH_3, respectively. IR spectra[113] of ethylene oxidation over Ag/SiO_2 catalyst at temperatures above 373 K have shown the formation of an alkoxide type surface structure, - CH_2 - CH_2 - O -. In addition, the presence of alkoxy species on Ag/Al_2O_3 catalysts were confirmed by a recent solid-state NMR study[32].

Of particular interest was detection of ethylene oxide which resonates at 40 ppm from TMS. Nevertheless, under experimental conditions employed in the present study at the temperature range used in ethylene oxidation (i.e., 473 - 573 K), we were not able to identify ethylene oxide without ambiguity over unpromoted and unmoderated Ag/SiO_2 catalysts. Despite the fact that various carbon-containing species were observed and identified on the surface of Ag/η-Al_2O_3 catalyst by ^{13}C NMR, Plischke and co-corkers[32] were not able to unambiguously detect ethylene oxide under epoxidation conditions. These authors have suggested that the absence of ethylene oxide in every spectra might be due to low signal-to-noise or different adsorbed states of ethylene. In a recent solid-state ^{13}C NMR investigation of ethylene oxidation over Ag/γ-Al_2O_3, however, ethylene oxide

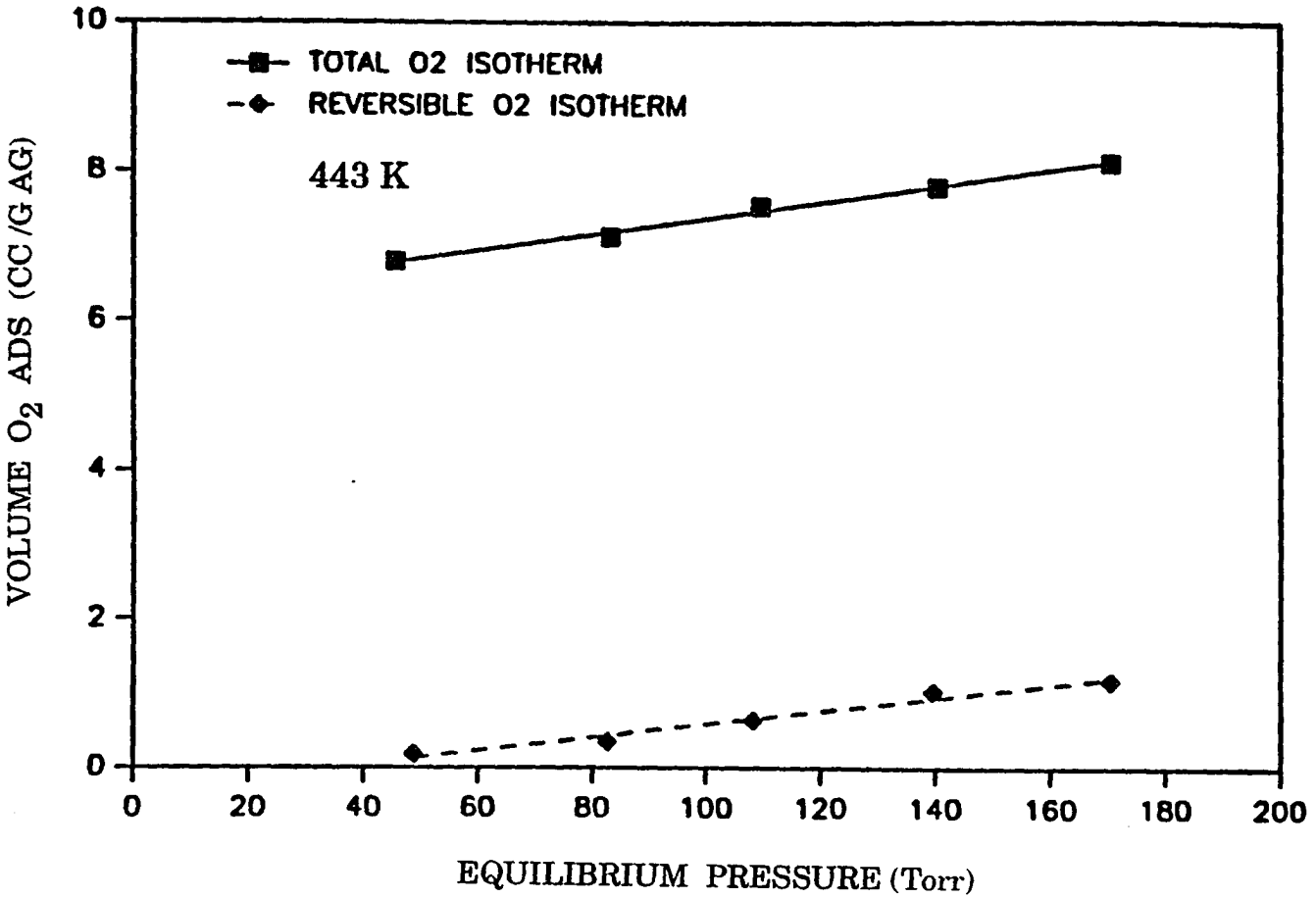

Fig. 14. Oxygen adsorption isotherms at 443 K for 20 % Ag/SiO_2.■,$(O_2)_{tot}$,◆ ,$(O_2)_{rev}$

has been reported to resonate at 61 ppm downfield with respect to TMS[35]. In the following, we attempt to understand the absence of a clear and distinct ethylene oxide peak in our spectra.

Aside from oxygen, the adsorption characteristics of the other species involved in the oxidation of ethylene have not been studied extensively. Therefore, in order to obtain further information on the chemistry of the ethylene oxidation over silica-supported silver catalysts, and explain the results of this study, we have further investigated the interaction of C_2H_4, C_2H_4O and CO_2 in the absence of oxygen with 20 % Ag/SiO_2 as well as pure SiO_2.The primary purpose of this study was to elucidate the adsorption characteristic of individual reactant and products on the surfaces of silica-supported silver catalyst and pure silica and to provide new valuable insight into the catalytic chemistry of ethylene oxidation.

The total and reversible O_2 isotherms on a 20 % Ag/SiO_2 are shown in Fig. 14. The dispersion of the catalyst was calculated to be 6.0 %. Sample preparations and pretreatments (B) were described before. Spectra were obtained at room temperature after heating the samples outside of the probe for 1 hr at 298 or 523 K. In each spectrum, only the chemical shifts range of 200 to 0 ppm is displayed since no features were observed outside of this region. Each spectrum results from 50,000 scans. Fig. 15 shows ^{13}C CP/MAS spectra of C_2H_4 on a 20 % Ag/SiO_2 as well as pure SiO_2 support at 298 and 523 K. The results reveal the existence of weakly adsorbed ethylene resonating at 123 ppm.A solid-state NMR study[36] of adsorption and reaction of C_2H_4 on Ru/SiO_2 in our laboratory has shown that ethylene

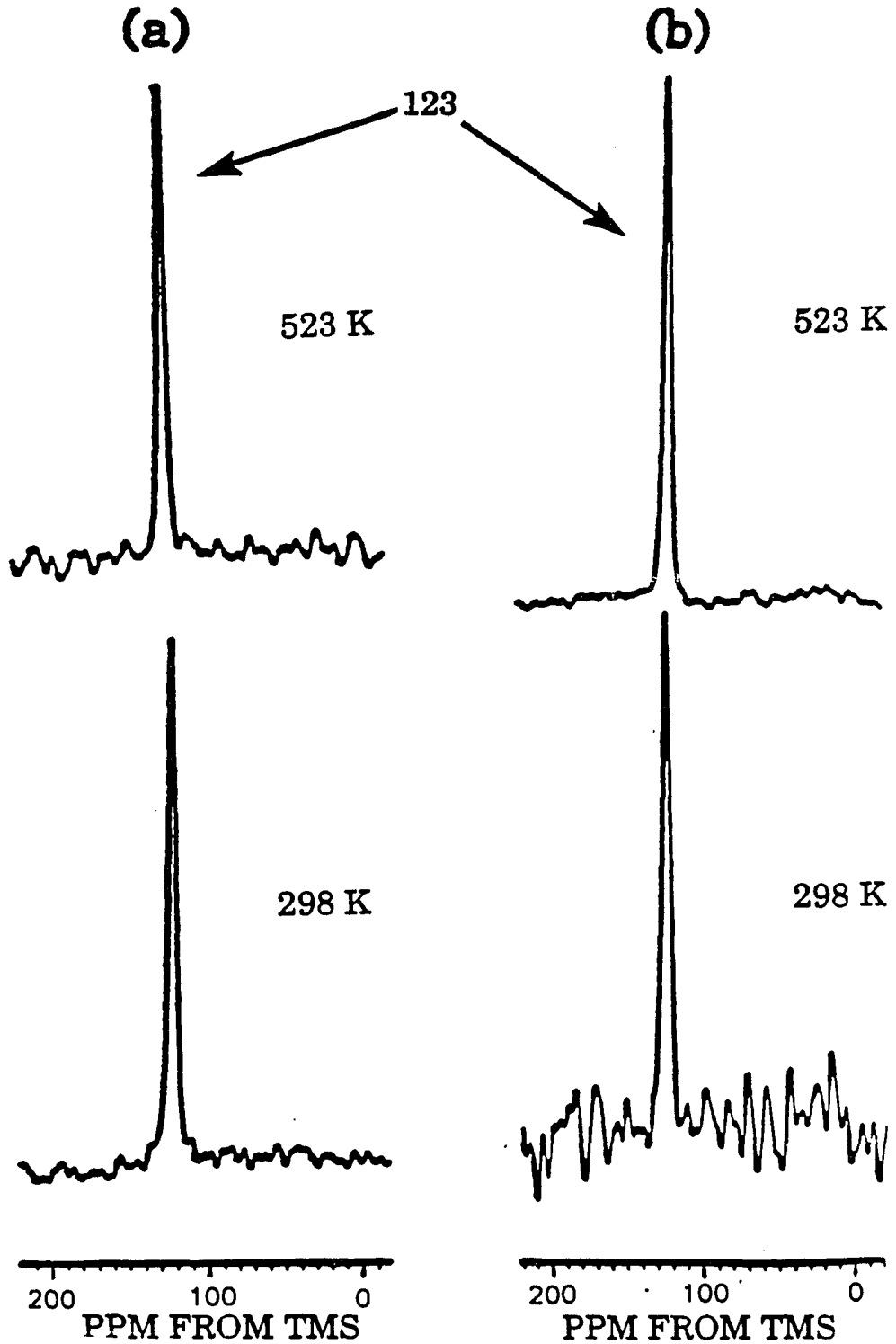

Fig. 15. ^{13}C CP/MAS spectra of only C_2H_4 on (a) 20 % Ag/SiO_2, (b) pure SiO_2 at 298 K and 523 K

adsorbed on pure silica produces a narrow peak located at 123 ppm. Ethylene on reduced Ru/SiO_2, however, could not be detected at room temperature since it decomposed to form strongly adsorbed acetylide and alkyl group followed by subsequent recombination of adsorbed alkyl species and hyrogenation of ethylene to form weakly adsorbed butane, butene and ethane. Gay[114] has shown that the adsorption of ethylene on Pt/SiO_2 or Pt/Al_2O_3 at room temperature resulted in the formation of a Π-bonded olefin. He further showed that the Π-bonded olefin on Pt/Al_2O_3 catalysts reacted to form σ -adsorbed species with an intact C = C double bond and surface alkyls. In contrast to these results, our finding indicates that the weakly adsorbed C_2H_4 on Ag/SiO_2 as well as pure SiO_2 does not react with silver and silica surfaces in the temperature range of 298 - 523 K.

Furthermore, we studied the interaction of CO_2 with Ag/SiO_2 and pure silica. Carbon dioxide, one of the byproducts in the oxidation of ethylene is formed either by direct oxidation of ethylene or by the further oxidation of ethylene oxide. The production of CO_2 which is a major engineering problem reduces the selectivity toward ethylene oxide. Since CO_2 is a nonprotonated molecule and there are no protons in its vicinity to polarize carbon atoms, CP/MAS is not an effective technique to detect carbon dioxide. Rather, direct ^{13}C excitation (Bloch decay) with a 2 sec recycle time was used to detect carbon dioxide. The Bloch decay pulse sequence is illustrated in Fig. 16. The Bloch decay spectra as shown in Fig. 17 indicate the presence of weakly adsorbed carbon dioxide (resonating at 124 ppm with respect to TMS), which in a manner similar to that of ethylene does not interact with either silver

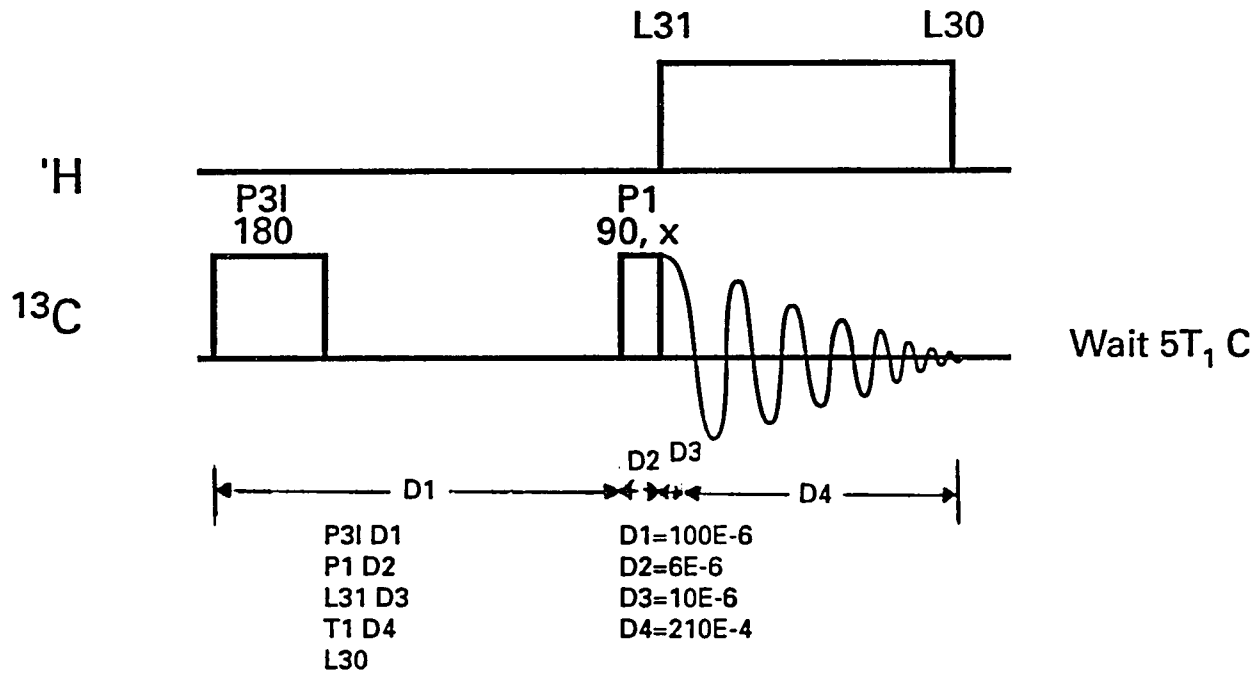

FIig. 16. Bloch decay pulse sequence

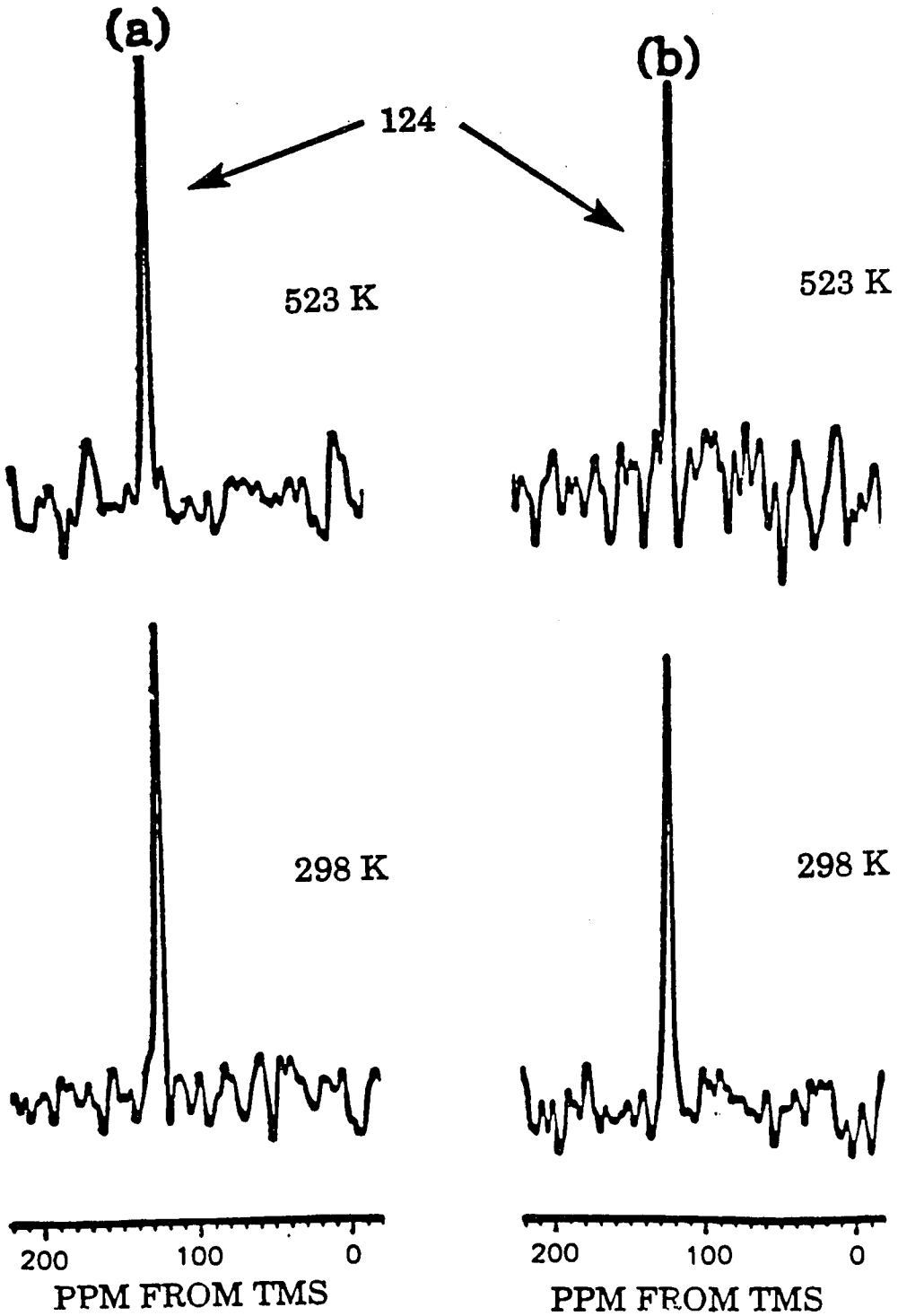

Fig. 17. Bloch decay spectra of only CO_2 on (a) 20 % Ag/SiO_2, (b) pure SiO_2 at 298 K and 523 K

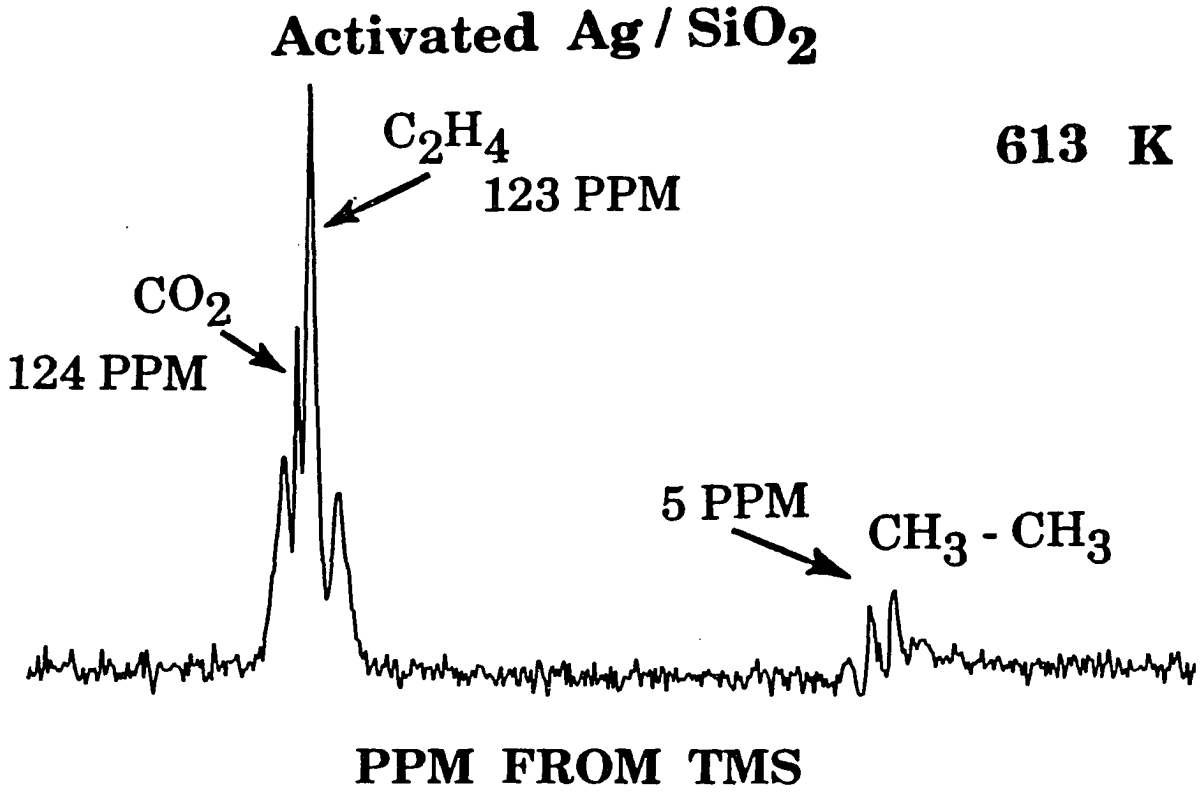

Fig. 18. Bloch decay spectra of C_2H_4O - N_2O on 10 % Ag/SiO_2 at 613 K

or silica surfaces at two different temperatures. It is known that under oxidation conditions, above 573 K complete cmbustion occurs to produce CO_2. Using the Bloch decay technique, we have been able to detect CO_2 under epoxidation conditions. Fig. 18 is the proton coupled Bloch decay spectrum of C_2H_4 - N_2O at 613 K. The formation of CO_2 resonating at 124 ppm is evident. The triplet and quartet peaks resonating at 123 and 5 ppm are the scalar-coupled methylenes and methyls from ethylene and ethane, respectively.

Finally, we investigated the species formed by reacting ethylene oxide with the supported catalyst as well as pure silica. Fig. 19 is the ^{13}C CP/MAS spectra of C_2H_4O on Ag/SiO_2 and pure SiO_2 at 298 and 523 K. There is evidence in the literature that ethylene oxide adsorbs readily on clean metallic silver[33,115]. Our results show that at 298 K, C_2H_4O (which resonates at 40 ppm from TMS) partially reacts with the supported silver catalyst to form species which resonate at 64 and 71 ppm. Cab-O-Sil HS5 is an amorphous nonporous silica support which has hydroxyl groups on the surface. The resonances at 64 and 71 ppm are therefore attributed to species $\equiv$Si-O-CH_2-CH_2-OH and $\equiv$Si$\langle$ O-CH_2-O $\rangle_n$ CH_2OH. The interaction of C_2H_4O with the silver surface is evident since the ethylene oxide peak is slightly broader and the peak at 64 ppm has lower intensity on Ag/SiO_2 than on pure SiO_2. Several interesting features are observed once the sample is heated to higher temperatures. At 523 K, C_2H_4O totally reacts with hydroxyl sites on silica surface as well as on Ag/SiO_2 to produce resonances at 64 and 71 ppm which we just assigned to species

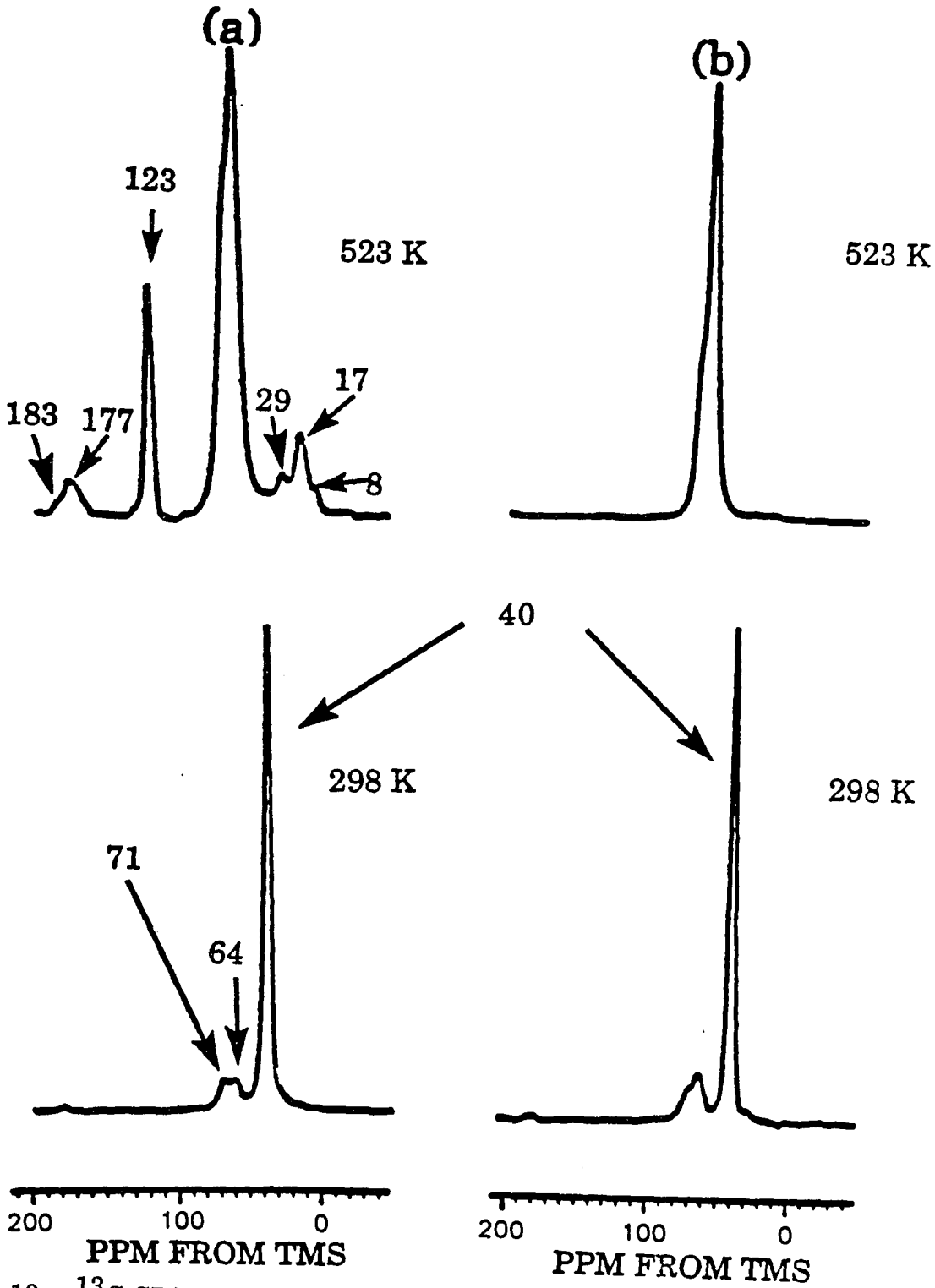

Fig. 19. ^{13}C CP/MAS spectra of only C_2H_4O on (a) 20 % Ag/SiO_2, (b) pure SiO_2 at 298 K and 523 K

≡Si-O-CH_2-CH_2-OH. Furthermore, interaction of ethylene oxide with silver results in additional resonances at 8, 17, 29, 123, 177 and 183 ppm. Based on the chemical shifts, the peaks resonating at 177 and 17 ppm are assigned to acetic acid and that at 123 ppm is assiged to ethylene. In addition, the resonances at 8, 29 and 183 ppm are assigned to species CH_3-CH_2-$\overset{O}{\overset{\|}{C}}$-OH.

The formation of ethylene over the activated silica-supported silver catalyst at 523 K presumably takes place through a reversal of the reaction by which ethylene oxide is formed, i.e., C_2H_4O -> $C_2H_4 + O_a$. It is known that silver would catalyze the isomerization of ethylene oxide to acetaldehyde when carried out in the absence of oxygen[115,116]. Under the conditions employed in the present study, however, no acetaldehyde (resonating at 30.7 and 199.7 ppm) could be detected. It can be assumed that any acetaldehyde formed via isomerization of ethylene oxide rapidly reacts with adsorbed oxygen to form acetic acid according to the following scheme: C_2H_4O -> CH_3-$\overset{O}{\overset{\|}{C}}$-H $\xrightarrow{O_a}$ CH_3-$\overset{O}{\overset{\|}{C}}$-OH. Our results reveal that at the temperature range which is normally used to produce C_2H_4O (i.e., 473 - 573 K), ethylene oxide reacts with both silver and silica surfaces and thus cannot be observed by NMR even if it is produced on the surface of the catalyst. Based on these observations, it could be reasonably argued that the absence of a clear and distinct ethylene oxide peak from spectra presented in Fig. 12 is mainly due to the interaction of C_2H_4O with Ag as well as SiO_2 surfaces.

There is evidence in the literature[117] that the silica support itself might be active in the conversion of ethylene oxide to acetaldehyde and

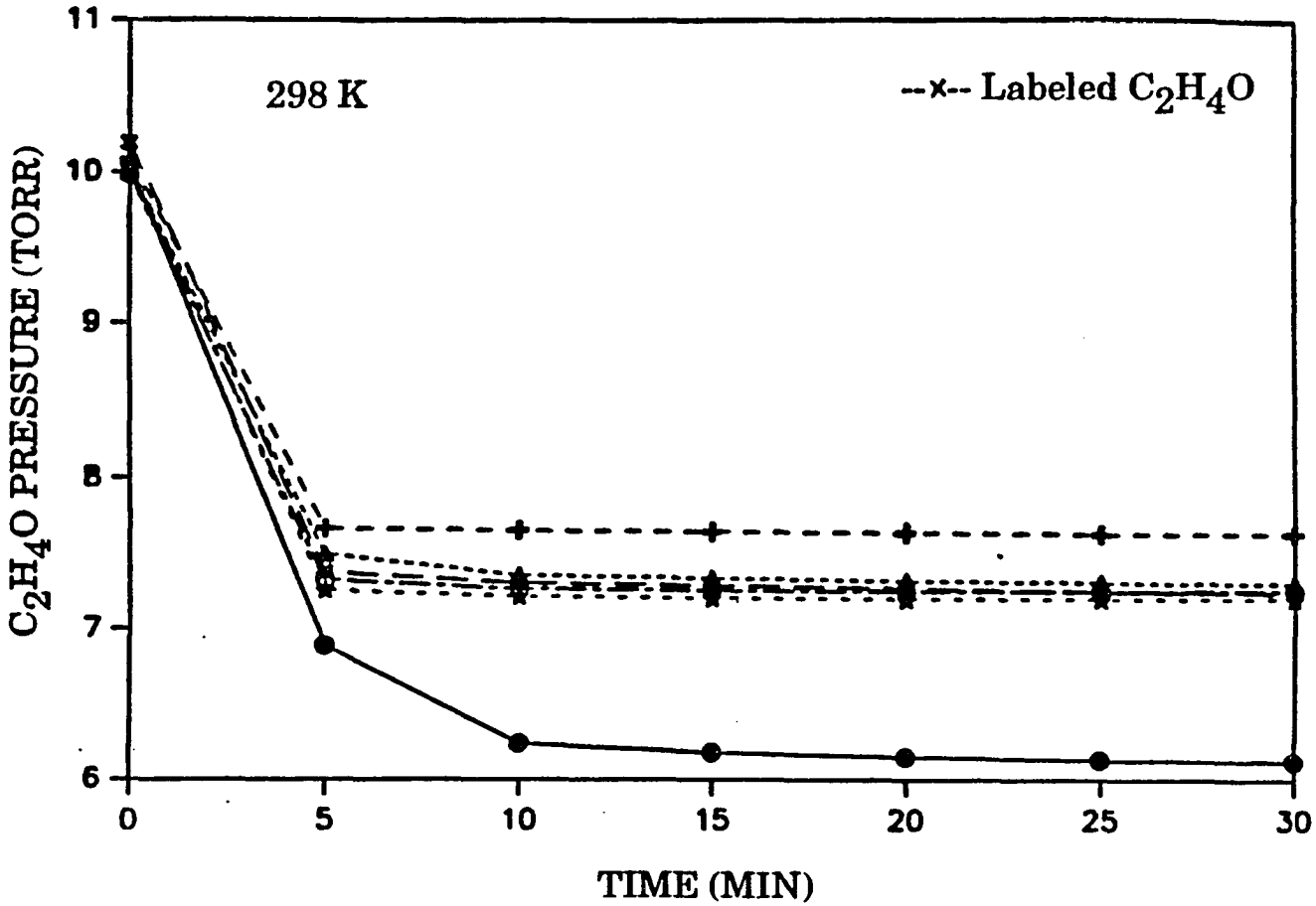

Fig. 20. Saturation of a 20 % Ag/SiO_2 catalyst with 10 Torr of unlabeled C_2H_4O for 2 1/2 hr followed by dosing with 10 Torr of labeled C_2H_4O for 30 min at 298 K. The sample was evacuated for 10 min after each unlabeled C_2H_4O saturation run

carbon dioxide. Lee et al.[118] have recently investigated the participation of the support in the chemistry of ethylene oxide oxidation on silver catalysts. These authors have shown that the low apparent selectivity of silica-supported silver catalysts toward the ethylene epoxidation reaction is primarily due to isomerization and oxidation of ethylene oxide on acidic sites supplied by the support. To test this hypothesis, they have modified the surface acidity of SiO_2 by impregnation with alkali or alkaline-earth metals. It was shown that activity toward isomerization was completely eliminated. Oxidation activity was reduced by alkali/alkaline earth impregnation. However, alkali-impregnated Ag/SiO_2 catalysts exhibited reduced selectivity to ethylene oxide and reduced overall activity. The authors have suggested that these results are probably due to poisoning of silver surfaces by deposition of alkali metals on them, either by surface migration under reaction conditions or during preparation of the catalysts. Lee and co-workers concluded that alkali-impregnation of supported silver catalysts is not a proper technique to eliminate support surface acidity so as to suppress its participation in chemistry of ethylene oxidation on silver catalysts.

In the present study, we have investigated the effect of the support on the performance of silver catalysts after saturating the catalyst with unlabeled ethylene oxide. The procedure outlined in pretreatment (C) was followed. The initial attempt was to saturate Ag/SiO_2 catalyst as well as SiO_2 support at 298 K. The result of saturating a Ag/SiO_2 catalyst with ethylene oxide is presented in Fig. 20. Evidently, saturation is achieved after 3 hr. Not shown here is the saturation experiment performed on a pure

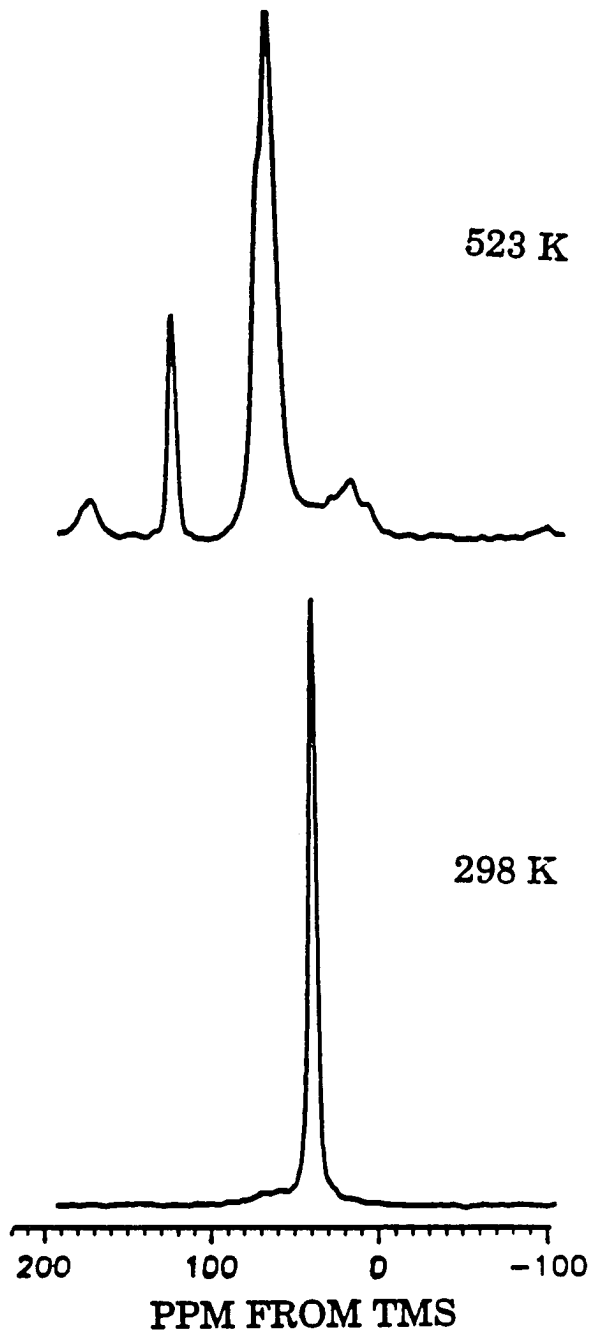

Fig. 21. ^{13}C CP/MAS obtained after saturating 20 % Ag/SiO_2 with 10 Torr of unlabeled C_2H_4O for 2 1/2 hr followed by dosing with 10 Torr of labeled C_2H_4O for 30 min at 298 K. The sample was evacuated for 10 min after each unlabeled C_2H_4O saturation run

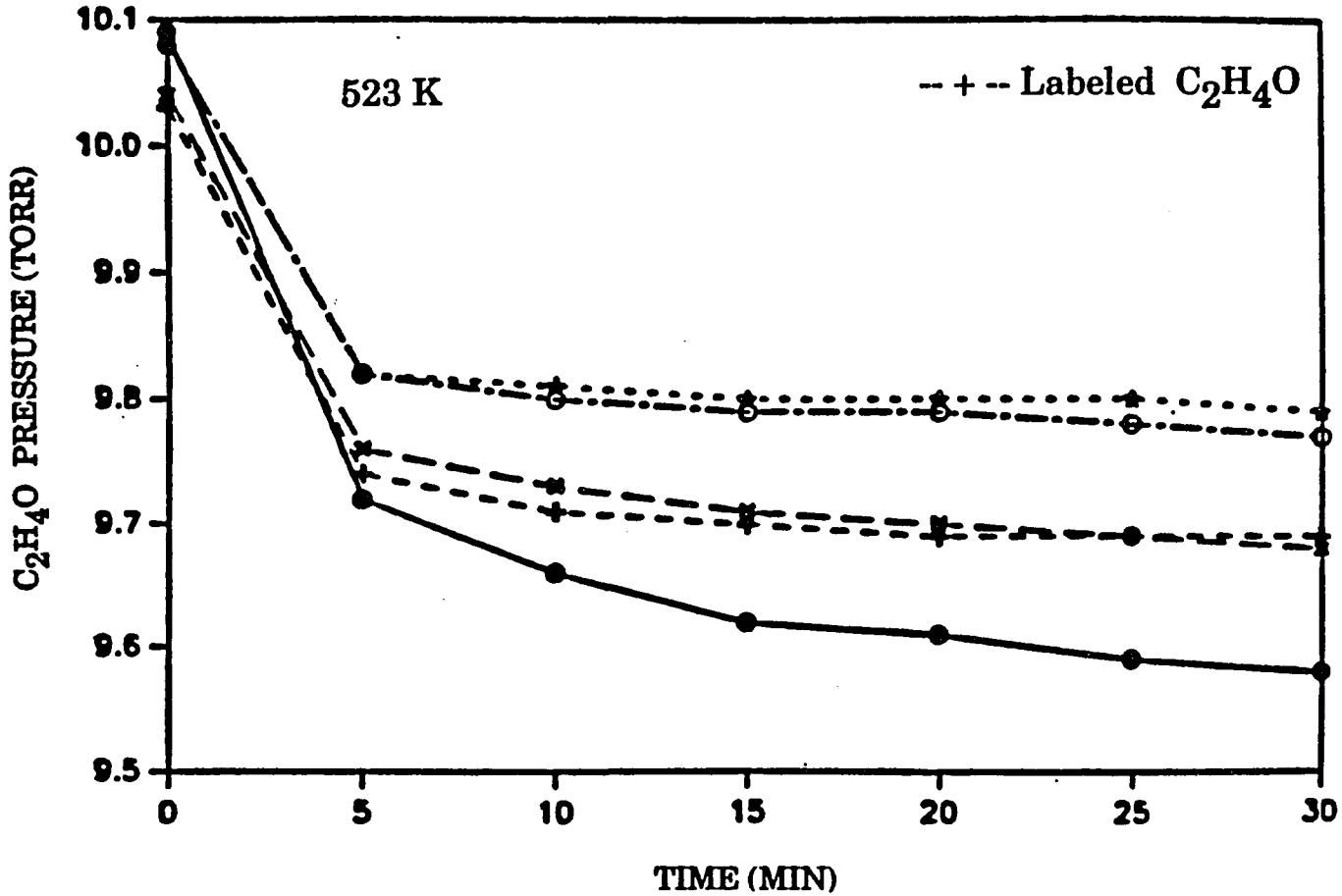

Fig. 22. Saturation of a 20 % Ag/SiO_2 catalyst with 10 Torr of unlabeled C_2H_4O for 2 hr followed by dosing with 10 Torr of labeled C_2H_4O for 30 min at 523 K. The sample was evacuated for 10 min after each unlabeled C_2H_4O saturation run

SiO_2 sample. Subsequently, ^{13}C CP/MAS experiments were performed on labeled ethylene adsorbed on Ag/SiO_2. The results as shown in Fig. 21 reveal the presence of identical resonances as was observed before (Fig. 19). Thus, saturation of the surfaces at 298 K is not an effective technique. The next attempt was to saturate Ag/SiO_2 as well as SiO_2 surfaces with C_2H_4O at 523 K. The result is presented in Fig. 22. Not shown here is the saturation experiment performed on a pure SiO_2 sample. Subsequently, ^{13}C CP/MAS experiments were performed on Ag/SiO_2 and pure SiO_2 samples. The results are presented in Fig. 23 and Fig. 24, respectively. The results indicate the presence of three resonances at 64, 71 and 40 ppm which have been previously assigned to species $\equiv$Si-O-CH_2-CH_2-OH and C_2H_4O, respectively. This finding clearly indicates that under the conditions employed in the present investigation, saturation populates the hydroxyl sites on the surface of silica such that the complete interactions of C_2H_4O with both SiO_2 and Ag surfaces at high temperature are prevented.

If this hypothesis is valid, C_2H_4O should be observed under conditions of ethylene epoxidation provided that the hydroxyl sites on the silica surface are saturated prior to oxidation reaction. Fig. 24 illustrates the ^{13}C CP/MAS NMR spectra of C_2H_4 - O_2 obtained after saturating a) 20 % Ag/SiO_2 and b) pure SiO_2 with unlabeled C_2H_4O. The pretreatment (D) was used to prepare the samples. Each sample was heated outside of the probe for 1 hr at 495 K. The spectra were then recorded at room temperature using 100,000 scans. Under conditions of oxidation employed in the present study, it can be seen that C_2H_4O (resonating at 40 ppm) is

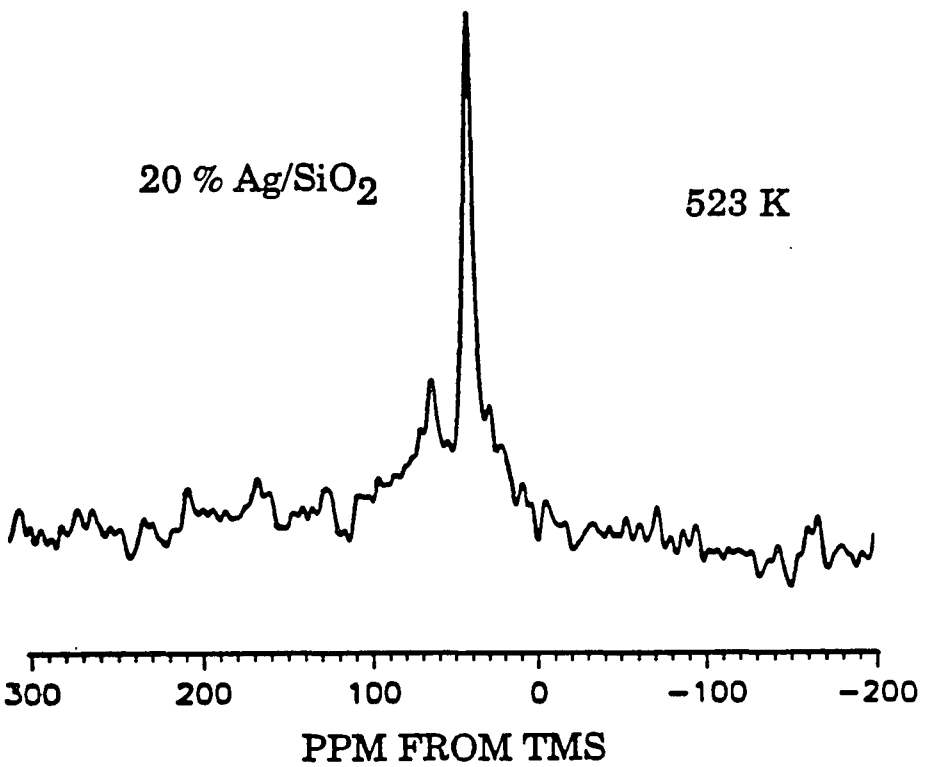

Fig. 23. ^{13}C CP/MAS obtained after saturating 20 % Ag/SiO_2 with 10 Torr of unlabeled C_2H_4O for 2 hr followed by dosing with 10 Torr of labeled C_2H_4O for 30 min at 523 K. The samples were evacuated for 10 min after each unlabeled C_2H_4O saturation run

indeed generated from the interaction of ethylene with chemisorbed oxygen. It was also determined, under identical conditions, that the silica support does not posses any oxidation activity toward ethylene. These results are in agreement with previous studies indicating that in the absence of promoters or moderators SiO_2 supported silver catalysts[50,117,119] exhibit activity/selectivity, whereas the silica support alone does not show any activity toward ethylene oxidation[118,120]. The possibility that the resonance at 40 ppm could be partially attributed to unlabeled C_2H_4O is disregarded due to the fact that 98.9 % of the naturally abundant carbons are inactive NMR nuclei. To examine this effect further, an experiment was carried out where the catalyst was saturated with unlabeled C_2H_4O only. No ethylene oxide was observed. Thus, the peak resonating at 40 ppm is assigned to ethylene oxide resulting from reaction of the labeled ethylene with the catalyst. Subsequent work is under way in our laboratory to further probe the effects of adding halogens as promoters.

Conclusion

Application of experimental nuclear spin dynamics, including conventional cross-polarization MAS, CP/MAS with dipolar dephasing as well as direct ^{13}C excitation (Bloch decay), allowed observation and identification of various carbon - containing species on the surface of SiO_2-supported silver catalysts in the absence of promoters and moderators. Under the oxidation conditions employed in the present investigation,

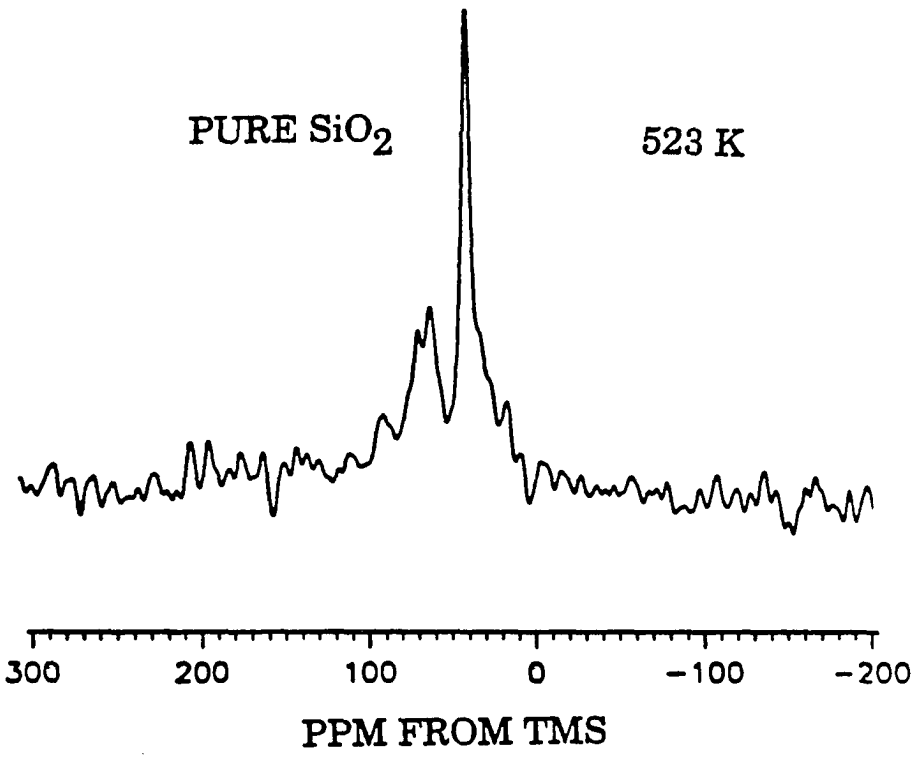

Fig. 24. ^{13}C CP/MAS obtained after saturating pure SiO_2 with 10 Torr of unlabeled C_2H_4O for 2 hr followed by dosing with 10 Torr of labeled C_2H_4O for 30 min at 523 K. The samples were evacuated for 10 min after each unlabeled C_2H_4O saturation run

ethylene, acetic acid, carbon dioxide, ethane and an alkoxy species are identified at temperatures ranging from 298 to 613 K. No ethylene oxide could be unambiguously detected.

We have further studied the interaction of CO_2, C_2H_4 and C_2H_4O with Ag/SiO_2 catalysts as well as pure SiO_2. This study has furnished valuable insight into the catalytic oxidation. In particular, it was found that under conditions employed in the present investigation, ethylene oxide reacts with both metal and silica support and thus could not be observed as the reaction product by NMR. Based on these observations, it has been shown that ethylene oxide could be detected if the catalyst is first saturated with unlabeled (natural abundance ^{13}C) ethylene oxide before reaction with labeled species. To test this hypothesis, samples of Ag/SiO_2 as well as pure SiO_2 were prepared under identical ethylene oxidation conditions. Ethylene oxide has been indeed observed after the saturation of a silica surface with unlabeled ethylene oxide prior to ethylene oxidation. It was also determined that silica support does not posses any activity toward ethylene oxidation.

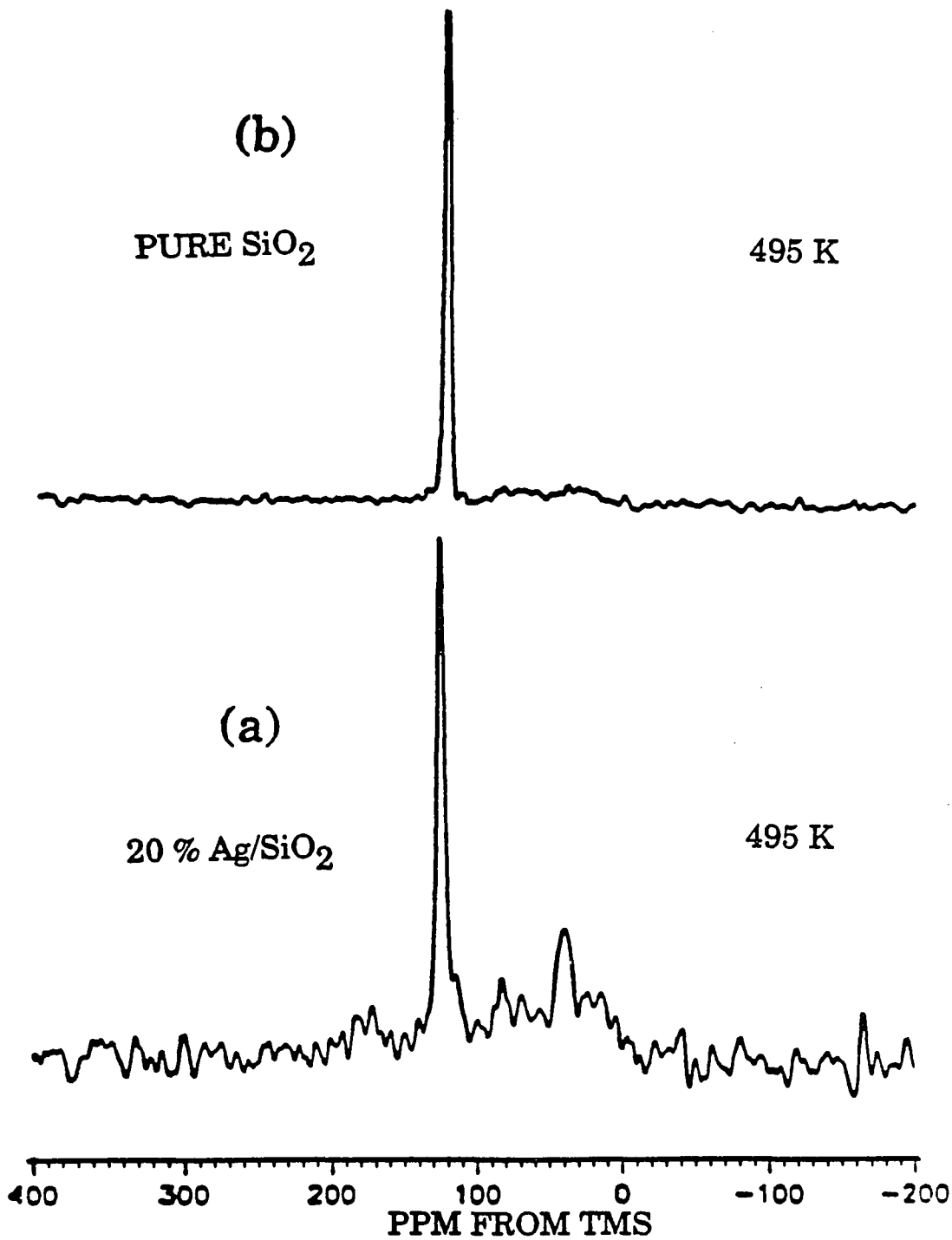

Fig. 25. ^{13}C CP/MAS spectra of C_2H_4 - O_2 obtained at 495 K after saturating (a) 20 % Ag/SiO_2 and (b) pure SiO_2 with 10 Torr of unlabeled C_2H_4O for 2 hr at 523 K

CHAPTER III. THE DESIGN OF A SINGLE - COIL DOUBLE RESONANCE PROBE AND A HIGH VACUUM GLASS APPARATUS

The Design of a Single - Coil Double - Resonance Probe

Introduction

A combination of high-power proton decoupling and sensitivity enhancement techniques like Cross Polarization (CP) with macroscopic spinning of the sample (MAS) at the "magic angle" of $54^{\circ}\ 44'$ to the magnetic field has provided a powerful tool for obtaining "high-resolution" ^{13}C NMR of molecules adsorbed on surfaces. In the Cross Polarization (CP) experiment which was developed by Hartmann and Hahn, polarization is transfered from abundant spins such as ^{1}H to rare spins such as ^{13}C via the coupling of two different nuclear species. Although dipolar broadening is removed by strong proton decoupling during data acquisition, chemical shift anisotropy may still severly complicate the ^{13}C spectrum. High-speed mechanical sample rotation at the magic angle as a line-narrowing technique in ^{13}C NMR studies of solids would average chemical shift anisotropic dispersions found in solid powder samples to their isotropic values.

Thus, the combination of cross polarization, dipolar decoupling, and magic angle spinning can produce ^{13}C NMR spectra of solids with high resolution. It is consequently desirable to design a probe for solids which is highly sensitive to the observed nuclide, is able to withstand sufficiently high

power ^{1}H decoupling, and is capable of magic angle spinning at high rates. We report here the design and construction of a single coil double resonance NMR "home - built" probe capable of performing experiments in solid-state cross-polarization magic angle spinning (CP/MAS). The probe was designed and constructed by the author. The probe is doubly tuned using the design of Doty with a modified version of the spinning assembly by Shoemaker - Apple - Pruski. Magic - angle spinning of sealed samples at rates exceeding 5 kHz is achieved. The probe to be described assumes the geometry associated with a 250 MHz superconducting magnet in our laboratory. The probe is lowered into the superconducting magnet from above.

Probe Body

Fig. 26 is the photograph of the entire probe assembly. The dimensions of this probe are given in Fig. 27. The probe consists of three parts : body, circuit and cap. Aluminum tubing with O.D. of 2.250 in and wall thickness of 0.194 in was used for construction of this probe. The circuit section consists of two brass bases which are connected by a brass partition with thickness of 0.128 in. The partition is used to isolate the ^{13}C and ^{1}H circuit compartments. The cap section consists of a brass rod which is screwed into the base and holds the stator to its side by a connector made of Kel-F. Tuning and matching capacitors are located within each compartment. Incorporation of the capacitors was difficult due to the limited space available in each compartment.

Fig. 26. Photograph of the entire probe assembly

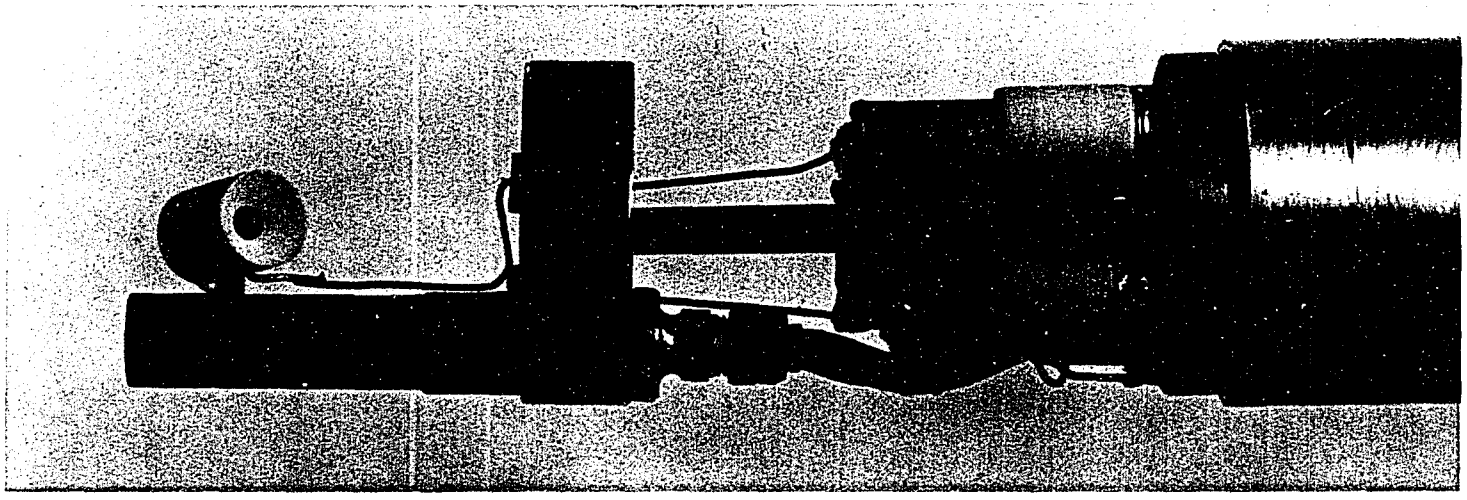

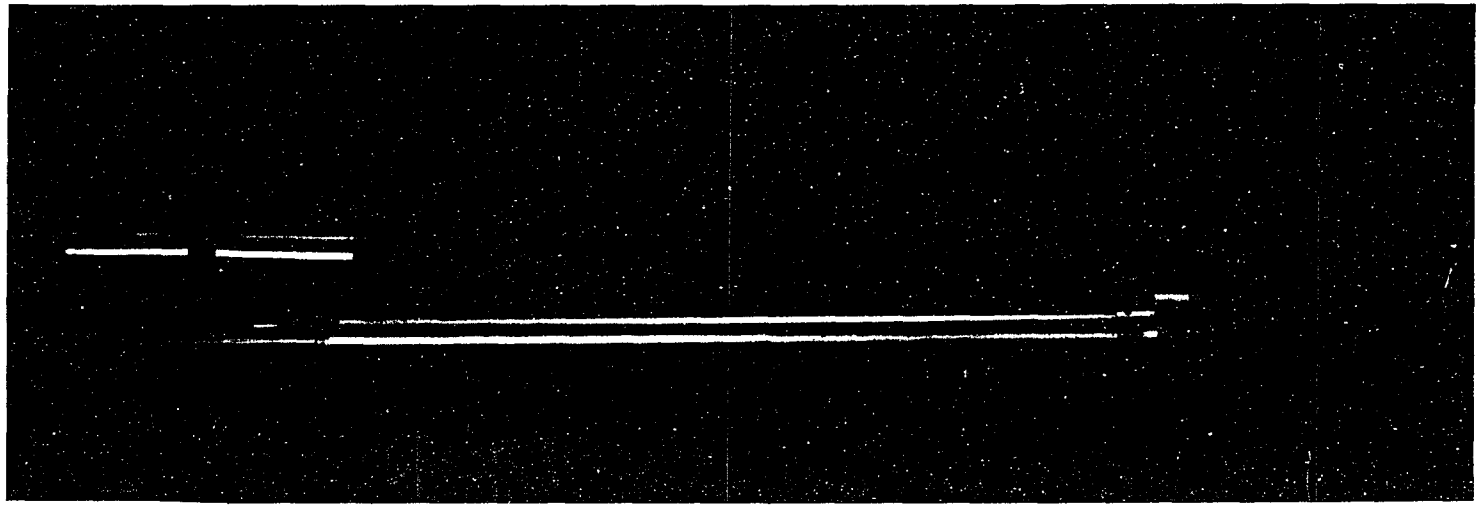

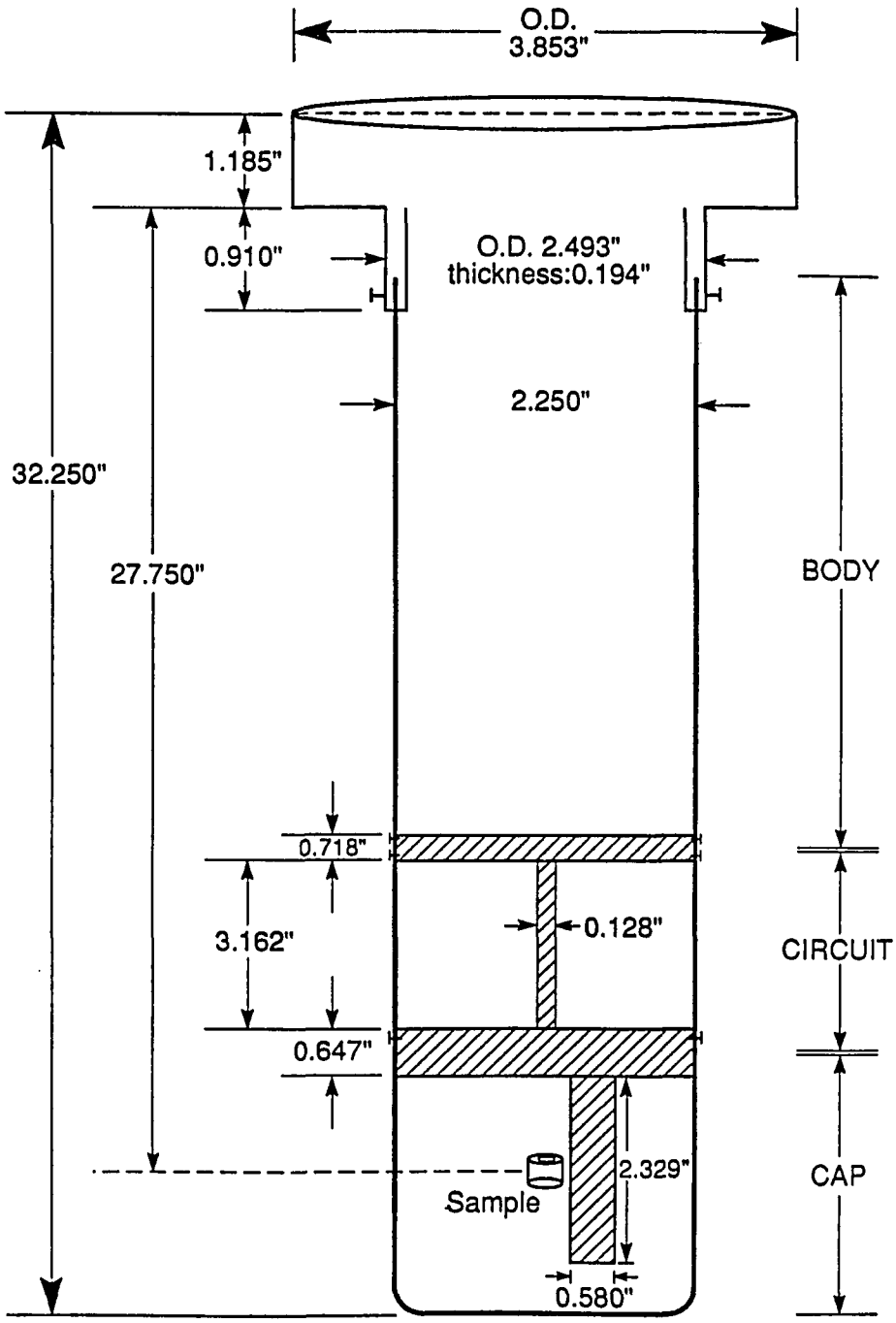

Fig. 27. Drawing of the dimensions of the probe body

The probe circuitry (the coil which generates B_1 and the tuning capacitors) must not arc during pulses. To avoid arcing, the capacitors were located as far as possible away from each other and the brass partition. The ^{1}H circuit compartment contains an inductor (.035 μH) and two polyflon high voltage rf variable capacitors with capacitance range of 5 - 25 and 0.8 - 10 pf, respectively. The ^{13}C circuit compartment contains two polyflon high voltage rf variable capacitors with capacitance range of 0.8 - 10 pf.

The probe assumes the geometry associated with a 250 MHz superconducting magnet in our laboratory and is lowered in to the superconducting magnet from above. Probe tuning is accomplished by tuning the vertically arranged variable capacitors with extension shafts from the top of the magnet.

Circuit Description

The schematic layout of the double- tuned ^{13}C / ^{1}H probe circuit for high-field CP/MAS NMR is shown in Fig. 28. The NMR coil is perhaps the most critical part of probe construction in modern solid-state NMR spectrometers. It is this coil which transmits the radiofrequency pulses to the sample and receives the NMR signals from the sample. The probe can efficiently perform this dual function only if the impedance of the coil is the same as that of the transmitter or the receiver.

Here L is the decoupling and observation coil for both ^{1}H and ^{13}C nuclei. The sample coil has an inductance of ~ 0.07 μH at 100 MHz.The

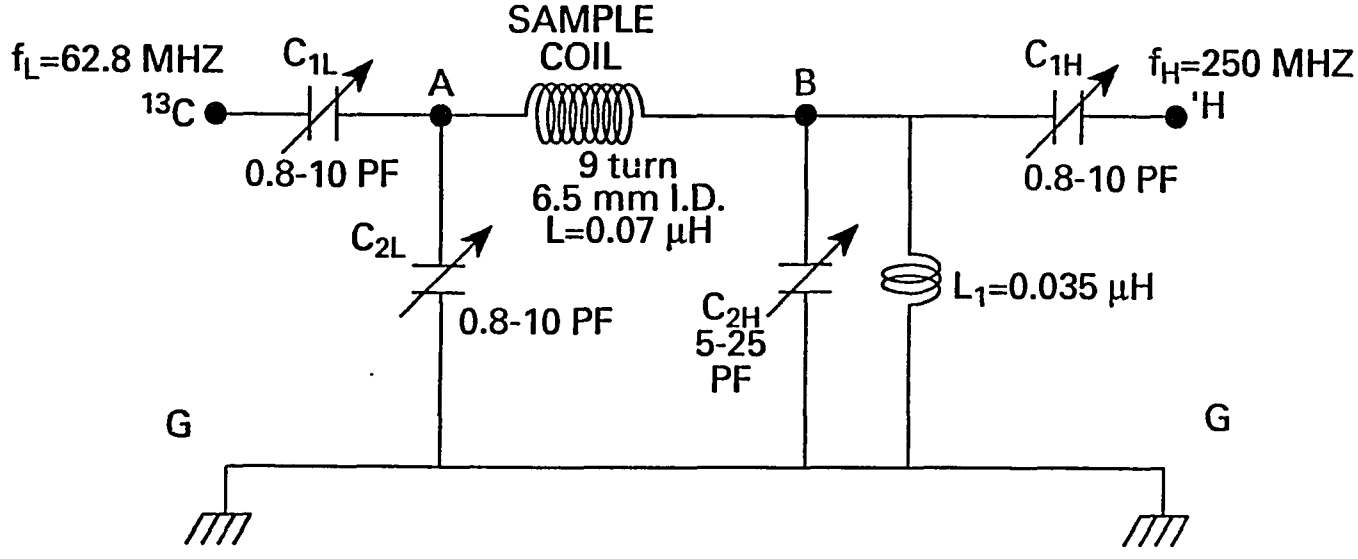

Fig. 28. The circuit of a single-coil probe for ^{1}H - ^{13}C cross-polarization and magic-angle spinning

inductance of the coil determines the quality factor Q which is a measure of the ability of a resonant circuit to store energy. The quality factor Q in most cases is a major factor determining both the overall sensitivity and the ring-down time of the spectrometer's receiving system. When S/N ratio is important, as for high Q probes, the best possible conductors such as silver-plated copper should be used. The coil which is made of silver-plated copper is cylindrical in shape and has 10 turns and a length-to-radius ratio of about 2. This is sufficient to produce a homogenous rf field over most of the coil volume. The coil is loosely wound (i.e., the spacing between its turns is about 1/2 the diameter of the wire) to prevent the reactance from becoming capacitive at higher frequencies.

In designing a double resonance probe for Cross Polarization of solids, there are two important criteria which need to be considered. The first criterion is that reasonably good power efficiency is achieved at both f_L and f_H. Tuning and matching which are accomplished by adjusting variable capacitors determine the impedance of the circuit (i.e., the extent to which the circuit opposes, or impedes alternating - current flow) and result in an efficient transfer of power from the amplifier to the probe. Optimum sensitivity will only be achieved when this adjustment is made correctly.

The tuning and matching in each channel can be adjusted separately to 50 Ω. The tuning and impedance matching of the ^{13} C channel at the lower frequency f_L (62.80 MHz in the present design) is done by adjusting the variable capacitors C_{2L} and C_{1L} and the ^{1} H channel at the higher frequency f_H (250 MHz in the present design) with C_{2H} and C_{1H}. If a very

high quality NMR spectrum is desired, then the probe has to be tuned by these adjustments whenever the sample is changed, because the effects on the inductance of the coil vary from sample to sample. The adjustments may be a little tricky as changing the setting of one capacitor affects the setting of the other capacitor, and one therefore has to alternately change each to obtain the optimum setting of the two.

The second criterion requires adequate isolation of the high frequency, f_H, from the low frequency, f_L. Isolation of f_H at the low frequency input is achieved by capacitance C_{2L} which acts as a virtual ground for the ^1H channel at 250 MHz. This makes point A in Fig. 28 at ground potential with zero impedance to the f_H. As a result there should be no f_H power on the f_L side of the probe. Isolation of low frequency f_L at the high frequency input is obtained with capacitor C_{2H} in parallel with inductor L_1 (.035 μ H). Point B is a virtual ground for the ^{13} C channel and presents an infinite impedance for the ^1H channel; thus all of the f_H rf power is avialable to the sample. Isolation between ^1H and ^{13} C channels was measured to be around 18 dB. With the above design, the probe produces a 5.6 μsec 90 proton pulse with 306 W power at 250 MHz using a 5 mm spherical doped water sample and a 5.2 μsec 90 pulse with 530 W power at 62.80 MHz using cylindrical ^{13}C-labeled acetic acid. The resolution of a sperical nonspinning sample of doped water was 0.14 ppm. The Q of the probe was measured to be around 86 and 125 for the ^1H and ^{13}C channels, respectively.

Stator and Rotar

Fig. 29 is a drawing of the stator. The stator was machined from Macor rod in the Ames lab machine shop by Steve Lee. There are eight equally spaced driving holes made with the stator held 45° with respect to the drill 0.212 in from the top edge and 0.100 in from the back edge of the stator cone. There are also eight bearing holes about the stator body. The eight driving holes in the conical surface of the stator are drilled with a No. 76 drill, and the eight bearing holes in the cylindrical part with a No. 78 drill. The inside diameter of the cylindrical portion of the stator is 0.200 in which can accept a 5 mm NMR tube. The stator has a length of 0.750 in and wall thickness of 0.033 in. The NMR coil is wrapped about the stator body such that partial covering of the bearing air holes is minimized, and a relatively homogenous rf field is maintained. Partial covering of the bearing air holes is an obvious concern to us since this leads to instabilities of the gas flow and unstable sample spinning.

Fig. 30 is a drawing of the Macor housing which has a length and outside diameter of 0.675 in and 0.600 in respectively. The Macor housing has two 0.0625 in holes for coil leads and a mounting and adjust screw with air inlet. The Macor stator and housing weigh about 5.0 gm. The stator is epoxied into the housing.

Fig. 31 is a drawing of the rotor. The rotor used here is constructed of Torlon, an easily machined polyimid polymer which exhibits little if any wear after many hours of use. The rotor is 1.53 cm in outside diameter and has

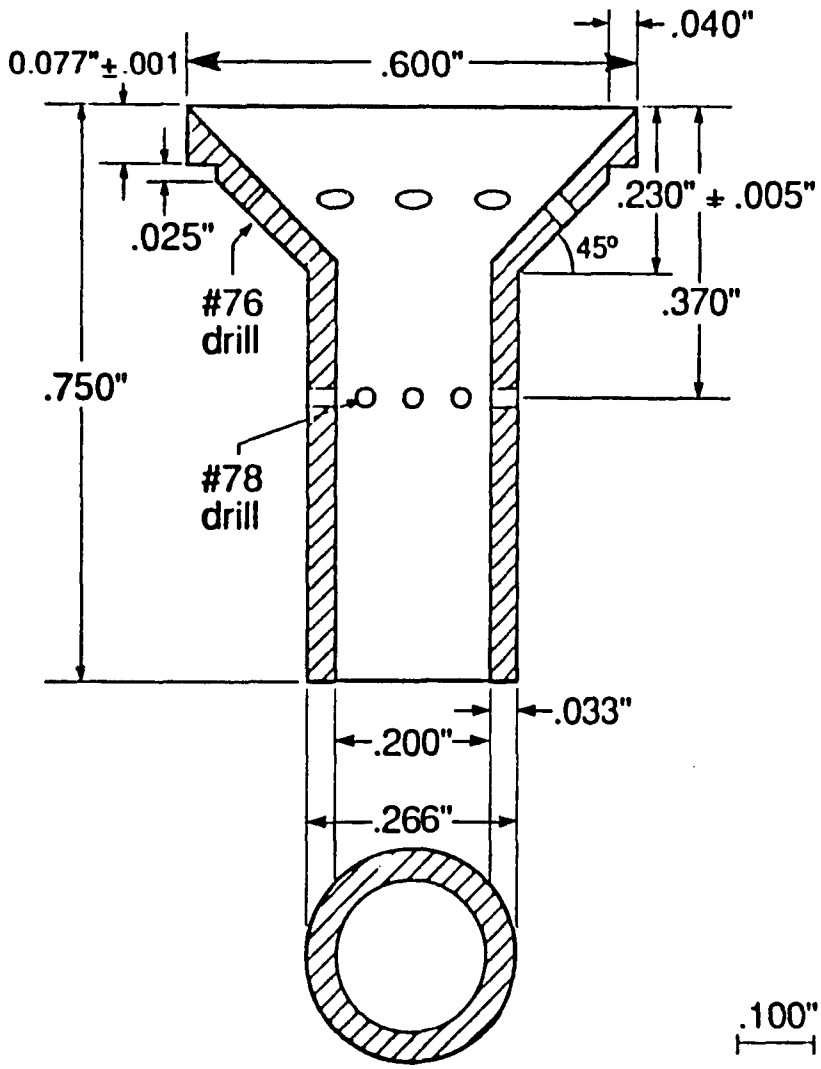

Fig. 29. Drawing of Macor stator

twelve flutes milled into the conical surface. The center hole to accomodate the NMR tube is drilled for a loose fit around the 5 mm NMR tube. The flutes are slit-like cavities which are made by an end mill. The flutes catch the stream of air and increase the rotor's speed. Caution must be taken while machining a rotor since slight imperfections can lead to instability at moderate or even relatively slow speed.

The sample is sealed in a 5 mm NMR tube to a length of 25 mm. Symmetrical sealing of the sample as much as possible is always desirable. If a grossly unbalanced sample is prepared, it will not spin at moderate speed and is in danger of breaking apart at high speed. A small amount of epoxy is applied to the top of the rotor to insure that the 5 mm NMR tube is firmly held while spinning. To achieve perfect centering, the sample is spun at low speed (~ 10 Hz) before complete hardening of the epoxy. The NMR tube is inserted into the stator from above such that the tube bottem is in line with the bottom of the stator.

Dry air as the spinning gas is passed through three air filters in series before reaching the probe. Dry air is used as driving gas due to its low cost relative to helium even though the use of helium as driving gas can usually double the spinning speed of rotor driven by dry air. The air flow enters the stator and is directed toward the rotor through eight bearing holes about the stator body and eight equally spaced driving holes in the conical surface of the stator. The arrangment of rotor flutes and stator holes is such that a clockwise movement of the rotor is produced.The Bernoulli forces lock the rotor into the correct position. Typically only 40 psig of pressure is used.

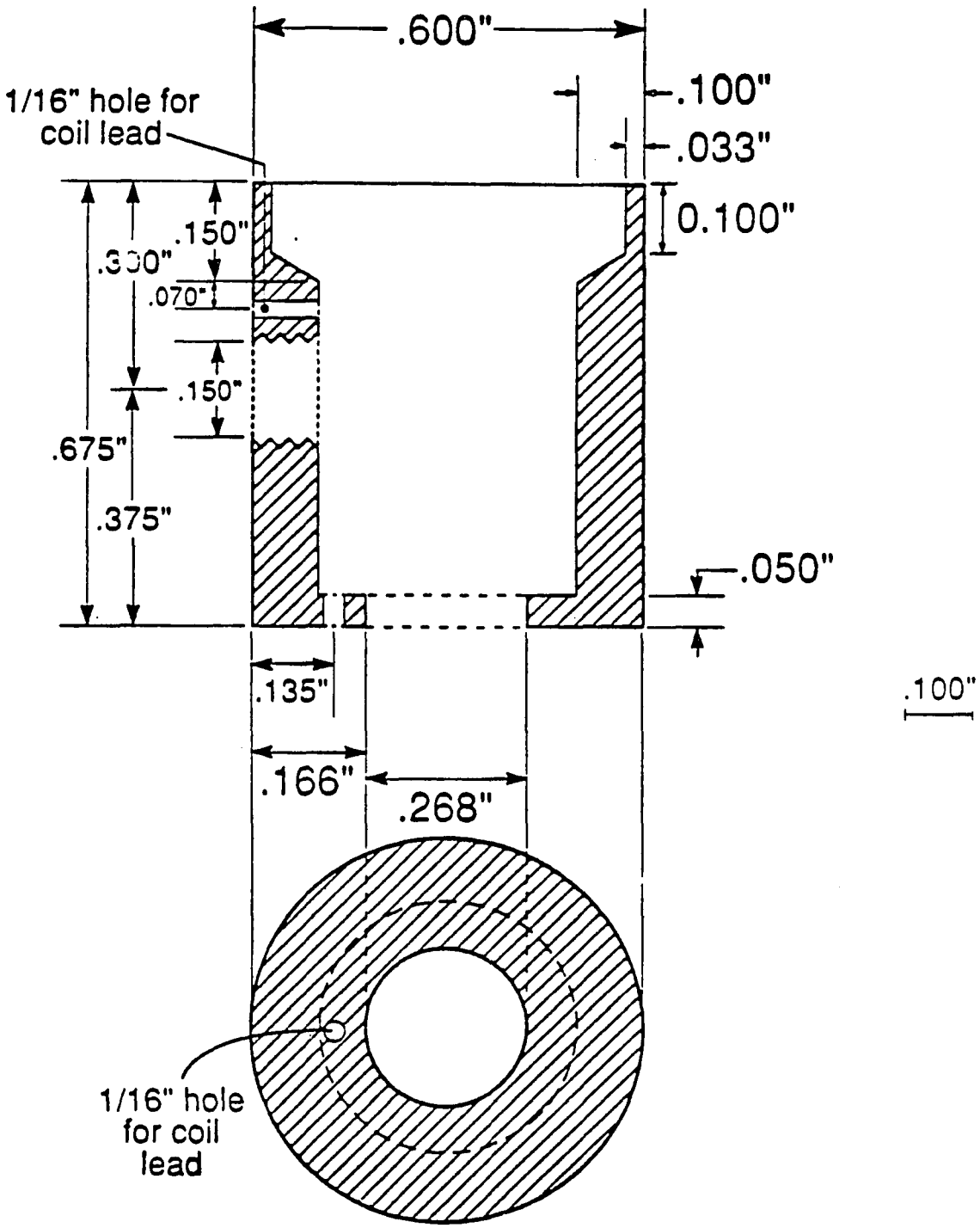

Fig. 30. Drawing of Macor housing

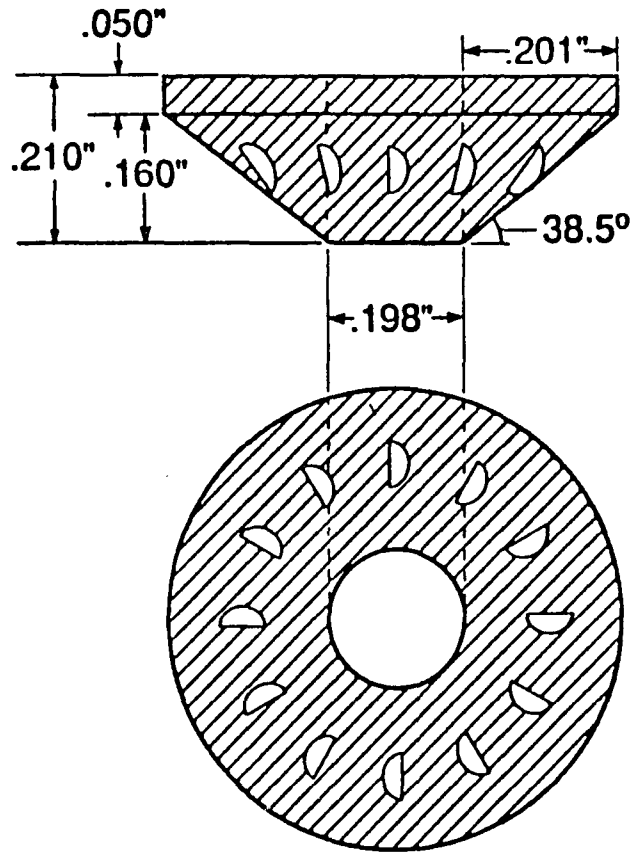

Fig. 31. Drawing of Torlon rotor

Further increase in pressure would break the sample. The symmetry of both rotor and stator is also critical for spinning at high speed. With the above design magic-angle spinning of sealed samples at 5 KHz is achieved.

An optical device is used to measure the rotation rate of the rotor. The procedure involves painting the rotor half black and half white as a reflector. The rotor is then illuminated by a strong light which is piped in through a bundle of optical fibers. The reflected light which varies as a function of the rotor spinning rate is then picked up by a light sensitive diode, the resistance of which causes a voltage variation across the diode. The voltage signal is then amplified and detected by an oscilloscope.

Setting the Magic Angle

Fourier transform magic-angle spinning NMR spectra of half-integer quadrupolar nuclei exhibit many spinning sidebands. The dependence of the sidebands' widths and intensities as a function of the angle the spinning axis makes with the magnetic field can be used in adjusting the magic angle. The NMR signal of ^{79} Br in powdered KBr is convenient for monitoring the angle in ^{13} C MAS experiments since ^{79} Br is an abundant half-integer spin nucleus (I= 3/2) with magnetogyric ratio close to that of ^{13} C thus resonating close to that of carbon (62.62 MHz versus 62.86 MHz at 5.85 Tesla).

The ^{79} Br MAS spectrum of solid KBr is shown in Fig. 32. The spectrum was obtained after taking 100 scans of 4-μsec 90 pulses with a 1-sec repetition time. Fig. 33 is FT/MAS ^{79} Br spectrum of KBr at the magic angle

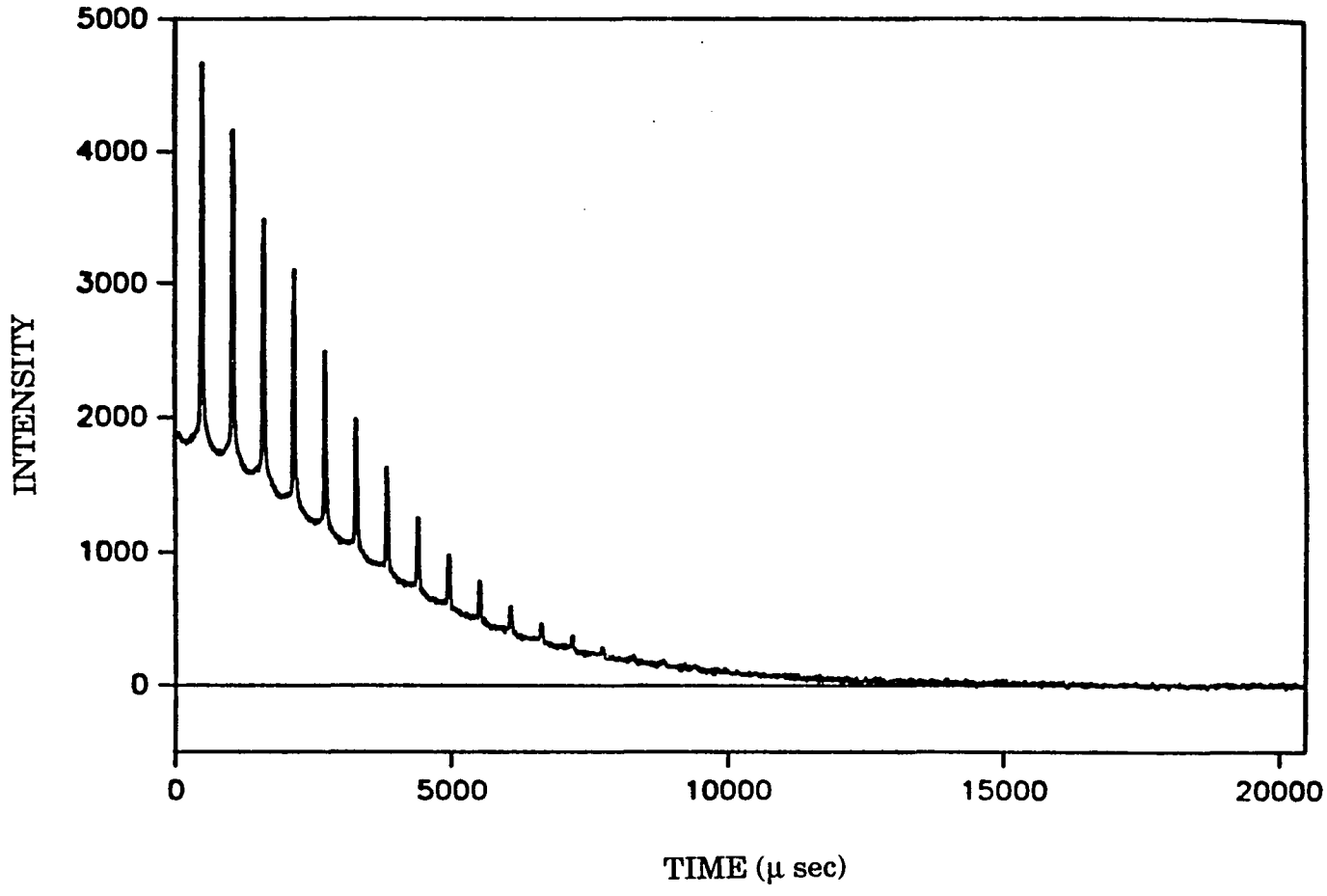

Fig. 32. ^{79}Br MAS spectrum of solid KBr

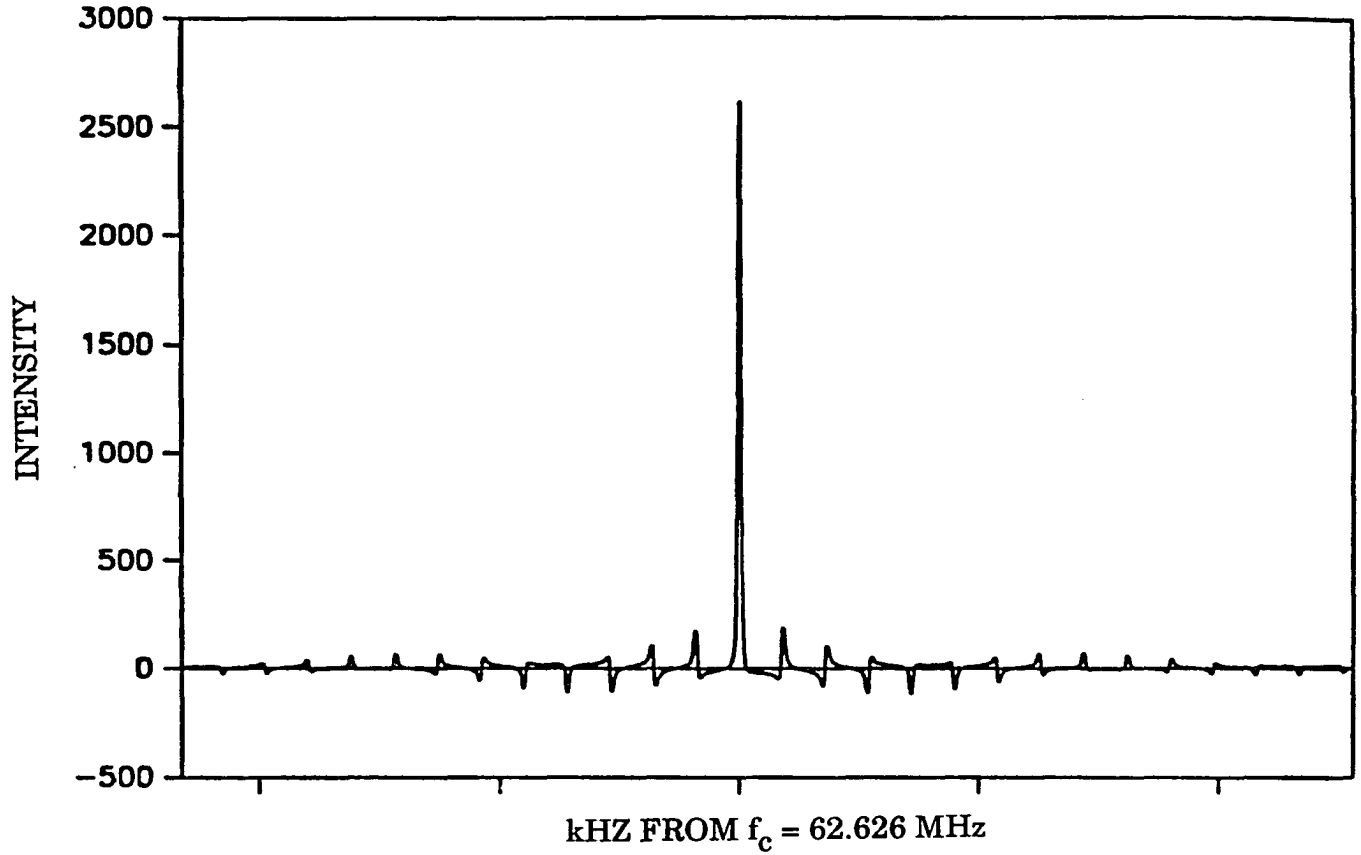

Fig. 33. FT/MAS ^{79}Br spectrum of KBr at the magic angle at 62.62 MHz. 100 4-μsec were taken with a 1.0 sec repetition time

at 62.626 MHz. The ^{79} Br resonance of KBr gives a single, central line, flanked by at least 20 spinning sidebands. The best resolution and the highest-order spinning sidebands are achieved at the exact magic angle. The sidebands in the frequency spectrum correspond to modulation in the time domain. One recognizes these modulations as patterns of spikes in the free induction decay (FID), and adjustment of the spinning angle can be set by monitoring the FID, without recourse to the Fourier- Transformed spectrum.

The magic angle was set by removing the probe from the magnet and turning the stator toward the magic angle until maximum number of spikes in the free induction decay was observed on the scope. The changes in linewidth and intensity are very sensitive to this adjustment in the vicinity of the magic angle. To keep the spinning angle constant and stable, the orientation of the stator was then fixed with epoxy.

The Design of a High Vacuum Glass Apparatus

Introduction

A multiport high-vacuum Pyrex glass apparatus which is used for sample preparation prior to the NMR experiments and chemisorption measurements as well as in-situ experiments is described. This apparatus was designed (as a copy of an apparatus built in the Chemical Engineering Department by Dr. Xi Wu) and constructed by the author. Fig. 34 is a

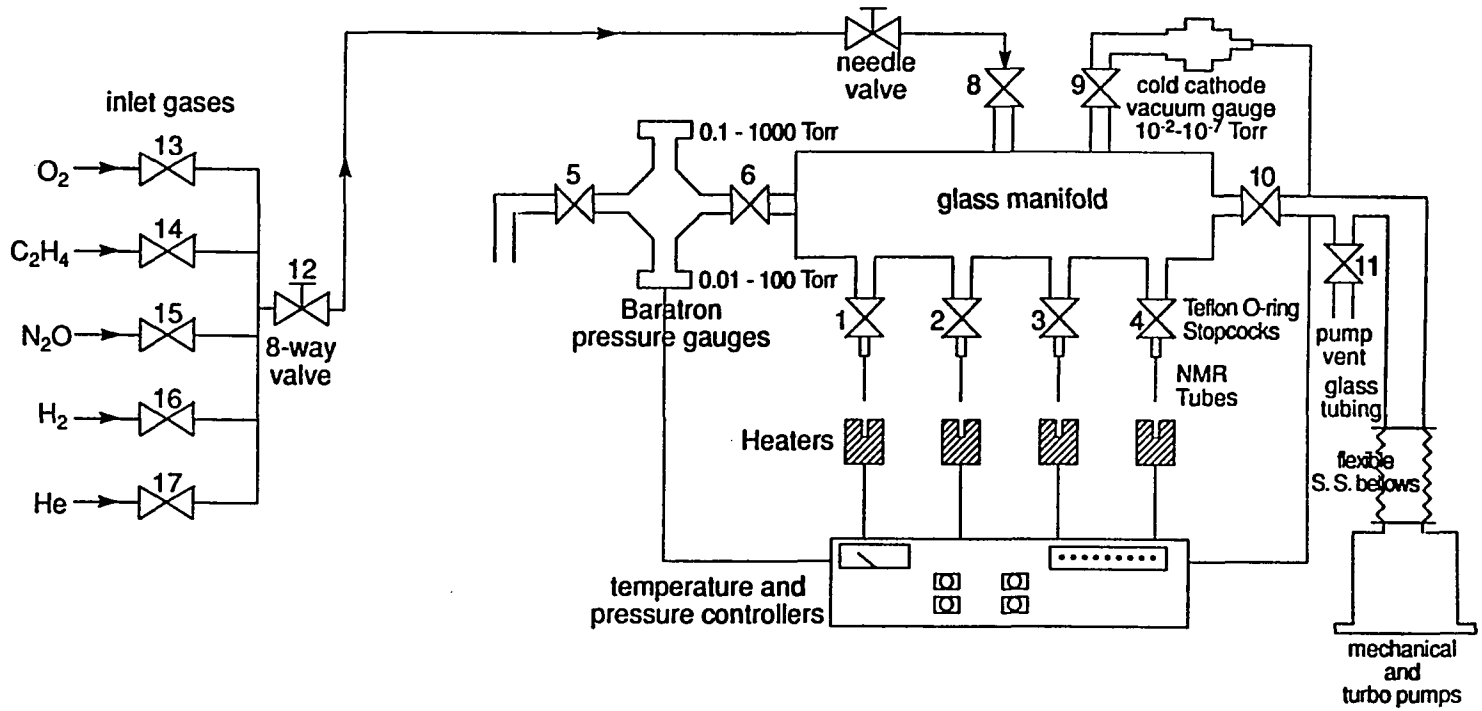

Fig. 34. Schematic diagram of the adsorption apparatus

schematic diagram of this adsorption apparatus. The system consists of a manifold, a pumping system, pressure sensing devices, temperature sensing devices, and gas inlet component. Each part is described in detail as follows:

Glass Manifold

Fig. 35 is the photograph of the adsorption apparatus. The glass manifold has a calibrated volume of 307.50 cm^3 as measured by the volume of distilled water. It connects to four sample-port stopcocks, the vacuum line, the pressure-sensing chambers, and the inlet gas line. High-vacuum greaseless bakeable (up to 200 C) stopcocks (Ace Glass) with teflon plugs and FETFE O-ring seals were employed to prevent any foreign materials from getting into the manifold and to manipulate gas dosage and storage in the manifold. Flexible electric heating cord (Cole-Parmer, 24 ft / max 454 C) is wrapped around the manifold for the purpose of bakeout.

High Vacuum Pumping System

A high vacuum pump (Pfeiffer Balzers, Model TPH050) which consists of a mechanical pump and a turbo molecular pump is connected to the glass manifold via a stainless steel flexible bellows. This particular pumping system is capable of achieving a vacuum better than 10^{-7} Torr (1 Torr = 133.3 pa) inside the glass manifold.

Fig. 35. A picture of the entire multiport high vacuum glass apparatus

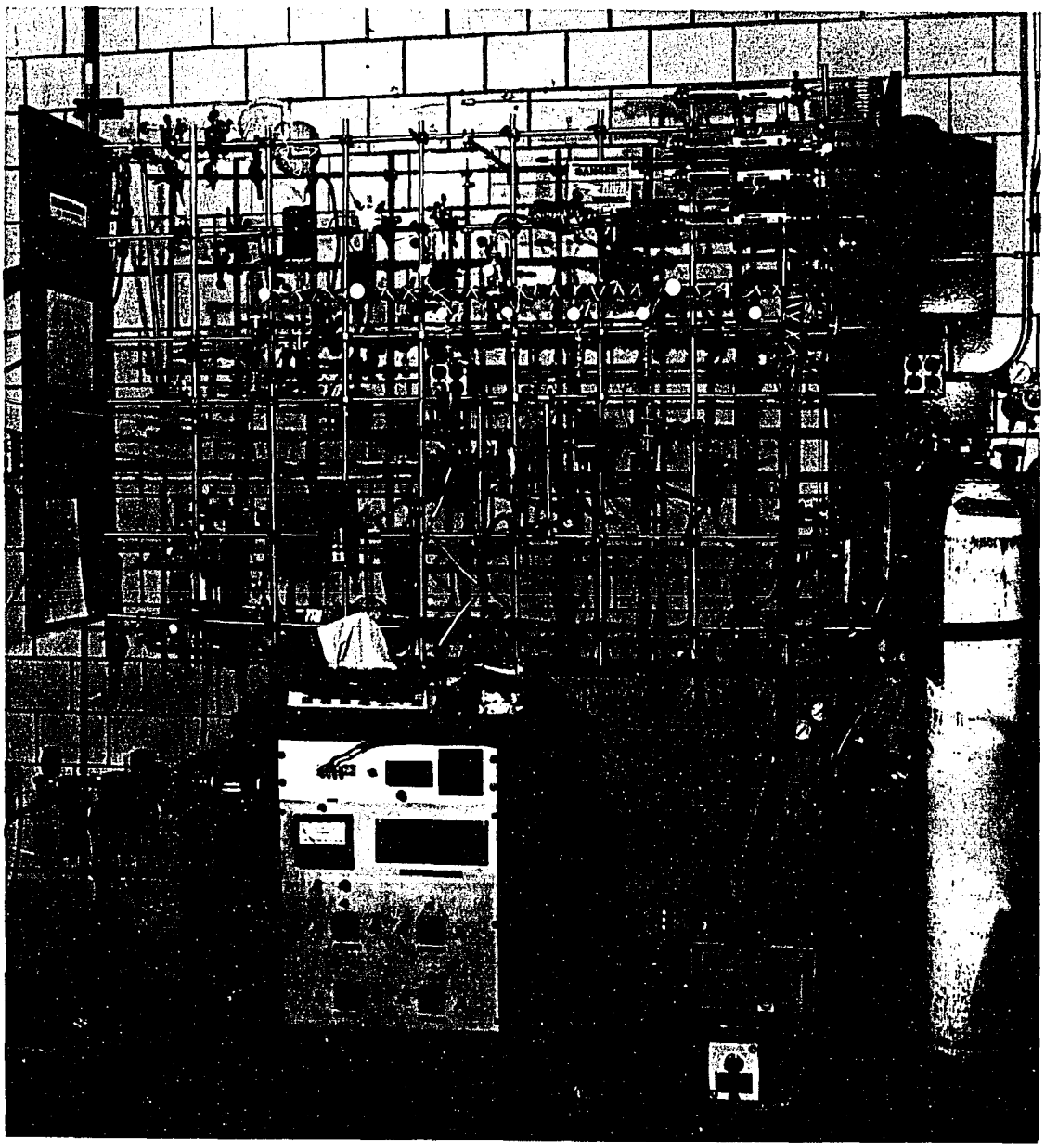

Pressure Sensing Devices

The pressure-sensing devices used to monitor the pressure inside the manifold include a cold cathode gauge (Varian Model 860 A) capable of monitoring pressures below 10^{-2} Torr and two Baratron absolute pressure gauges (MKS instruments) capable of measuring pressure from 10^{-2} Torr to 10^{3} Torr. The cold cathode gauge sensor is connected to the manifold by a stopcock and a piece of stainless steel bellows. The gauge meter is mounted on the instrument panel. The gauge should be turned on when the pressure in the manifold is zero Torr. To achieve a better performance the cold cathode sensor is occasionally baked out (maximum bake out temperature is 120 C). One should be careful to avoid the exposure to high voltage from the sensor. The two Baratron pressure sensors are mounted to the pressure-sensing chamber and the Baratron digital readout unit is mounted on the instrument panel. The digital readout is capable of automatically switching from one sensor to the other. It also provides a number of different pressure units to be displayed.

Temperature Sensing Devices

There are four sample ports available for the NMR sample preparation and chemisorption measurements. The 5mm-OD Norell XR-55 NMR sample tubes are attached to sample ports via Cajon connectors. For each sample port, a small furnace is used to heat the NMR sample tube containing the

catalyst. The temperature controllers (mounted on the instrument panel) regulate the heating within 1 K according to the feedback signals from the built-in thermocouples inside the furnaces. The thermocouples are of K-type (Chromel-alumel or Cr-Ni to Al-Ni). A second thermocouple for each furnace is also provided to measure the true temperature around the sample tube inside the furnace. This temperature is displayed by a digital thermometer (Omega) mounted on the instrument panel. The temperature reading from different furnaces can be monitored separately by turning the rotary selector switch to the desired channel. The true temperatures and setpoint temperatures have been accordingly calibrated and do not need to be recalibrated. All furnaces are supported by clamps with fiber glass sleeves. There are also two extra channels available for monitoring temperatures of the heating tapes around the manifolds and the cold cathode gauge sensor.

Gas Inlet Component

Before their use, helium (zero grade, Air Products & Chemical) is passed through an Oxytrap (Alltech Assoc.) and gas purifier with Drierite and a 5-A molecular sieve (Alltech), oxygen (99.99 %, Scott Specialty Gases), hydrogen(Airco), and nitrous oxide (99.9 %, Scott Specialty Gases) are passed through gas purifiers. A 250 ml in volume glass flask containing ethylene (1,2-$^{13}C_2$, 99.9 %,ISOTEC INC), a 1000 ml in volume glass flask containing carbon dioxide (^{13}C, 99 %,CIL) and a 100 ml in volume glass flask containing ethylene oxide (1,2-$^{13}C_2$, 99 %,CIL) and unlabeled ethylene

oxide (99.7 %,LINDE) were also connected to the manifold without further purification. A single gas may be selected by the eight-way gas selector. All gases are allowed to pass a needle valve and an inlet stopcock before they are introduced into the glass manifold. The inlet gas pressure should never exceed 1000 Torr or the Baratron diaphragms will suffer irreversible deformation due to overpressure. Corrosive gases such as Cl_2, F_2, HCl and concentrated H_2S should also be avoided since they will damage the diaphragms of the Baratron gauges.

REFERENCES

1. Bloch, F.; Hansen, W.W.; Packard, M.E. Phys. Rev. 1946, 69, 127.
2. Purcell, E.M.; Torrey, H.C.; Pound, R.V. Phys. Rev. 1946, 69, 37.
3. Grestein, B.C.; Dybowski, C.R. Transient Techniques in NMR of Solids; An Introduction to Theory and Practice; Academic Press: New York, 1985.
4. Abragam, A. Principle of Nuclear Magnetism; Oxford Univ Press: London, 1961.
5. Slichter, C.P. Principle of Magnetic Resonance; Harper and Row: New York, 1963.
6. Packer, K.J. Prog. Nucl. Reson. Spectroscopy. 1967, 3, 87.
7. Tabony, J. Prog. Nucl. Magn. Reson. Spectroscopy. 1980, 14, 1.
8. Delgass, W.N.; Haller, G.L.; Kellerman, R.; Lunsford, J.H. Spectroscopy in Heterogenous Catalysis; Academic Press: New York, 1979, Chapter 7.
9. Derouane, E.G.; Fraissard, J.; Fripiat, J.J.; Stone, W.E.E. Catalysis Rev. 1972, 7, 121.
10. Fripiat, J.J. Cat Rev. 1971, 5, 269.
11. Pfeifer, H. Phys. Rep. 1976, 7, 293.
12. Pfeifer, H. NMR Basic Principles and Progress; Diehl, P., Ed.; Springer Verlag: New York, 1975; Vol. 7.
13. a) Hartmann, S.R.; Hahn, E.L. Phys. Rev. 1962, 128, 2042.
    b) Jones, E.P.; Hartmann, S.R. Phys. Rev. 1972, 36, 757.
14. a) Lurie, F.M.; Slichter, C.P. Phys. Rev. 1964, 133, A1108.

b) Slichter, C.P.; Holton, W.C. Phys. Rev. 1961, 122, 1701.

15. a) Pines, A.; Gibby, M.G.; Waugh, J.S. J. Chem. Phys. 1972, 56, 1776.
b) Pines, A.; Gibby, M.G.; Waugh, J.S. J. Chem. Phys. Letters. 1972, 15, 373.
16. Mehring, M. High Resolution NMR Spectroscopy in Solid; NMR Basic Principles and Progess; Springer Verlag: New York, 1976; Vol. 11.
17. Pines, A.; Gibby, M.G.; Waugh, J.S. J. Chem. Phys. 1973, 59, 569.
18. Solomon, I. Compt. Rend. 1959, 92, 248.
19. Demco, D.E.; Tegenfeldt, J.; Waugh, J.S. Phys. Rev.B1. 1975, 11, 4133.
20. Mehring, M. Principles of High Resolution NMR in Solids; Springer: New York, 1983; 2nd ed, pp 392.
21. a) Andrew, E.R. Arch. Sci. 1959, 12, 103.
b) Lowe, I.J.; Phys. Rev. Letters. 1959, 2, 285.
22. a) Dixon, W.T. J. Magn. Reson. 1981, 44, 220.
b) Dixon, W.T.; Schaefer, J; Sefeik, M.D.; Stejskal, E.O.; McKay, R.A. J. Magn. Reson. 1981, 45, 173.
23. Shoemaker, R.K.; Apple, T.M. J. Magn. Reson. 1986, 67, 367.
24. Kilty, P.A.; Sachtler, W.M.H. Cat. Rev. Sci. Eng. 1974, 10, 1.
25. Sachtler, W.M.H.; Backx, C.; Van Santen, R.A. Cat. Rev. Sci. Eng. 1981, 23, 127.
26. Hucknell, D. J. Selective Oxidation of Hydrocarbons; Academic Press: New York, London, 1974.
27. Verykios, X.E.; Stein, F.P.; Coughlin, R.W. Cat. Rev. Sci. Eng. 1980, 22 (2), 197.

28. Voge, H.H.; Adams, C.R. Adv. Catal. 1967, 17, 154.

29. Duncan, T.M.; Dybowski, C. Surf. Sci. Rep. 1981, 1, 157.

30. Slichter, C.P. Ann. Rev. Phys. Chem. 1986, 37, 25.

31. Wang, P.K.; Ansermet, J.P.; Rudaz, S.L.; Wang, Z.; Shore, S.; Slichter, C.P.; Sinfelt, J.H. Science. 1986, 35, 234.

32. Plischke, J.K.; Benesi, A.; Vannice, M.A. In Press.

33. Force, E.L.; Bell, A.T. J. Catal. 1975, 38, 440.

34. Force, E.L.; Bell, A.T. J. Catal. 1975, 40, 356.

35. Chin, Y. H.; Ellis, P.D. J. Am. Chem. Soc. In Press.

36. Pruski, M.; Kelzenberg, J.C.; Gerstein, B.C.; King, T.S. J. Am. Chem. Soc. 1990, 112, 4232.

37. a) Pines, A.; Gibby, M.G.; Waugh, J.S. J. Chem. Phys. 1973, 59, 569.
b) Lowe, I. J. Phys. Rev. Lett. 1975, 2, 285.

38. a) Fyfe, C.A. Solid State NMR for Chemist; C.F.G. Press: Ontario, Canada. 1983, p. 474.
b) Opella, S.J.; Frey, M.H. J. AM. Chem. Soc. 1979, 101, 5854.

39. Brownstein, A.M. Trends in Petroleum Technology; Petroleum Publishing Co: Tulsa. 1976.

40. Thomas, C.L. Catalytic Processes and Proven Catalysts; Academic Press: New York. 1970, p. 214.

41. Lefort, T.E. French Patent 729, 952, 1931.

42. Van Santen, R.A.; Kuipers, H.P.C.E. Advan. Catal. 1987, 35, 265.

43. Verykios, X.E.; Stein, F.P; Coughlin, R.W. Catalysis. Rev. Sci. Eng. 1980, 22, 197.

44. Sachtler, W.M.H.; Backx, C.; Van Santen, R.A. Cat Rev. Sci. Eng. 1981, 23, 127.

45. Barteau, M.A.; Madix, R.J. Surf. Sci. 1981, 103, L171.

46. Campbell, C.T.; Pafferr, M.T. Surf. Sci. 1984, 139, 396.

47. Grant, R.B.; Lambert, R.A. J. Catal. 1985, 92, 364.

48. Yong, Y.S.; Cant, N.W. J. Catal. 1990, 22, 122.

49. Seyedmonir, S.R.; Plischke, J.K.; Vannice, M.A.; Young, H.W. J. Catal. 1990, 123, 534.

50. Wu, J.C.; Harriott, P. J. Catal. 1975, 39, 395.

51. Seyedmonir, S.R.; Strohmayer, D.E.; Geoffroy, G.L.; Vannice, M.A.; Young, H.W.; Linowski, J.W. J. Catal. 1984, 87, 424.

52. Seyedmonir, S.R.; Strohmayer, D.E.; Guskey, G.J; Geoffroy, G.L.; Vannice, M.A. J. Catal. 1985, 93, 288.

53. Seyedmonir, S.R.; Strohmayer, D.E.; Geoffroy, G.L.; Vannice, M.A. Adsorption. Sci. Technol. 1984, 1, 253.

54. Czanderna, A.W. J. Phys. Chem. 1964, 68, 2765.

55. Scholten, J.J.F. J. Catal. 1973, 28, 209.

56. Smeltzer, W.W. Can. J. Chem. 1956, 34, 1046.

57. Strohmayer, D.E.; Geoffroy, G.L.; Vannice, M.A. Appl. Catal. 1983, 7, 189.

58. Seyedmonir, S.R.; Strohmayer, D.E.; Geoffroy, G.L.; Vannice, M.A. J. Catal. 1981, 87, 424.

59. Engelhardt, H.A.; Menzel, D. Surf. Sci. 1976, 57, 591.

60. Rovida, G. J. Phys. Chem. 1976, 80, 150.

61. Rovida, G.; Pratesi, F. Surf. Sci. 1975, 52, 452.

62. Barteau, M.A.; Madix, R.J. Surf. Sci. 1980, 97, 101.

63. Clarkson, R.B.; Cirrllo, A.C. J. Vac. Sci. Technol. 1972, 9, 1073.

64. Janssen, M.M.P.; Moolhuysen, J.; Sachtler, W.M.H. Surf. Sci. 1972, 33, 624.

65. Mattera, A.M.; Goodman, R.M.; Somorjai, G.A. Surf. Sci. 1967, 7, 26.

66. Heiland, W.; Iberl, F. Surf. Sci. 1975, 53, 383.

67. Kilty, P.A.; Rol, N.C.; Sachtler, W.M.H. Proceedings of The 5th Congress of Catalysis. 1973, 2, 929.

68. Bradshaw, A.M.; Menzel, D. Faraday. Discuss. Chem. Soc. 1974, 58, 46.

69. Honig, R.E. J. Appl. Phys. 1985, 29, 549.

70. Bagg, J.; Bruce, L. J. Catal. 1963, 2, 93.

71. Kulkova, N.V.; Temkin, M.I. Russ. J. Phys. Chem. 1962, 36, 931.

72. Rovida, G.; Pratesi, F. Surf. Sci. 1975, 52, 542.

73. Wachs, I.E.; Klemen, S.R. J. Catal. 1981, 68, 213.

74. Campbell, C.T. J. Catal. 1985, 94, 436.

75. Grant, R.B.; Lambert, R. Surf. Sci. 1984, 146, 256.

76. Bradshaw, A.m.; Menzel, D. Faraday. Discuss. 1974, 58, 46.

77. Rovida, G.; Ferroni, E.; Magleilta, M. Adsorption Desorption Phenomena; F. Ricca, Ed.; Academic Press: London, 1972; p 417.

78. Eichmans, J.; Goldman, A.; Otta, A. Surf. Sci. 1983, 127, 153.

79. Backx, C.; DeGroot, C.P.M. Surf. Sci. 1981, 104, 300.

80. Sexton, B.A.; Madix, R.J. Chem. Phys. Lett. 1980, 76, 294.

81. Campbell, C.T.; Paffett, M.T. Surf. Sci. 1984, 143, 517.

82. Campbell, C.T. Surf. Sci. 1985, 43, 157.

83. Backx, C.; Van Santen, R.A. J. Catal. 1981, 72, 364.

84. Worbs, H. Ph.D. Dissertation, Technische Hochshule, 1942.

85. Voge, H.H.; Adams, C.R. Adv. Catal. 1967, 17, 151.

86. Kilty, P.A.; Sachtler, W.M.H. Catal. Rev. Sci. Eng. 1974, 1, 10.

87. Kilty, P.A.; Rol, N.C.; Sachtler, W.M.H. Proceedings of The 5th International Congress on Catalysis, Palm Beach, CA, 1973; P. 64

88. Grant, R.B.; Lambert, R.M. Langmuir. 1985, 1, 29.

89. Van Santen, R.A.; de Groot, C.P.M. J. Catal. 1986, 98, 530.

90. Anderson, J.R. Structure of Metallic Catalysts; Academic Press: London, 1975.

91. Czanderna, A.W.; Frank, O.; Schmidt, W.A. Surface. Sci. 1973, 38, 129.

92. Kagawa, S.; Masakasa, I.; Morita, S.J. J. Chem. Soc. Faraday. Trans I. 1982, 78, 143.

93. Backx, C.; Moolhuysen, J.; Geenen, P.; Van Santen, R.A. J. Catal. 1981, 72, 364.

94. Grant, R.B.; Lambert, R.M. J. Chem. Soc. Chem. Commun. 1983, 58, 124.

95. Czanderna, A.W. J. Phys. Chem. 1966, 70, 2120.

96. Kholyavenko, K.M.; Rubanic, M.Y.; Cheryukhiva, N.A. Kinet. Catal. 1964, 5, 437.

97. Scholten, J.J.F.; Konvalinka, J.A.; Beekman, F.W. J. Catal. 1973, 28, 209.

98. Smeltzer, W.W.; Tollefson, E.L.; Cambson, A. Can. J. Chem. 1956, 34, 1046.

99. Pruski, M.; Sanders, D.K.; King, T.S.; Gerstein, B.C. J. Magn. Reson. 1992, 96, 574.

100. Stejskal, E.O.; Schaefer, J. J. Magn. Reson. 1975, 18, 560.

101. Engelhardt, G.; Michel, D. High - Resolution Solid-State NMR of Silicates and Zeolites; John Wiley and Sons: New York, 1987; pp 368 - 478.

102. Alemany, L.B.; Grant, D.M.; Alger, T.D.; Pugmire, R.J. J. Amer. Chem. Soc. 1983, 105, 6697.

103. DuBois, M.P.; Gerstein, B.C. J. Mag. Reso. 1985, 62, 303.

104. Kobayashi, M. Catalysis Under Transient Conditions. A.T. Bell and L.L. Hegedus, Eds; Amer. Chem. Soc. Symp. Ser: Washington, D.C., 1980.

105. Herzog, V.M. Ber. Bunsenges. Phys. Chem. 1970, 74, 216.

106. Avery, N. Surf. Sci. 1983, 131, 501.

107. Shi, S.K.; Lee, H.I.; White, J.M. Surf. Sci. 1981, 102, 56.

108. Harbraken, F.H.; Bootsma, G.A. Surf. Sci. 1979, 87, 333.

109. Tan, S.A.; Grant, R.B.; Lambert, R.M. J. Catal. 1987, 104, 156.

110. Bremser, W.; Frank, B.; Wagner, H. Chemical Shift Ranges in Carbon - 13 NMR Spectroscopy; Verlag Chemic: Weinheim, West Germany. 1982.

111. Mudrukovskii, I.L.; Mustikhin, V.M.; Bogdanchikova, N.E.; Khasin, A.V. React. Kinet. Catal. Lett. 1987, 34, 185.

112. Kobayashi, M.; Yamamoto, M.; Kobayashi, H. Proceedings of The 6th International Congress on Catalysis. A 24, 1976.

113. Kilty, P.A.; Rol, N.C.; Sachtler, W.M.H. Proceedings of The 5th International Congress on Catalysis. North - Holland: Amsterdam. 1972, paper 67A.

114. Gay, I.D. J. Catal. 1987, 108, 15.

115. Twigg, G.H. Proc. R. Soc. London. 1946, 188 A, 105.

116. Lapkin, R.E. J. Phys. Chem. 1970, 74, 1493.

117. Harriott, P. J. Catal. 1971, 21, 56.

118. Lee, J.K.; Verykios, X.E.; Patchai, R. Appl. Catal. 1988, 44, 223.

119. Riassian, M.; Trimm, D.L.; Williams, P.M. J. Catal. 1977, 46, 82.

120. Lee, J.K.; Verykios, X.E.; Pitchai, R. Appl. Catal. 1989, 50, 171.

ACKNOWLEDGMENTS

I must express my gratitude to the following people :

1. My gracious and wonderful parents who have sacrificed everything for me to have the best possible education. There are simply no words for me to express their love, dedication, encouragement, emotional as well as financial supports throughout the years I have been in the United States.
2. My lovely wife Mitra, who is my biggest treasure. Her enormous love, encouragement and support are beyond my imagination. Without her help and sacrifice, I could not possibly complete this work. Worthful to mention that writing up this thesis coincides with the birth of our first child.
3. Dr. B. C. Gerstein for his patience, guidance, encouragement, support and invaluable comments throughout the course of this project.
4. Dr. T. S. King of the Chemical Engineering Department for suggesting me this project, providing numerous comments and sharing his knowledge and expertise on heterogenous catalysis.
5. Dr. M. Pruski for his comments on this project and allowing me to use his probe and the 100 MHz NMR spectrometer.
6. Mr. Son-Jong Hwang who taught me so much about nuts and bolts of NMR and emotionally supported me when I needed help. His friendship is invaluable to me and I will always remember him as an outstanding scientist and more importantly as a very nice individual.

7. Mr. Steve Lee who sincerely taught me so much about various techniques involved in the machine shop. His cooperation and friendship are always appreciated and remembered.
8. Special thanks go to the people in the glass shop , the electronic shop and the store room who fully cooperated with me when I needed their assistance.
9. Last but certainly not least, I am grateful to my colleagues Hongjun Pan, Luisita C. Dela Rosa, Deniz Uner, Sandeep Bhatia, Xi Wu and David Lang for their friendship and beneficial discussions.

This work was performed at Ames Laboratory under contract no. W-7405-eng-82 with the U.S. Department of Energy. The United States government has assigned the DOE Report number IS-T 1623 to this dissertation.